NTIS #PB95-185419

SSC-381

RESIDUAL STRENGTH OF DAMAGED MARINE STRUCTURES

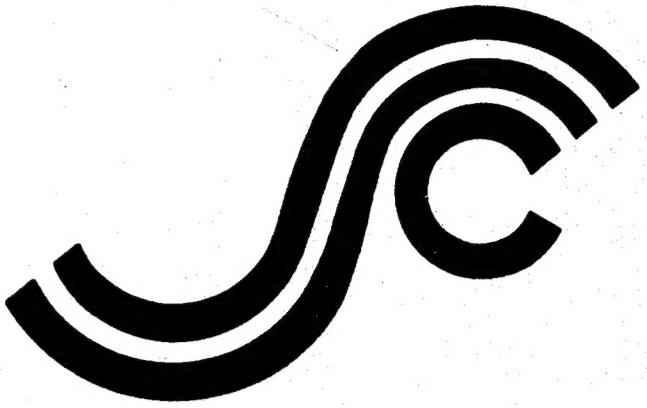

SHIP STRUCTURE COMMITTEE

1995

SHIP STRUCTURE COMMITTEE

The SHIP STRUCTURE COMMITTEE is constituted to prosecute a research program to improve the hull structures of ships and other marine structures by an extension of knowledge pertaining to design, materials, and methods of construction.

RADM J. C. Card, USCG (Chairman)
Chief, Office of Marine Safety, Security
and Environmental Protection
U. S. Coast Guard

Mr. Thomas H. Peirce
Marine Research and Development
Coordinator
Transportation Development Center
Transport Canada

Mr. Edwin B. Schimler
Associate Administrator for Ship-
building and Technology Development
Maritime Administration

Dr. Donald Liu
Senior Vice President
American Bureau of Shipping

Mr. Edward Comstock
Director, Naval Architecture
Group (SEA O3H)
Naval Sea Systems Command

Mr. Thomas W. Allen
Engineering Officer (N7)
Military Sealift Command

Mr. Warren Nethercote
Head, Hydronautics Section
Defence Research Establishment-Atlantic

EXECUTIVE DIRECTOR

CDR Stephen E. Sharpe, USCG
U. S. Coast Guard

CONTRACTING OFFICER TECHNICAL REPRESENTATIVE

Mr. William J. Siekierka
Naval Sea Systems Command

SHIP STRUCTURE SUBCOMMITTEE

The SHIP STRUCTURE SUBCOMMITTEE acts for the Ship Structure Committee on technical matters by providing technical coordination for determinating the goals and objectives of the program and by evaluating and interpreting the results in terms of structural design, construction, and operation.

MILITARY SEALIFT COMMAND

Mr. Robert E. Van Jones (Chairman)
Mr. Rickard A. Anderson
Mr. Michael W. Touma
Mr. Jeffrey E. Beach

MARITIME ADMINISTRATION

Mr. Frederick Seibold
Mr. Richard P. Voelker
Mr. Chao H. Lin
Dr. Walter M. Maclean

U. S. COAST GUARD

CAPT G. D. Marsh
CAPT W. E. Colburn, Jr.
Mr. Rubin Scheinberg
Mr. H. Paul Cojeen

AMERICAN BUREAU OF SHIPPING

Mr. Stephen G. Arntson
Mr. John F. Conlon
Mr. Phillip G. Rynn
Mr. William Hanzelek

NAVAL SEA SYSTEMS COMMAND

Mr. W. Thomas Packard
Mr. Charles L. Null
Mr. Edward Kadala
Mr. Allen H. Engle

TRANSPORT CANADA

Mr. John Grinstead
Mr. Ian Bayly
Mr. David L. Stocks
Mr. Peter Timonin

DEFENCE RESEARCH ESTABLISHMENT ATLANTIC

Dr. Neil Pegg
LCDR Stephen Gibson
Dr. Roger Hollingshead
Mr. John Porter

SHIP STRUCTURE SUBCOMMITTEE LIAISON MEMBERS

U. S. COAST GUARD ACADEMY

LCDR Bruce R. Mustain

U. S. MERCHANT MARINE ACADEMY

Dr. C. B. Kim

U. S. NAVAL ACADEMY

Dr. Ramswar Bhattacharyya

CANADA CENTRE FOR MINERALS AND
ENERGY TECHNOLOGIES
Dr. William R. Tyson

SOCIETY OF NAVAL ARCHITECTS AND
MARINE ENGINEERS
Dr. William Sandberg

U. S. TECHNICAL ADIVSORY GROUP TO THE
INTERNATIONAL STANDARDS ORGANIZATION
CAPT Charles Piersall

NATIONAL ACADEMY OF SCIENCES -
MARINE BOARD
Dr. Robert Sielski

NATIONAL ACADEMY OF SCIENCES -
COMMITTEE ON MARINE STRUCTURES
Mr. Peter M. Palermo

WELDING RESEARCH COUNCIL

Dr. Martin Prager

AMERICAN IRON AND STEEL INSTITUTE

Mr. Alexander D. Wilson

OFFICE OF NAVAL RESEARCH

Dr. Yapa D. S. Rajapaske

STUDENT MEMBER

Mr. Trevor Butler
Memorial University of Newfoundland

Member Agencies:

American Bureau of Shipping
Defence Research Establishment Atlantic
Maritime Administration
Military Sealift Command
Naval Sea Systems Command
Transport Canada
United States Coast Guard

Ship Structure Committee

An Interagency Advisory Committee

Address Correspondence to:

Executive Director
Ship Structure Committee
U.S. Coast Guard (G-MI/SSC)
2100 Second Street, S.W.
Washington, D.C. 20593-0001
Ph:(202) 267-0003
Fax:(202) 267-4677

SSC-381
SR-1341

March 17, 1995

RESIDUAL STRENGTH OF DAMAGED MARINE STRUCTURES

Deep draft merchant vessels built during the past few decades are less robust than their predecessors. Finite element analysis, reduction of corrosion allowances, and other design practices have provided a means for the designer to reduce scantlings overall to the minimum required. Where older structures had significant redundancies the newer structures have relatively little. Following the impacts of several marine disasters, operators, regulators, and classification societies have had to more closely monitor the strength of aging and damaged structures.

In 1983 the Ship Structure Committee sponsored a symposium on "The Role of Design, Inspections and Redundancy in Marine Structures Reliability". This report is the third follow-on project since that symposium. It is intended to introduce to the industry a means of assessing residual strength. Some currently available methods to measure residual strength are presented and evaluated for effectiveness and applied to case studies. It outlines practical analytical procedures to make decisions to respond to failures found in marine structures.

J. C. CARD
Rear Admiral, U.S. Coast Guard
Chairman, Ship Structure Committee

Technical Report Documentation Page

1. Report No.	2. Government Accession No.	3. Recipient's Catalog No.
SSC-381	PB95-135419	

4. Title and Subtitle	5. Report Date
"Residual Strength of Damaged Marine Structures"	September 1994
	6. Performing Organization Code
	8. Performing Organization Report No.
7. Author(s) Dhruba J. Ghose, Natale S. Nappi and Christopher J. Wiernicki	"SR-1341"
9. Performing Organization Name and Address	10. Work Unit No. (TRAIS)
Designers & Planners, Inc. 2120 Washington Blvd., Suite 200 Arlington, VA 22204	11. Contract or Grant No. DTCG23-92-C-E01090-1
	13. Type of Report and Period Covered
12. Sponsoring Agency Name and Address	FINAL
Ship Structure Committee U.S. Coast Guard 2100 Second Street, S.W. Washington, D.C. 20593	14. Sponsoring Agency Code G-M

15. Supplementary Notes

Sponsored by the Ship Structure Committee and its member agencies.

16. Abstract

Traditionally assessment of ship's longitudinal strength has been made by comparing the elastic stresses at the deck or bottom shell to fractions of the material yield strength. This results in high reserve capacity due to inherent redundancies in ship structures. Residual strength, which is defined as the strength of the structure after damage, has rarely been considered either during design or at the time of repair. In this report, key elements required to undertake an engineering analysis to evaluate the residual strength have been identified. Emphasis has been placed on assessing the residual strength of marine structures damaged due to normal operating loads. Methods available to industry for evaluation of damage such as, fracture and ultimate strength have been summarized. An example problem, illustrating the application of an integrated approach to residual strength assessment on a particular ship type, is presented.

17. Key Words	18. Distribution Statement
Residual Strength, Ultimate Strength, Fracture Mechanics, Fatigue, Permanent Deformation, Plasticity, Hull Structure	Available from: National Technical Information Service Springfield, VA 22161 Distribution Unlimited

19. Security Classif. (of this report)	20. Security Classif. (of this page)	21. No. of Pages	22. Price
Unclassified	Unclassified	180	$27.00 Paper $12.50 Micro

Form DOT F 1700.7 (8-72) Reproduction of completed page authorized

United States Department of Commerce
Technology Administration
National Institute of Standards and Technology
Metric Program, Gaithersburg, MD 20899

METRIC CONVERSION CARD

Approximate Conversions to Metric Measures

Symbol	*When You Know*	*Multiply by*	*To Find*	*Symbol*
LENGTH				
in	inches	2.5	centimeters	cm
ft	feet	30	centimeters	cm
yd	yards	0.9	meters	m
mi	miles	1.6	kilometers	km
AREA				
in^2	square inches	6.5	square centimeters	cm^2
ft^2	square feet	0.09	square meters	m^2
yd^2	square yards	0.8	square meters	m^2
mi^2	square miles	2.6	square kilometers	km^2
	acres	0.4	hectares	ha
MASS (weight)				
oz	ounces	28	grams	g
lb	pounds	0.45	kilograms	kg
	short tons (2000 lb)	0.9	metric ton	t
VOLUME				
tsp	teaspoons	5	milliliters	mL
Tbsp	tablespoons	15	milliliters	mL
in^3	cubic inches	16	milliliters	mL
fl oz	fluid ounces	30	milliliters	mL
c	cups	0.24	liters	L
pt	pints	0.47	liters	L
qt	quarts	0.95	liters	L
gal	gallons	3.8	liters	L
ft^3	cubic feet	0.03	cubic meters	m^3
yd^3	cubic yards	0.76	cubic meters	m^3
TEMPERATURE (exact)				
°F	degrees Fahrenheit	subtract 32, multiply by 5/9	degrees Celsius	°C

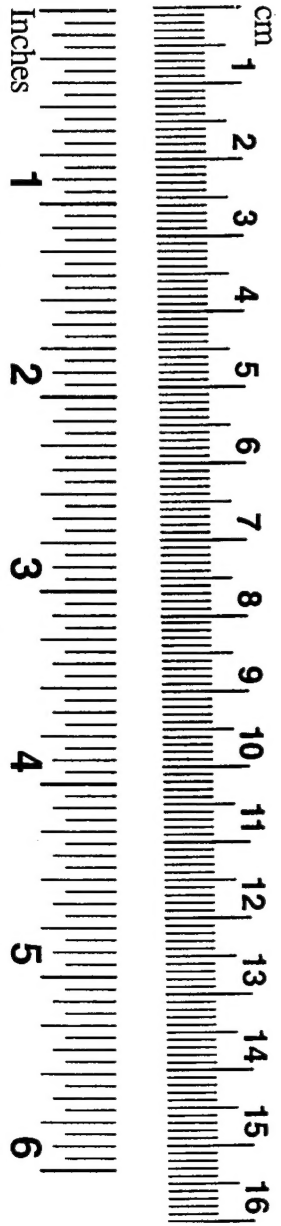

Approximate Conversions from Metric Measures

Symbol	*When You Know*	*Multiply by*	*To Find*	*Symbol*
LENGTH				
mm	millimeters	0.04	inches	in
cm	centimeters	0.4	inches	in
m	meters	3.3	feet	ft
m	meters	1.1	yards	yd
km	kilometers	0.6	miles	mi
AREA				
cm^2	square centimeters	0.16	square inches	in^2
m^2	square meters	1.2	square yards	yd^2
km^2	square kilometers	0.4	square miles	mi^2
ha	hectares (10,000 m^2)	2.5	acres	
MASS (weight)				
g	grams	0.035	ounces	oz
kg	kilograms	2.2	pounds	lb
t	metric ton (1,000 kg)	1.1	short tons	
VOLUME				
mL	milliliters	0.03	fluid ounces	fl oz
mL	milliliters	0.06	cubic inches	in^3
L	liters	2.1	pints	pt
L	liters	1.06	quarts	qt
L	liters	0.26	gallons	gal
m^3	cubic meters	35	cubic feet	ft^3
m^3	cubic meters	1.3	cubic yards	yd^3
TEMPERATURE (exact)				
°C	degrees Celsius	multiply by 9/5, add 32	degrees Fahrenheit	°F

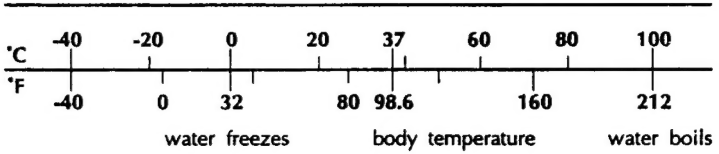

TABLE OF CONTENTS

LIST OF FIGURES

LIST OF TABLES

Nomenclature

β	plate slenderness ratio b/t $\sqrt{(\sigma_y/E)}$
γ_s, γ_a, γ_t	partial coefficients for safety factor treatment (see table 4.4)
$\Delta\sigma$	applied stress range (N/mm^2)
δ_c	crack tip opening displacement (CTOD) (mm)
δ_{CR}	critical crack tip opening displacement (onset of unstable fracture) (mm)
δ_I	applied crack tip opening displacement (mm)
ΔK_I	applied stress intensity factor range ($N \cdot mm^{-3/2}$)
ΔK_{rms}	root mean square stress intensity factor range ($N \cdot mm^{-3/2}$)
ΔK_{th}	threshold stress intensity factor range ($N \cdot mm^{-3/2}$)
ΔP_b	bending stress range (N/mm^2)
ΔP_m	membrane stress range (N/mm^2)
δ_r	fracture ratio using CTOD parameter
ϵ	strain
ϵ_y	yield strain
θ	rotation
ρ	plasticity correction factor
σ	stress (N/mm^2)
σ_1	applied tensile stress (N/mm^2)
σ_f	flow stress (N/mm^2)
σ_H	horizontal wave bending stress (N/mm^2)
σ_n	net section stress (N/mm^2)
$\sigma_{r\,i}$	stress range corresponding to the i^{th} sea-state (N/mm^2)
$\sigma_{r\,max}$	maximum stress range (N/mm^2)
σ_R	residual stress (N/mm^2)
σ_{rms}	root mean square stress range (N/mm^2)
σ_u	ultimate tensile strength (N/mm^2)
σ_{VH}	hogging wave bending stress (N/mm^2)
σ_{vs}	sagging wave bending stress (N/mm^2)
σ_y	yield strength (N/mm^2)
Φ	complete elliptic integral of the second kind

2a	crack length for through thickness cracks (see figure 4.5) (mm)
2c	crack length for surface or embedded flaw (see figure 4.5) (mm)
a	length of panel of plating (long edge) (mm)
A	material constant used for K_f (mm)
a_0	initial crack length (mm)
a_1	half length of the real crack, including the plastic zone (mm)
a_f	final crack length (mm)
$\bar{a}_m$, a_m	tolerable crack size (mm)
b	breadth of panel of plating (short edge) (mm)
B	section thickness in the plane of through flaw (see figure 4.5) (mm)
B_c	cross-section margin
C	constant in crack growth law
d	depth of the web plus the flange thickness
D	damage ratio
da/dN	crack growth rate (mm/cycle)
E	Young's modulus of elasticity (N/mm^2)
$E_{d\ imp}$	dynamic impact energy (MJ)
E_{imp}	static impact energy (MJ)
F	peak stress (N/mm^2)
f^*_{r2}	stress range due to fluctuating pressure loading (N/mm^2)
H	equivalent half thickness
$H_{s\,i}$	significant wave height in the i^{th} sea-state
$H_{s\,max}$	maximum significant wave height
I_{yy}	moment of inertia about the horizontal N.A. (m^2-cm^2)
I_{zz}	moment of inertia about the vertical N.A. (m^2-cm^2)
J_{mat}	material toughness measured by J-method (N/mm)
K	stress intensity factor ($N \cdot mm^{-3/2}$)
K_e	equivalent stress intensity factor ($N \cdot mm^{-3/2}$)
K_f	fatigue strength reduction factor
K_I	applied stress intensity factor ($N \cdot mm^{-3/2}$)

K_{IC}	plain strain fracture toughness ($N \cdot mm^{-3/2}$)
K_{mat}	material toughness measured by stress intensity factor ($N \cdot mm^{-3/2}$)
K_r	fracture ratio (K_I/K_{mat})
K_t	stress concentration factor
l	length of beam
l_i	hinge line
m	exponent in crack growth law
M	bending moment (N-mm)
M_Y	full plastic moment (N-mm)
M_{Des}	allowable design collapse moment (N-mm)
M_{km}, M_{kb}	
M_m, M_b,	stress intensity factor magnification factors
M_u, M_{ULT}	ultimate collapse moment (N-mm)
N	number of cycles
N_f	number of cycles to failure
n_i	number of cycles in the i^{th} range
N_i	number of cycles for crack initiation
N_p	number of cycles for crack propagation
p	applied lateral pressure (N/mm^2)
P	applied load (N)
P_Y	full plastic axial force (N)
$P^{(1)}_f$	probability of failure of a structural member
$P^{(s)}_f$	probability of system failure
P^*_r	probabilistic measure of redundancy
P_b	primary bending stress (N/mm^2)
P_m	primary membrane stress (N/mm^2)
Q	secondary stress (N/mm^2)
Q_b	secondary bending stress (N/mm^2)
Q_m	secondary membrane stress (N/mm^2)
r	notch radius (mm)
R	stress ratio ($\sigma_{min}/\sigma_{max}$)
REF	reserve resistance factor
RIF	residual resistance factor

r_y	length of the plastic zone (mm)
S	stress range (N/mm^2)
S_i	i^{th} stress range (N/mm^2)
SM	sectional modulus ($m\text{-}cm^2$)
S_r	plastic collapse ratio (σ_n/σ_f)
t	thickness of plating (mm)
W	plane width in plane of flaw (see figure 4.5) (mm)
w	displacement (mm)
Y	form factor (stress intensity factor correction)

1.0 INTRODUCTION

The increasing demands being placed on existing marine structures and the trends toward lightweight structures and limit state design require a thorough understanding of the reserve and residual strength capacity of structures.

Historically, in traditional engineering practice, the role of residual strength is not explicitly defined. However, since the Ship Structure Committee (SSC) Symposium in 1983, which addressed "The Role of Design, Inspections, and Redundancy in Marine Structure Reliability", events in the marine industry have pointed to a reevaluation of the role of residual strength in the context of safety, and reliability of marine structures. This project titled "Residual Strength Assessment of Damaged Marine Structures" attempts to introduce the subject to the practicing engineering community and form the basis for continued future work. Specifically, this project will identify characteristic types of damage based on review of ship casualty records and present supporting analytical methods capable of assessing both the local individual component and global system residual strength. The ability to assess both intact and damaged structures will lead to the proper exploitation of inherent structural redundancy, identification of desired local and global safety levels and the development of inspection, maintenance and repair procedures in a more rational, cost effective and complete manner than has been possible in the past.

1.1 Background

Two previous Ship Structure Committee (SSC) projects; SSC-354, "Structural Redundancy for Discrete and Continuous Systems" and SSC-355, "Relation of Inspection Findings to Fatigue Reliability", were conducted which investigated the role of structural redundancy and the reliability of current marine inspection procedures, respectively. The significant conclusions of these projects included the following:

- Even simple structures have high levels of redundancy;
- The relationship between reserve strength, residual strength and redundancy is difficult to quantify, even for simple marine structural systems;
- Decisions to repair damage found during inspections are based upon a particular inspector's experience rather than analytical methods.

This SSC project builds on the conclusions of these two previous projects emphasizing residual strength assessment of damaged marine structures due to normal operating loads.

1.2 Objectives

The primary objectives of this project are as follows:

1. Introduce the subject of residual strength assessment of damaged marine structures.

2. Summarize the state of the art technology and methods available in the marine and non-marine industry for quantifying residual strength.

3. Recommend future work to integrate current engineering procedures in the areas of crack growth, permanent deformation and global ultimate strength to assess residual strength of damaged marine structures.

Because of the implicit relationship between residual strength and inspection procedures, a secondary objective of this report is to present an outline for a practical analytical procedure to react to detected cracks.

1.3 Approach

To accomplish the objectives of the project, the following approach was undertaken:

Task 1 - Literature Review:

A literature review was conducted to benchmark the state of the art in residual strength assessment. Technical papers from both the marine and non-marine industries were reviewed to identify the key elements that form the basis for residual strength analysis.

Task 2 - Collection and Evaluation of Marine Structure Damage Data:

Various databases and hull survey records maintained by regulatory bodies, classification societies and owners were studied to identify characteristic forms of damage, extent and shipboard locations. Interviews with owners and inspectors were held, to get practical information on criteria followed during inspection and reaction to damages.

Task 3 - Evaluation of Various Methods for Assessing Residual Strength:

Current methods used by the marine and non-marine industries, to assess residual strength which are consistent with the forms of damage identified in Task 2, were reviewed and representative case studies were summarized. Both indirect and direct methods were reviewed. In the indirect method, analysis is carried out at the local component level (cracks and ductile damage) and based on

damage extent assumptions integrated upward to the global system level (ultimate collapse) using service life experience, approximate closed form solutions, industry recognized guidelines and two dimensional ultimate strength analysis. In the direct method, analysis is carried out using three dimensional non-linear finite element methods.

Task 4 - Residual Strength Analysis of a Typical Tanker:

The Residual Strength of a typical single skin tanker is assessed using the indirect method. Fracture assessment is based on procedures outlined in British Standard Institute's published document, PD 6493: 1991 entitled "Guidance on Methods For Assessing the Acceptability of Flaws in Fusion Welded Structures" [4.16]*. Ultimate strength is evaluated using an ultimate strength analysis program, ULTSTR [4.1], developed by the U.S. Navy.

Task 5 - Conclusions and Recommendations for Future Work:

Based on the review of current industry practice, conclusions regarding limitations and key assumptions are made. Recommendations for future research efforts are presented.

* [ ] Reference at the end of section 4.0.

2.0 COLLECTION AND EVALUATION OF MARINE STRUCTURE DAMAGE DATA

The purpose of this section is to identify characteristic forms of damage, categorize forms of damage as either local or global, and determine damage locations. This information is of importance to this project because the engineering methods and analytical procedures investigated to assess the residual strength of damaged structures must be consistent with the form of damage observed. The data collection process involved literature reviews, interviews with ship owners and operators and searches of available databases. Collection of enough relevant data to be able to confidently correlate damage type and location with inspection histories was very difficult. The majority of the ship owners and operators would not release or disclose damage records of their fleet. As a result of the limited available data, only broad trends could be cautiously established that correlate ship types with damage forms, and locations.

The impact that damage has on the overall residual strength of the structure is a function of its (i) extent, (ii) mode of failure and (iii) relative shipboard location. While isolated small cracks, also known as "nuisance" cracks, at the toe of a bracket or at a cutout for a longitudinal will hardly affect the overall strength of the structure, a crack of considerable length on the main deck or side shell can seriously affect the structure's residual strength. The mode of failure also influences the remaining residual stiffness of the structure. A structure under ductile failure, like buckling, usually possesses post-buckled strength which allows it to continue to carry load after damage. Conversely, a structure with brittle failure hardly possesses any reserve strength and the failure can lead to total collapse of the structure. Various modes of failure are shown in table 2-1. The relative shipboard location of damage also affects the structure's residual strength. For example, damage in the middle cargo block can lead to greater loss of residual strength than those at the ends due to the high bending moments in the middle cargo block.

2.1 Collection of Data

The form of damage and its effect on residual strength assessment are the result of various factors and their interaction. In an effort to correlate these factors and identify trends, without going into any rigorous statistical evaluation, a task was undertaken to gather as much information as possible on damage to marine structures. Primary sources of damage information were the in-house casualty report database called CASMAIN maintained by the U.S. Coast Guard Marine Investigation Division, G-MMI, and other hull survey reports prepared by various tanker owners, which included reports on surveys required by the Critical Area Inspection Plans (CAIP). The ship casualty reports in the USCG

TABLE 2-1 TYPES OF FAILURE IN MARINE STRUCTURES

TYPE OF FAILURE		EXTENT	RELEVANT PROPERTIES	POSSIBLE LOCATIONS	REMARKS
Yielding		Local	σ_y	At discontinuities, joints, etc. In plating under pressure. Near concentrated loads.	May not be damaging unless it occurs repeatedly.
		Global	σ_y	In structures under axial tension; beams or grillages under lateral load.	Resulting gross distortions cannot be accepted at loads below collapse load. Energy absorption will depend on ductility also.
Buckling		Local	E, σ_y	In thin plating between stiffeners; deep webs in shear or compression. Pillars.	Elastic local buckling may not be damaging unless it overloads the remaining structure.
		Global	E, σ_y	In stiffened panels in compression or shear.	Will generally involve yielding, hence unacceptable permanent distortions. Final collapse strength may also depend on ductility.
Fracture	Ductile	Local	U.T.S.		Unlikely in view of high strains required.
		Global	U.T.S.		Unacceptable. Design will be governed by general yielding load; but safety depends on U.T.S.
	Brittle	Local	Toughness and Impact Properties	At discontinuities; or where ductility is reduced by triaxial stresses, or metallurgical damage.	Undesirable, though not serious if propagation prevented by fail-safe devices and remaining material is sufficiently tough.
		Global			Unacceptable, but hardly calculable. Good material properties, detail design and workmanship must be ensured.
	Fatigue	Local	Endurance at low or high cycles	At stress concentrations, joints, etc.	Undesirable, but not serious if material prevents development of brittle crack. Generally unacceptable in longitudinal material.
		Global			No known cases. Preventive action should be possible before crack propagates generally.

σ_y = Yield Strength
E = Young's Modulus in Tension
U.T.S. = Ultimate Tensile Strength

CASMAIN database were in a standardized format. The content varied depending on the inspector making the report. In most of the cases the cause of damage was identified based on experience and precedents. Classification societies require hull surveys to be conducted at regular intervals. The hull survey reports obtained from some oil tanker owners/operators were very professionally documented. They contained the symptoms of the damages that were observed during the hull surveys without any reference to the causes. A lot of relevant information was available from the Critical Area Inspection Plans prepared by the Trans Alaska Pipeline Service (TAPS) tanker operators. CAIP's were instituted by the USCG through their Navigation and Vessel Inspection Circular (NVIC) No. 15-91 as a management tool that serves to track the historical performance of a vessel, identify problem areas, and provide greater focus to periodic structural examinations. The CAIP's obtained from the TAPS tanker operators were usually for different classes of ships based on their sizes. Within each class all the ships were more or less similar with respect to their structural configuration. This similarity was reflected in the damage patterns of the ships which closely resembled each other. But at the same time there were some instances of damage which were unique to each ship. Since these CAIP's are primarily the responsibility of the owners and operators, most of the damages mentioned are well researched and have been rationally analyzed.

From these sources, 41 instances of damage were chosen which had complete description of the damage in terms of location, cause, mode of failure, extent of the damage, etc. and were felt to be of relevance to the project.

For brevity and ease of identification of trends, the information on these instances of damages was put in the form of a matrix in table 2-2, which is described below.

2.2 Summary of Casualty Data

The matrix in table 2-2, is divided into two parts. The first four columns give a description of the vessel and the last seven give a concise description of the damage. Under description of the vessel the first column indicates the type of vessel and its age in years when the damage occurred. The column titled "Route" gives an indication of the specific body of water in which the ship primarily operates. This gives an indication of the sea conditions that the vessel encounters during its usual operation. The next column gives the physical dimensions of the vessel in terms of its length, breadth and depth. The fourth column gives the displacement of the vessel. In cases where displacements are not available, the deadweight of the vessel is provided, indicated by a "(1)" next to the figure. The last two columns give a feel for the size of the vessel and fineness of the hull form. Under a particular type of vessel, the cases have been presented in an ascending order of displacement/deadweight.

The description of damage consists of the cause of damage, location (structural component as well as relative shipboard location), category of failure and miscellaneous comments. In some cases, the cause of damage was determined analytically and/or by laboratory testing of the damaged samples during post-damage analysis conducted by the classification societies or the owners/operators. In other cases, the cause was determined from practical experience and judgment. In some cases the damage extends through a number of structural components, for example the main deck plating, the deck longitudinals, the side shell plating and shell longitudinals. In such cases all the structural components are mentioned irrespective of the origin of damage. The relative shipboard location of the damage was broadly identified in terms of its longitudinal, transverse and vertical location. Longitudinally each vessel was divided into forward, cargo block and aft portions. The cargo block has been further divided into forward, middle and aft regions. The vessel has been divided into three regions transversely, two outboard regions at the port and starboard side and the region around the centerplane. No broad divisions have been made vertically, however vertical locations have been identified as the main deck level, base level, waterline region, turn of bilge, etc. The extent of damage, wherever available, was provided in parenthesis in one of the three columns giving its relative location depending on the orientation of the crack or fracture. For example, a 10′ long crack at the side shell running vertically is mentioned as (10′) under the column titled "vertical."

In the last column, titled "comments", the damage was categorized according to the classification method provided in the U.S. Coast Guard NVIC 15-91, which describes three classes of structural failures according to the size and the location of the fracture. These are:

Class 1 Structural Failure

1. A fracture of the oil/watertight envelope that is visible and of any length or a buckle that has either initiated in or has propagated into the oil/watertight envelope of the vessel; or

2. A fracture 10 feet or longer in length that has either initiated in or propagated into an internal strength member.

TABLE 2-2 MATRIX OF CASUALTY DATA

	DESCRIPTION OF THE VESSEL				SUMMARY OF DAMAGE							
	TYPE (AGE)*	ROUTE	LxBxD (m)	DISPL (TONS)	CAUSES	LOCATION				FAILURE TYPE	COMMENTS
						STRUCTURAL COMPONENT	LONGL. (Extent, cm)	TRANSV. (Extent, cm)	VERTICAL (Extent, cm)		
1	Bulk Carrier (31)	Grt. Lakes	213x21x11	30,054	High Stress Poor Fabrication Notches	Spar Deck Side Shell Longl. Longl. Bulkhead	Amidship	Starboard (Outbrd 1/3rd)	Top Deck	Brittle Fracture	Class 1 Cracks Occurred Where a New Midbody Was Added
2	Bulk Carrier	NA	NA	NA	Stress Conc. Due to High Constraint. Existence of Fatigue Fracture	Main Deck Side Shell	Between Fr. 78 & Fr. 79	40m from Side Shell (P) (370)	Top Deck	Mixed Fracture Fatigue + Brittle	Class 1 Cracks Arrested By Redundant Structure (Hatch Coaming)
3	Bulk Carrier (32)	Grt. Lakes	217x23x12	NA	Weld Flaw Excess. Slamming and Whipping	Main Deck Main Deck Longl. Tunnel Side Bhd. Stbd. Side Stringer Plt.	Midship	Starboard (Outbrd 1/3rd) (381)	Top Deck	Brittle Fracture	Class 1 Cracks Arrest. By Riveted Seam Construction
4	Bulk Carrier (14)	Pacific	247x41x24	115,721 (1)	Heavy Corrosion Loss of Stiffness Heavy Seas	Side Shell and Associated Hold Frames	Midship (640 Long & 396 Wide Side Shell Opening [P]) (130 Crack on [S] Side Shell Plate)	(P&S)	Top Side Tank Bottom	Corrosion Fatigue Crack Large Deflection Buckling	Class 1 Wastage of Cargo Hold and Wing Ballast Tank Structure
5	Bulk Carrier (10)	Great Lakes	277xNAxNA	NA	Stress Conc.	Side Shell Plating	Midship	Port	Just Above Turn of Bilge (~5")	Brittle Fracture	Class 1 Origin of Fracture at a Hard Spot Fracture Does Not Enter Bilge Radius
6	Containership (10)	N. Pacific	175x25x15	16,796 (1)	Severe Bow Slam Fabrication Flaw	Side Shell (Bow Flare)	Forward (671)	Side Shell (S)	Abv. Waterline (335)	Fatigue Crack Brittle Fracture Severe Buckling	Class 1 Fractured at a Site of Previous Cracking
7	Containership (20)	N. Atlantic	201x23x14	26,942	Faulty Design Poor Welding Notches	Bottom Shell Plating	(Throughout Primary Structure)			Corrosion Fatigue Crack Brittle Fracture	Class 1 Converted from General Ship after 17 Years
8	Containership (2)	N. Pacific	247x32x20	29,963 (1)	High Torsional Stress Faulty Structural Detail. Stress Conc.	Transverse Bhd.	Forward	Hatch Corner (P)	Main Deck Lvl. (~61)	Fatigue Fracture	Class 2
9	Containership (1)	N. Atlantic	288x32x20	50,315	Heavy Seas Insufficient Torsional Stiffness	Main Deck Hatch Corner	Forward	Port & Stbd. (61)	Top Deck	Fatigue Fracture	Class 1 Type of Steel Used was Good to Prevent Brittle Fracture but not Fatigue Fracture
10	Tank Barge (1)	Docked	178x27x14	15,579 (1)	Faulty Detail Design High Local Stress Residual Stress Notch	King Post Base	Midship	Ship Broke in Two		Brittle Fracture	Tress on Upper Deck 2.5 Times Allowable. No Provision for Crack Arrest
11	Tanker (32)	NA	175x21x12	Less than 20,000	Weld Flaw	Main Deck	Between Fr. 62 - Trns Bhd	Middle 1/3rd (597)	Top Deck	Brittle Fracture	Class 1 Fracture Originated at a Repair Weld

Age, when damage was discovered.

TABLE 2-2 MATRIX OF CASUALTY DATA (Continued)

	DESCRIPTION OF THE VESSEL				SUMMARY OF DAMAGE							
	TYPE (AGE)	ROUTE	LxBxD (m)	DISPL (TONS)	CAUSES	LOCATION				FAILURE TYPE	COMMENTS
						STRUCTURAL COMPONENT	LONGL. (Extent, cm)	TRANSV. (Extent, cm)	VERTICAL (Extent, cm)		
12	Tanker (6)	N. Atlantic	183x27x14	31,400 (1)	Poor Weld Fatigue Structural Overload	Bilge Keel Flat Bar	Midship	Ship Broke In Two		Fatigue Fracture (Local) Brittle Fracture	From Stress Analysis Done Later Stress Values Found Very High. Almost Near Allowable.
13	Tanker (4)	Alaskan	247x32x17	70,000 (1)	Improper Fabrication Wrong Steel Type Stress Conc.	Bottom Bleeder Plug Insert	Midship	Wing Tank (S)	Bottom Shell	Fatigue Fracture	Class 1 Insert Plate Thickness at the Drainage Groove Less Than Reqd. Groove In Athwart Direction.
14	Tanker (18)	TAPS	247x32x17	70,200 (1)	Heavy Weather High Stress	Top of CVK Web	Throughout the Cargo Block	Centerline	1/3rd Depth Above Baseline (2.5-15)	Fatigue Fracture	Class 2
15	Tanker (18)	TAPS	247x32x17	70,200 (1)	Heavy Weather High Stress	Side Shell Longl. (Flange & Web)	Aft Half of Cargo Block	Starboard	1/3rd Depth Below Main Deck (2.5-20)	Fatigue Fracture	Class 2
16	Tanker (18)	TAPS	247x32x17	70,200 (1)	Heavy Weather High Stress	Longitudinal BHD Longl. (Flange & Web)	Aft Half of Cargo Block	Starboard Wing Tank	1/3rd Depth Below Main Deck (2.5-20)	Fatigue Fracture	Class 2
17	Tanker (21)	TAPS	247x38x17	75,000 (1)	High Stresses Heavy Weather	Vertical Girder Abv. CVK	Midship (122 & 213)	Center Cargo Tank	Base Lvl.	Fatigue Fracture	Class 2 Temporary Repair Using Stopper Holes. Damage to be Monitored.
18	Tanker (19, 20, 21)	TAPS	247x38x17	75,000 (1)	Stress Conc.	Bottom Transverse and Connection to Longitudinal BHD	Throughout the Cargo Block (<30)			Fatigue Fracture	Class 2
19	Tanker (21)	TAPS	247x38x17	75,000 (1)	Stress Conc.	Lap Weld Joints in Transverse Web Frame	Throughout the Cargo Block (30-91)			Fatigue Fracture	Class 2 Stress Concentration Due to Unsymmetrical Nature of Lap Weld Joints
20	Tanker (20)	TAPS	247x38x17	75,000 (1)	Panting Stress Due to One-Sided Load & Fluctuating Pressure	Longitudinal O.T. BHD Between Center Cargo & Wing Ballast Tank	Midship (366)	Stbd.	1/3rd Depth Above Baseline	Fatigue Fracture	Class 1 Severe Weather Condition
21	Tanker (10)	NA	249x39x19	100,000 (1)	Excessive Flexure of Side Shell Longl.	Side Shell	Midship	Port	Bel. Waterline	Brittle Fracture + Shear Fracture	Class 1 Weld Failure Between Transverse Web Stiffener & Side Shell Longl.
							(1646 Long & 488 Deep Side Shell Plate Came Off)				

TABLE 2-2 MATRIX OF CASUALTY DATA (Continued)

	DESCRIPTION OF THE VESSEL				SUMMARY OF DAMAGE						
	TYPE (AGE)	ROUTE	LxBxD (m)	DISPL (TONS)	CAUSES	LOCATION				FAILURE TYPE	COMMENTS
						STRUCTURAL COMPONENT	LONGL. (Extent, cm)	TRANSV. (Extent, cm)	VERTICAL (Extent, cm)		
22	Tanker (9)	TAPS	265x41x22	123,000(1)	Local Residual Stress	Weld Seam of Longitudinal BHD Main Deck	Midship	Centerline	Main Deck Lvl (Thru Thickness)	Fatigue Fracture + Brittle Fracture	Class 1 Origin of Fracture 183 cm Below Main Deck in the Weld Seam of Longitudinal BHD
23	Tanker	TAPS	265x41x22	123,000(1)	Propulsion Vibration	Transverse BHD Horizontal Stringers	Aft of the Ship	Port & Stbd.		Fatigue Fracture	Class 2 Stringers are on Aft BHD of the Ballast Tank Between Engine Room & Aft Peak Tank
24	Tanker (2, 11)	TAPS	276x53x23	149,900(1)	Poor Detail Design High Local Stress	Side Shell Plating at the Terminal of the Bilge Keel	Midship	Port & Stbd.	Bilge (76 & 15)	Brittle Fracture	Class 1 Modification Done to Bilge Keel Detail After 2 Years of Service, Quite Successful
25	Tanker (3 - 12)	TAPS	276x53x23	149,900(1)	Poor Detail Design High Local Stress	Side Shell Longl. in Way of Connection to Transverse Web Frame	Midship	Port & Stbd.	Bet. LWL & Bilge	Fatigue Fracture	Class 2 Despite Modification Problem Still Exists. Propagation Slow.
26	Tanker (7 - 11)	TAPS	268x53x23	149,900(1)	Poor Detail Design High Local Stress Fabrication Defects	Upper Deck Longl. Deck Plating	Midship	Wing Tk. (P&S)	Main Deck Lvl	Brittle Fracture	Class 1 Since Last Modification No Further Damage
27	Tanker (12)	TAPS	276x53x23	149,900(1)	High Stresses Heavy Weather	Center Vertical Keel (CVK)	Midship (61)	Center Cargo Tk.	Base Level	Fatigue Fracture	Class 2
28	Tanker (12)	TAPS	276x53x23	149,900(1)	Stress Concentration From Weld Defects	Bottom Shell Plating in Way of Limber Hole in Bottom Longitudinal	Forward	Port	Base Level (Thru Thkns)	Fatigue Crack	Class 1
29	Tanker	TAPS	268x54x20	155,000(1)	Poor Detail Design Stress Concentration Heavy Weather	Bottom Plate Longl. Connecting Bracket	Midship	Centerline	Base Level (2.5 - 15)	Fatigue Fracture	Class 2 Cracks Occurred in 2 Cargo Tanks in Both of Them Near the Aft Transverse BHD
30	Tanker	TAPS	268x54x20	155,000(1)	Poor Detail Design Stress Concentration Heavy Weather	Bottom Plate Longl. Connecting Bracket	Aft of the Cargo Block	Middle 1/3rd (2.5 - 20)	Base Level (2.5 - 56)	Fatigue Fracture	Class 2 Cracks Occurred Along the Whole Breadth of #4 Center Tank
31	Tanker	TAPS	268x54x20	155,000(1)	Poor Detail Design Stress Concentration Heavy Weather	Bracket Connecting Side Shell Longl. To Transverse Frame	Midship	Port & Stbd. (~13)	Base Level	Fatigue Fracture	Class 2 Cracks Occurred in Ballast Tank

TABLE 2-2 MATRIX OF CASUALTY DATA (Continued)

	DESCRIPTION OF THE VESSEL				SUMMARY OF DAMAGE						
	TYPE (AGE)	ROUTE	LxBxD (m)	DISPL (TONS)	CAUSES	LOCATION				FAILURE TYPE	COMMENTS
						STRUCTURAL COMPONENT	LONGL. (Extent, cm)	TRANSV. (Extent, cm)	VERTICAL (Extent, cm)		
32	Tanker	TAPS	268x54x20	155,000(1)	Poor Detail Design Stress Concentration Heavy Weather	CVK Bracket	Midship	Centerline	Base Level	Fatigue Fracture	Class 2
33	Tanker (7)	TAPS	276x53x23	170,000(1)	Stress Concentration from Construction Detail	Transverse BHD	Aft	Stbd. S. B. Tk.	~945 Abv. B.L. (41)	Fatigue Crack	Class 2 Fracture Occurred in Heat Affected Zone of Weld
34	Tanker (7)	TAPS	276x53x23	173,000(1)	Notch	Upper Deck Longl. Main Deck	Aft	Middle 1/3rd (91 to 823)	Top Deck	Fatigue Fracture Brittle Fracture	Class 1 Fatigue Crack Reached a Critical Length Which Initiated Brittle Fracture
35	Tanker (12)	TAPS	276x53x23	173,400(1)	Heavy Weather High Stress	Side Shell Longitudinal	Midship	Port (2 x 46)	Just Above Turn on Bilge	Fatigue Fracture	Class 2 Crack Did Not Reach Side Shell. Stopped at Pre-Existing Stopper Hole.
36	Tanker (12)	TAPS	276x53x23	173,400(1)	Heavy Weather High Stress	Side Shell Longitudinal (Flange & Web)	Midship	Port (46)	Just Above Turn on Bilge (30)	Fatigue Fracture	Class 2 Web Crack Arrested at Pre-Existing Stopper Hole; Longl. Almost Broke Apart at the Damage.
37	Tanker (12)	TAPS	276x53x23	173,400(1)	Heavy Weather High Stress	Side Shell Longitudinal	Midship	Starboard (5 - 46)	Near WL	Fatigue Fracture	Class 2 These Cracks Not Found During Inspection Held 14 Months Before the One in Which They Were Found
38	Tanker (5)	Atlantic	348x52x20	250,000(1)	Heavy Seas Poor Weld Job	Side Shell Main Deck Longl. (SS + Mndk)	Midship	Stbd. S. Shell (52)	Main Deck Level (1646)	Brittle Fracture	Class 1 Loss of Side Shell Longl. Due to Locked in Stresses
39	VLCC/ULCC (5 - 13)	NA	NA	250,000(1) & abv	Poor Detail Design Fatigue Stress Conc.	S. Shell Longl. in Way of Connection to Transverse Web Frame	Throughout the Cargo Block	Mostly Port Side	LWL	Fatigue Fracture	Class 2
40	VLCC/ULCC (5 - 13)	NA	NA	250,000(1) & abv	Poor Detail Design	Web Frame Flat Bar Stiffener at Connection to Side Shell Longl.	Throughout the Cargo Block	Mostly Port Side	LWL	Fatigue Fracture	Class 2
41	VLCC/ULCC (5 - 13)	NA	NA	250,000(1) & abv	Poor Detail Design	Side Shell Plating at Weld of Web Frame	Throughout the Cargo Block	Mostly Port Side	LWL	Fatigue Fracture	Class 1

Class 2 Structural Failure

A fracture less than 10 feet in length or a buckle that has either initiated in or propagated into an internal strength member during normal operating conditions.

Class 3 Structural Failure

A fracture or buckle that occurs under normal operating conditions that does not otherwise meet the definition of either a Class 1 or Class 2 structural failure.

Definitions of some of the terms used above are:

(1) oil/watertight envelope: the strength deck, side shell and bottom plating of a vessel, including the bow and stern rakes of barges.

(2) internal strength members: the center vertical keel; deep web frames and girders; transverse bulkheads and girders; side, bottom and underdeck longitudinals; longitudinal bulkheads; and bilge keels.

(3) buckle: any deformation in the oil/watertight envelope whereby the adjoining internal structural members are also bent to such an extent that structural strength has been lost.

In addition to identifying the class of damage, additional information regarding the cause of damage, history of the vessel, cause of crack arrest, etc. has been provided where available.

2.3 Discussion of Findings

Some broad trends and characteristics have been observed from the damage instances presented in table 2-2. Based on the data in table 2-2, various correlations between forms of damage, extent, location and their interaction were attempted. Since the form of failure is usually determined based on visual inspections and other circumstantial evidence, the accuracy depends on the experience of the inspector. Therefore for the purpose of this report all types of fractures, whether fatigue or brittle, are classified as cracks. The following observations based on review of the available data are made:

1. Table 2-3 shows the correlation between distribution of damage among the various structural components and ship type. Horizontally the table is divided into three, corresponding to the three broad classes of structural components, namely; primary longitudinal, primary transverse and secondary. Each of the three classes contains the components listed in the

table below:

LETTER CODES USED FOR THE STRUCTURAL COMPONENTS

STRUCTURAL COMPONENT	CODE
Side Shell Longitudinal	SL
Bottom Longitudinal	BL
Deck Longitudinal	DL
Main Deck	MD
Side Shell	SS
Bottom Plate	BP
'Tween Deck	TD
Longitudinal Bulkhead	LB
Longitudinal Girder	LG
Transverse Bulkhead	TB
Web Frame	WF
Horizontal Girder	HG
Brackets	BK
Flat Bar Stiffeners	FB
Others (Double Plates, etc.)	OT

Two statistics for each structural component are presented. The first one is the fraction of the total damage in a particular class that is due to that component, and the second one is the fraction of the overall damage for the particular ship type. For example, the number of damage incidences occurring in side shell longitudinals of tankers is 30% of the number of damage incidences in primary longitudinal members and 16% of the total number of damage incidences in tankers. These two numbers give a feel for the relative significance of the component locally in its class and overall in terms of the number of damage incidences it suffers. According to the present classification of the structural components, the table indicates that for all three ship types, the primary longitudinal components suffer the most number of damages; 53% for tankers, 54% for bulk carriers and 83% for containerships.

Tankers: Overall, the side shell longitudinal (16%) and secondary connecting structures, bracket (13%) and flat bar stiffeners (10%) are the components most often damaged. Among primary longitudinal members, the side shell longitudinals are most often damaged (30%), followed by the main deck plating and associated longitudinal (33%). Among primary transverse members the web frames (55%), due to the presence of lap joints, are the most affected. Among secondary connecting structures, brackets (50%) account for the most number of

damage incidences. Another trend to be noted is a comparison of the ratios of side shell longitudinal to side shell (30/17) damage and deck longitudinal to deck plate (13/20) damage. The former ratio is much higher. This is because cracks originating at the side shell longitudinal are usually repaired before they reach the side shell, whereas cracks originating on the main deck plating are not repaired as quickly and therefore propagate along the deck, cracking any deck longitudinal they encounter.

Bulk Carrier: Overall side shell plating suffers the most (30%), followed closely by web frames and connecting brackets (23% each). This follows closely the reasoning put forward in observation number 1, that the main cause of damage is side shell flexing.

Containerships: Most often damaged components are the main deck (33%) and side shell plating (33%). The present survey does not show any damage to secondary structure, which implies that for containerships, damage to secondary structure is negligible.

2. Location of damage plays a critical role in the residual strength assessment of damaged structure. The overall structural response to damage is affected by the location and extent of damage. Table 2-4 indicates that for tankers and bulk carriers most of the longitudinal damage occur in the middle cargo block, whereas for containerships the forward section is affected more. Transversely, in case of tankers, damage incidences are evenly distributed among the port, starboard and the centerplane areas, whereas in the case of bulk carriers and containerships, damage occur mostly at the sides. Vertically, except for bulk carriers which hardly show any damage at the bottom, tankers and containerships show an even distribution of damage at all three levels. Bulk carriers show a greater amount of damage at the main deck (62%) because, in addition to the damage that occurs solely on the main deck, much of the damage that occurs at the middle third depth of the side shell (38%) extends to the main deck level also.

3. The predominant form of local failure among all ship types is fracture, as indicated in table 2-5 and in [1, 2]*. Over the years extensive research into failure due to buckling under compressive loads has resulted in local structure which is fairly resistive to buckling. The few instances of buckling that are observed are due mainly to the reduction of scantlings due to corrosion [3, 4, 5] or excessive warping of the cross decks, on wide-hatched ships like bulk carriers and containerships, due to hull girder torsion [6].

* [ ] Reference at end of section.

TABLE 2-3 PERCENTAGE OF TOTAL FAILURE BY STRUCTURAL COMPONENT AND SHIP TYPE

SHIP TYPE		TANKER(%)		BULK CARRIER(%)		CONTAINER(%)	
STRUCTURAL COMPONENT		(A)	(B)	(A)	(B)	(A)	(B)
PRIMARY (LONGITUDINAL)	SL	30	16	11	6	-	-
	BL	7	4	-	-	-	-
	DL	13	7	6	3	-	-
	MD	20	11	11	6	4	33
	SS	17	9	55	30	4	33
	BP	3	2	-	-	2	17
	LB	7	3	11	6	-	-
	LG	3	2	-	-	-	-
	TD	-	-	6	3	-	-
TOTAL		100	53	100	54	100	83
PRIMARY (TRANSVERSE)	TB	27	5	-	-	100	17
	WF	55	11	100	23	-	-
	HG	18	4	-	-	-	-
TOTAL		100	20	100	23	100	17
SECONDARY	BL	50	13	100	23	-	-
	FB	36	10	-	-	-	-
	OT	14	4	-	-	-	-
TOTAL		100	27	100	23	100	-
TOTAL		100		100		100	

A: Percentage of Failure by Category

B: Percentage of Total Failure

TABLE 2-4 PERCENTAGE OF FAILURE BY LOCATION AND SHIP TYPE

SHIP TYPE / **LOCATION**		TANKER(%)	BULK CARRIER(%)	CONTAINER(%)
LONGITUDINAL	FWD	2	-	62
	MID	82	100	38
	AFT	16	-	-
	TOTAL	100	100	100
TRANSVERSE	PORT	33	44	38
	CENTER	31	-	12
	STBD	36	56	50
	TOTAL	100	100	100
VERTICAL	TOP	31	62	38
	LWL	29	38	25
	KEEL	40	-	37
	TOTAL	100	100	100

TABLE 2-5 PERCENTAGE OF FAILURE BY FAILURE MODE AND SHIP TYPE

SHIP TYPE / **FAILURE MODE**	TANKER(%)	BULK CARRIER(%)	CONTAINER(%)
CRACKING	100	65	88
BUCKLING	0	35	12

2.4 Conclusions

The complex interaction that exists between the various forms of damage, their location and ship type, compounded by the amount of available data, makes it difficult to draw many definite conclusions. Therefore, the trends and patterns shown in the tables presented in their section are only qualitative and should not be taken in any absolute quantitative sense.

The significant conclusions that can be drawn from the data collected in this section of relevance to investigating methods to assess the residual strength of damaged marine structures are:

1. Fracture is the most dominant form of damage to ship structure. Fatigue cracks have no serious effects on ship's longitudinal strength if the crack length is less than the crack length which starts fast fracture (critical crack length) and the temperature is not extremely low.

2. Ductile failure in the form of permanent deformation is quite common in ship structure and excessive gross deformation can lead to fracture.

3. Extent of damage is localized to particular regions and individual components in ship structures and predominant damage locations are very much a function of ship type.

2.5 References

1. "Service Experience - Ships", Proceedings of the 10th International Ship and Offshore Structures Congress, Denmark, 1988.

2. Weber, P.F., "Structural Surveys of Oil Tankers", Trans 1 Mar E Vol. 96, Paper No. 65, 1984.

3. "Lessons Learned from Failures and Damage of Ships", Presented at the 8th International Ship Structures Congress, Gdansk, 1982.

4. Grove, T.W., Rynn, P.G. and Ashe, G.M., "Bulk Carriers, A Cause for Concern", ABS Report (Draft Copy).

5. "Study Report on Bulk Carrier Loss", January 1992, Nippon Kaiji Kyokai.

6. Hong, D.P., et al., "Analysis of Structural Damage of a Large Ore/Coal Carrier". SNAME, STAR Symposium, Spring Meeting, May 27-30, 1987.

3.0 ELEMENTS OF RESIDUAL STRENGTH ASSESSMENTS OF MARINE STRUCTURES

3.1 Introduction

Residual strength is defined as the capability of a structure to continue to carry load after damage. The ability to measure the structure's residual strength after damage and determine the structure's suitability for continuing service, requires an understanding of the interrelationship between the following four elements:

1) design philosophy of the existing structure

2) structural redundancy

3) types of damage

4) inspection practices

The ability of a structure to sustain damage, its residual strength, depends largely on the design philosophy (design strength and ultimate strength of intact structure) and the structural redundancy within the system. Engineering methods to assess the residual strength of damaged structures are dependent on the types of damage, locations of damage and operational profile. Damage to marine structures may occur at the local, or component level, and at the global, or system level. The damage may be small affecting only local components or very significant in which total strength is lost. Decisions to repair damage are a function of the engineering calculations required to assess the residual strength of the damaged structure and the existing inspection practices.

3.2 Design Philosophies

Safety and reliability are the primary goals of any design philosophy. Safety and reliability are measures of a structure's ability to resist loads in excess of the design load and to sustain damage without catastrophic collapse. Design philosophies which are employed and incorporated within structures subjected to cyclic loadings can comprise one or both of the following:

1. Safe life design philosophy.
2. Fail safe design philosophy.

Safe life design procedures are expressed in terms of operational life time, or number of load applications during which the probability of failure of the marine structure is likely to be extremely remote. This can be estimated early in the design stage from fatigue data already available or obtained from laboratory tests. The safe life approach, in its pure form, assumes that the structure would not incur any damage during its life. This raises

the objection that it makes no allowance for damage due to fabrication defects. Structure is designed such that crack propagation is only remotely possible, hence is often very conservative. At the end of the design life the structure is either scrapped or extensively reworked, as there is no consideration for periodic inspection and repair in the design philosophy.

Fail safe design philosophy established a forgiving nature of a structure to damage. It is used to describe a structure designed to withstand a certain degree of failure and still maintain sufficient strength and stiffness in the remaining part of the structure to permit continued use until the next inspection period. Fail safe design became common practice early in the development of commercial aircraft structure. It is based on the following premises:

(a) Existence of Flaws and Cracks - due to fabrication defects, day-to-day operations or faulty structural designs (specifically structural details).

(b) Existence of Damage Control Plan - which consists of:

(i) Structurally Robust Design - Robustness is derived from a combination of reserve strength (excess capacity of the components making up the total structure), redundancy (existence of alternative load paths in the structure to carry loading from damaged components) and ductility (ability to sustain large plastic strains without significant loss in strength).

(ii) Damage Analysis Capability - Primarily a Fracture Mechanics based approach which allows prediction of crack growth rate and residual strength given the initial crack length, the material characteristics and the stress field.

(iii) Inspection Program - The inspection program should be able to identify the smallest flaw. For efficient inspection, knowledge of critical locations should be available. This could be based on stress analysis, the designer's experience or previous records. The inspection interval is important and could be based on fracture mechanics. The whole success and reliability of fail safe design philosophy is based on the fact that cracks will be detected before they reach a critical length. The structure could be designed such that there could be a number of alternative load paths but if cracks are not detected during inspection, before they reach critical length, there could be a catastrophical failure.

Preferred Design Philosophy - Although the forgiving nature of the fail safe design philosophy makes it an attractive option, its full implementation in the marine world could be difficult. A critical aspect of fail safe philosophy is the detection of cracks and flaws. While this may be possible in the aircraft industry under controlled environment and easy accessibility, it is difficult in the marine industry due to the immense size of the structure and the harsh environment the surveys are accomplished in. Typically a modern VLCC or ULCC involves 100 to 200 acres of structural steel surface and 1,000 to 2,000 miles of welding. Therefore chances of cracks and flaws going unnoticed are quite high. Consequently, ship structural design is based on a combination of safe life and fail safe design principles and assessment of residual strength is based on fail safe principles.

3.3 Redundancy

Redundancy implies the ability of a structure to "sustain overload" or the existence of "alternative load path" in a structure. Hence redundancy can be expressed in two ways: (i) reserve strength and (ii) residual strength. Reserve strength is the margin between the demand imposed by the load and the ultimate capacity of the structure. It is due to the conservatism in the design of individual components and ultimately the ensemble of components making up the structure. Residual strength refers to the safety of the structure against failure after damage has occurred. If all the components that make up the system are not fully stressed under a given load, there is a potential for stress redistribution upon the failure of one or more components and prevention of complete failure of the structure. Various methods to measure redundancy for discrete and continuous structure are available [1-5][1] but none of them has been widely used. For the present study, deterministic measures of reserve strength and residual strength, as presented in [1] are used. In [1] reserve strength is defined in terms of Reserve Resistance Factor (REF) given by the ratio of the ultimate system strength to the design load.

$$REF = \frac{\text{Environmental Load At Collapse (Undamaged)}}{\text{Design Environmental Load}}$$

Residual strength is given in terms of Residual Resistance Factor (RIF) which is defined as the ratio of the residual system strength to the system collapse strength.

$$RIF = \frac{\text{Environmental Load At Collapse (Damaged)}}{\text{Environmental Load At Collapse (Undamaged)}}$$

[1]Numbers in [ ], refer to references at the end of the section.

Finding an appropriate probabilistic measure of redundancy is a more complex issue. One way to measure the ability of a structure to tolerate damage is by the conditional probability of system survival given that one of its members has failed. The redundancy measure has been used in several studies [4, 5].

$$P_r^* = 1 - \frac{P_f^{(s)}}{P_f^{(1)}}$$

where,

P^*_r is the measure of redundancy

$P_f^{(s)}$ is the probability of system failure

$P_f^{(1)}$ is the probability of failure of any one structural member

and $P_f^{(s)} \leq P_f^{(1)}$

In marine structures, the presence of numerous failure paths make it practically impossible to accurately determine the probabilistic measure of redundancy. Therefore to limit the number of failure paths, the approach adopted both in the deterministic and probabilistic methods, is to identify critical elements of the system whose failure leads to catastrophic consequences.

Various classifications of redundancy can be found in literature. Four of them are presented below. Lloyd [1] suggests a member redundancy hierarchy for indeterminate structures. The levels of this hierarchy vary from 0 to 5. Members belonging to level 0 are the least redundant while those at level 5 are the most redundant. Klingmuller [6], in the context of "systems" reliability, identified structures as having either "active" (hot) or "standby" redundancy. Active redundancy refers to components which are fully active in normal response and can be used to maintain stability after failure of a parallel component but otherwise are additional, unnecessary components. Standby redundancy refers to additional components which are not used in normal response performance but have to replace components that have failed. For continuous stiffened plate based structures, [7] suggests a three level hierarchy. An example for a multi-columned semi-submersible is as follows:

- "Tertiary" relating to individual stiffeners on a panel,
- "Secondary" relating to an individual stiffened panel, and
- "Primary" relating to an assemblage of stiffened panels forming a cylindrical column.

Depending on the structural configuration various levels of redundancies would be exhibited by a structure. For example, a multi-column semi-submersible with unstiffened columns exhibits only primary redundancy. A monohull will exhibit only secondary and tertiary redundancy while a SWATH ship with single or twin struts would exhibit primary, secondary, and tertiary redundancy. Stiansen [8] has classified redundancies into two categories, local and global. Local redundancy refers to local reserve strength which exists in individual members and joints. Global redundancy refers to the overall structure.

3.4 Types of Damage and Failure

As stated in section 2.0, to make an assessment of residual strength of damaged marine structure it is imperative to investigate the various types of damage and resulting forms of failure, both locally and globally.

The various types of damage include cracking, buckling, excessive deformation and yielding of the cross-section. Damage to local components can lead to either ductile or fracture failure. Globally the failure of a local component can have one of two general effects:

- the structure responds with a redistribution of internal forces depending on the form of local failure and the level of redundancy or

- the damage precipitates progressive failure which results in loss of overall stiffness and load carrying ability.

While local ductile failure involves gross deformation in the form of yielding or buckling and results in gradual redistribution of local internal forces, local fractures do not involve any significant deformation but result in rapid redistribution of local internal forces.

In an attempt to highlight the fundamental forms of damage and provide engineering solutions this report will concentrate on just ductile failure and fracture. Figure 3-1 shows a typical ductile failure of a structural component and compares that with a brittle failure scenario.

3.4.1 Ductile Failure:

Figure 3-2 shows the various categories of ductile failure. Ductile failure can involve elastic buckling, inelastic buckling, plastic collapse or an interaction of all three. Each of these failure modes, for simple components like beams and plates, has been widely discussed in readily available literature [9, 10]. Because of the consequences of gross deformation on ship structure, and the significance of permanent deformation [11], to repair

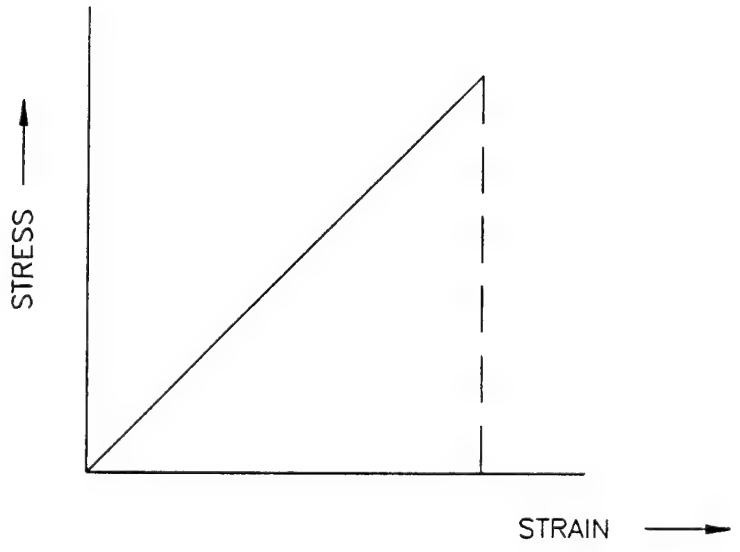

(A) – COMPLETE FAILURE, ' BRITTLE ' SYSTEM
– STRUCTURE EITHER CRACKED THROUGH OR COMPLETE FAILURE

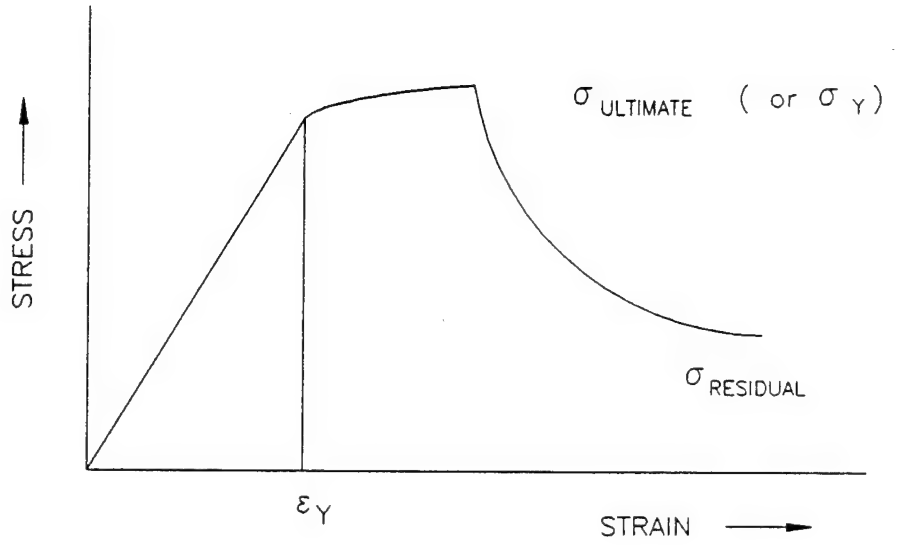

(B) – DUCTILE FAILURE
– FOLLOWING COLLAPSE IN COMPRESSION, RESIDUAL COMPRESSIVE STRENGTH

FIGURE 3.1 FAILURE OF BRITTLE AND DUCTILE SYSTEMS [7]

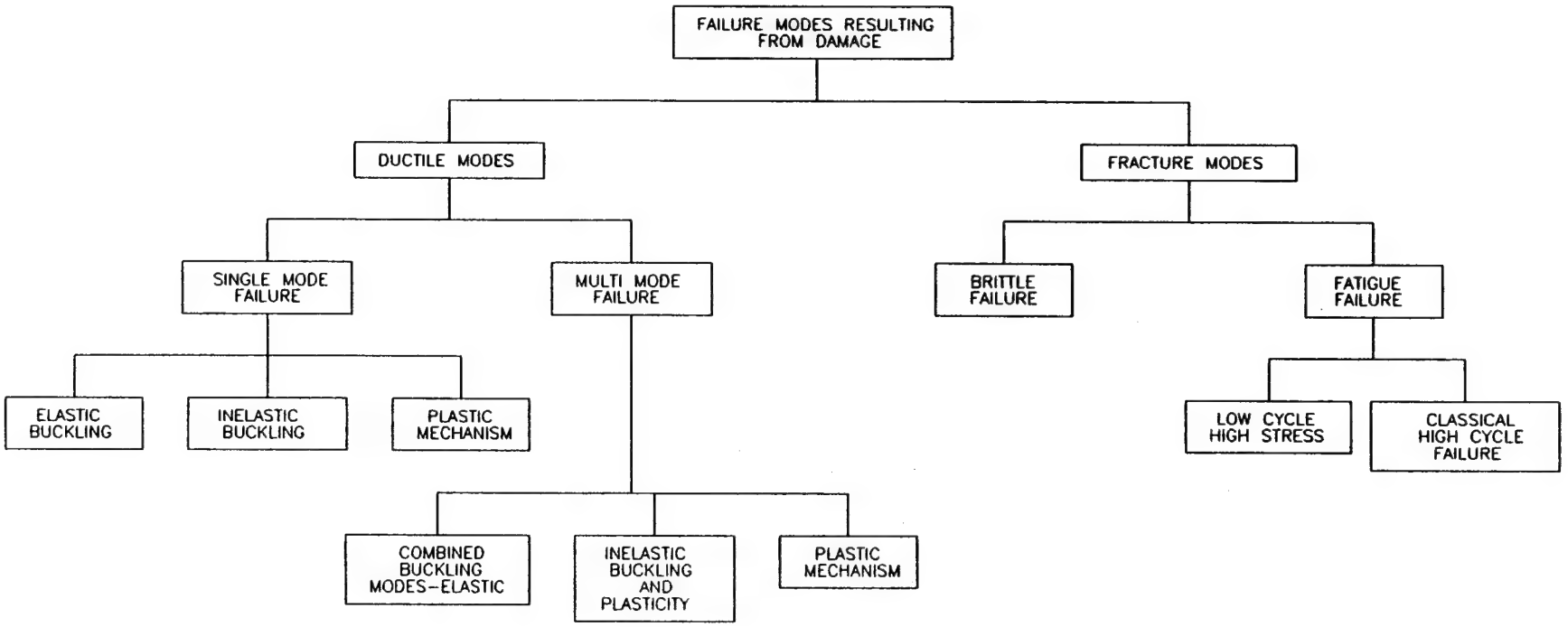

FIGURE 3.2 VARIOUS STRUCTURAL FAILURE MODES

decisions, this report will focus only on the ductile failure as a result of plastic collapse due to lateral loadings. The ship's hull structure is a complex combination of plating, longitudinal stiffeners and supporting frames. Plating together with stiffeners make up a stiffened panel. The stiffened panel together with the supporting frames compose a grillage structure. For a grillage structure subjected to lateral loads there are three basic levels of load and response:

1. The plating between the stiffeners deflects according to its stiffness and transfers the load to the stiffeners.

2. The stiffeners along with an effective width of plating act as beams to carry the load to the supporting frames.

3. The supporting frames yield and the grillage deflects transferring the load to the bulkheads and decks.

The basic modes of failure for a laterally loaded grillage structure are summarized in table 3-1.

TABLE 3-1 FAILURE MODES OF LATERALLY LOADED GRILLAGE

	Unserviceability	Ultimate Failure
plating	unacceptable amount of permanent set	rupture or large amount of permanent set
stiffeners	partial yield of stiffener flange or unacceptable amount of permanent set	collapse due to formation of plastic hinges
grillage	unacceptable permanent set	yield of supporting frames

In general, stiffened panels that fail in a ductile manner generally do so through a series of progressive stages:

- the onset of non-linear response, where the load carrying capability begins to increase at a rate which is less than the rate of strain or deflection.

- the development of a plateau, that is almost a constant load carrying capability regardless of deflection.

- a post ultimate strength load deflection curve, which will generally be dependent upon the type of component, and which will often show an unloading trend.

3.4.1.1 Strength of Damaged Structure Under Lateral Load

The predominant form of damage caused by collisions with piers and hydrodynamic impact is lateral plastic deformations (due to plastic collapse) of stiffened plate panels forming the shell or deck of a ship's hull structure. It is important to note that this form of damage is usually found in thin plated, strongly stiffened structure typical of combatant hull structural systems and gives a "hungry horse" appearance to the ship hull, whereby the plating deforms symmetrically between stiffeners. In general the permanent deformation of stiffened plate panels affects the residual strength characteristics of the stiffened plate panel.

Possible consequences of such permanent deformations are [12]:

- a reduction in stiffness and strength of the panels under subsequent lateral loads; but it has been generally found that such reductions are insignificant.

- a loss of local stiffness and strength under in-plane loads and subsequent reduction in ultimate hull girder bending strength.

Data on rectangular plates of aspect ratio (a/b) greater than 2 and slenderness ratio (b/t) less than 60, suggest that the longitudinal compressive strength is only slightly reduced when subjected to single lobe damage. The effect of lateral pressure [13] and therefore probability of damage deformation is more prominent in slender plates (b/t > 80).

Damage of the "hungry horse" type, is likely to induce more significant loss of stiffness and strength under in-plane load applied in the shorter or transverse direction, causing:

(a) a reduction of hull-girder bending strength in way of transversely framed bottom shell and deck structure, as commonly employed in the fore and aft regions of a ship's hull;

(b) loss of effective flexural stiffness in transverse frames where the shell plating acts as a flange to the frames, notably in double bottom structures.

As illustrated in figure 3-3 [12] the behavior of a long rectangular plate under transverse compression depends mainly on the relative form of initial deformation in the plate panel. Much greater loss of stiffness and strength occurs when the distortions are antisymmetric than when distortions are approximately symmetric, i.e. of the "hungry horse" form. In the case of symmetric distortion, initial deformations grow symmetrically until the buckling load is almost attained, at which point the panel snaps into an antisymmetric configuration. In the case of

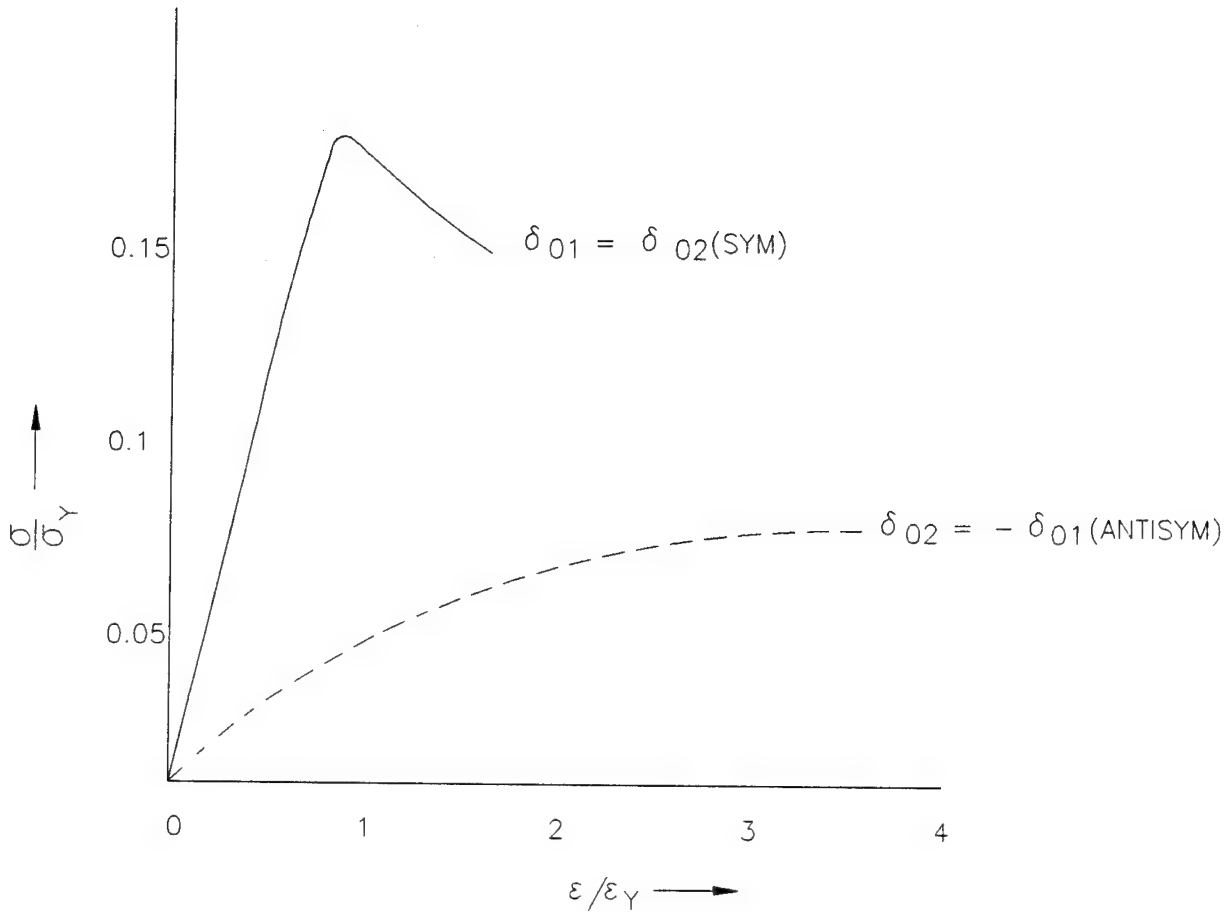

FIGURE 3.3 LOAD–SHORTENING CURVES FOR LONG, TRANSVERSELY–COMPRESSED PLATES WITH SYMMETRIC AND ANTISYMMETRIC DEFORMATIONS [12]

antisymmetric initial distortion, deformation remains antisymmetric throughout the load range and failure occurs gradually but with a much greater reduction of stiffness and strength. It is clear from these scenarios that correct evaluation of characteristic plate strength requires statistical assessment of both plate distortion amplitudes and the relative form of distortion in the panels.

Damage caused by hydrodynamic overload will tend to induce the symmetric, more favorable form of deformation. This effect has been approximately evaluated, for the case of a long steel plate (large a/b) by examining the behavior of a transverse strip of plating subjected to:

(a) application and removal of lateral pressure causing elasto-plastic deformation and associated residual stresses;

(b) transverse compression up to and beyond collapse.

Results of a study presented in reference [12] are summarized in figure 3-4 in the form of compressive load shortening curves for various ratios of b/t and levels of permanent deformation. It is evident that for slender plates in which the elastic buckling stress is substantially lower than the yield stress, damage may cause significant loss of stiffness but has little effect on peak load capability. Conversely, in stocky plates, which buckle elasto-plastically, damage will cause loss of both transverse stiffness and strength.

More general damage involving elasto-plastic bending of stiffeners may also result from lateral loads. A typical lateral load-displacement curve for a stiffened panel is shown in figure 3-5. The design load, indicated by point B, commonly corresponds to 0.80 of the load to cause first yield, indicated by point C. Deformation under a static or dynamic load is likely to correspond to a curve of form ABCDF. Where damage has not progressed beyond point F and where no marked evidence exists of local failure (i.e., local shear buckling of web, tripping of stiffener, tearing of welds), residual strength under subsequent lateral loads is likely to remain adequate. It is important to note that residual stiffness, as indicated by the slope DE, is also unlikely to differ significantly from the original stiffness. Provided that the damaged structure is not required to withstand large in plane compressive loads and that overriding hydrodynamic or aesthetic reasons do not exist for restoring the original geometry, repair may be unnecessary. If clear evidence exists of local failures and damage is judged to have progressed beyond point F, residual strength and stiffness are likely to be substantially reduced.

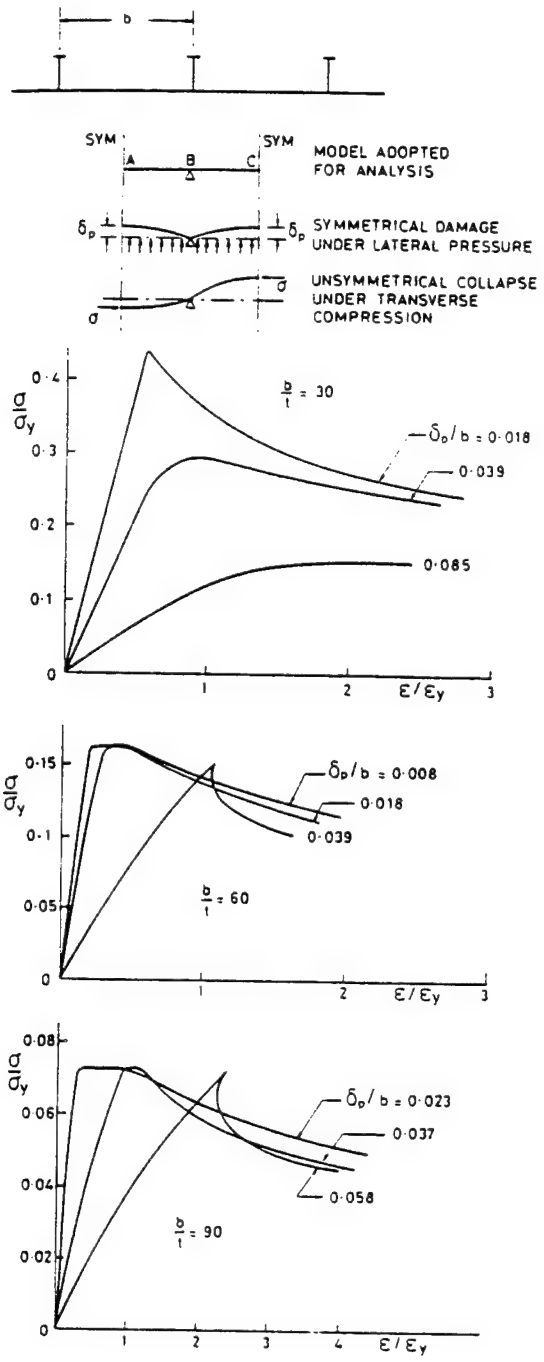

FIGURE 3-4 EFFECT OF SYMMETRIC DAMAGE ON STIFFNESS AND STRENGTH OF LONG PLATES UNDER TRANSVERSE COMPRESSION. (A) MODEL ADOPTED IN ANALYSIS. (B) LOAD-SHORTENING CURVES

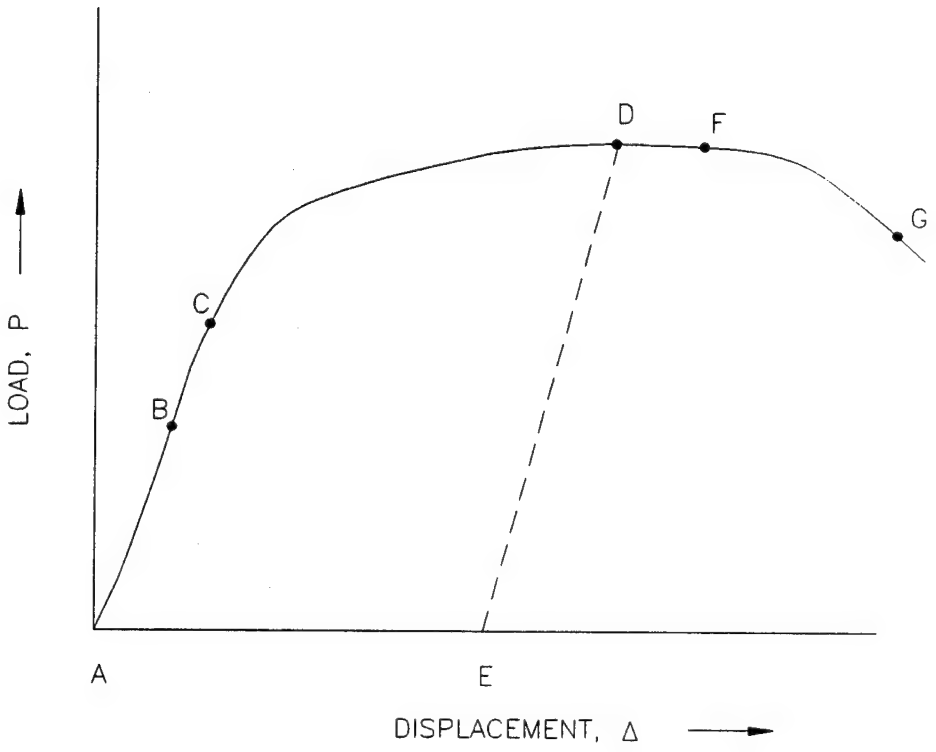

FIGURE 3.5 LATERAL LOAD–DISPLACEMENT RELATIONSHIP FOR STIFFENED PANEL [12]

3.4.1.2 Effect of Localized Imperfection

In addition to overall initial deflection, localized initial deflections are often observed in long rectangular plates on marine structures. The localized initial deflections also influence stiffness and strength of plates. The effect of localized imperfection is very similar to that of initial deflection due to welding. For long thin plates, with initial deflection under longitudinal compression, ultimate strength is reached after loss of stiffness due to large deflection, but for thicker plates it is by loss of strength due to spread of the localized plastic zone.

According to figure 3-6, from [14] the localized effect is not very sensitive to the shape of the dent. Isolated sinusoidal dents of moderate amplitude influence plate strength only slightly less than ripple distortions having the same amplitude and wave-length. A marginally greater loss of strength is caused by an isolated sinusoidal dent of length 0.8b than others. The location of an isolated dent slightly influences the loss of compressive strength of a long plate. The imperfection effect is marginally greater when the dent is located close to a plate end. Localized initial deformation causes less precollapse loss of plate stiffness and leads to failure at a lower compressive strain with more rapid postcollapse unloading than ripple distortion of the same amplitude. Addition of a localized imperfection of moderate amplitude to the overall distortion causes loss of strength.

3.4.2 Fracture Failure

Fracture failure is broken into two categories: fatigue cracking and brittle fracture. Fatigue cracks differ from brittle fractures by the following characteristics:

1. Life: While brittle fractures are instantaneous, given the right conditions, fatigue fractures take time to develop. Usually fatigue crack propagation consists of three stages namely, initiation, propagation and onset of unstable fracture.

2. Location: In most cases fatigue cracks originate at the surface whereas brittle fractures can initiate at subsurface defects where the triaxiality of stress is generally noticeably greater.

3. Causes: Fatigue cracking is initiated by repeated reversing loads at a region of stress concentration, while a combination of mechanical and metallurgical factors may affect the initiation of brittle fracture in three ways - (i) by supplying additional energy, (ii) by carrying local embrittlement of the material and (iii) by stress corrosion.

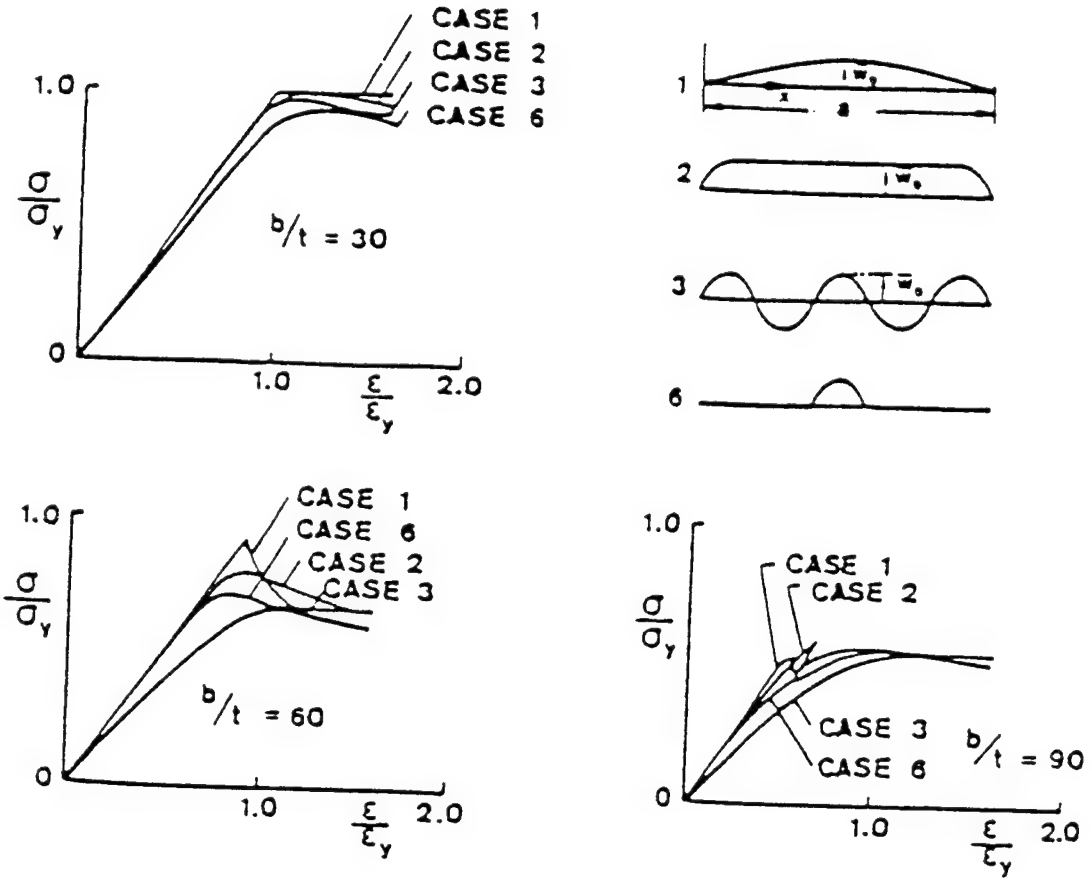

FIGURE 3-6 COMPARISON OF LOAD-END SHORTENING CURVE FOR LONG PLATES (a/b=4) WITH OVERALL, PERIODIC AND LOCALIZED DISTORTION

3.4.2.1 Fatigue Analysis

Traditionally, the fatigue characteristics of a material are represented by the S-N (cyclic stress S, versus number of cycles to failure, N) diagram as shown in figure 3-7. These diagrams can be split into high cycle fatigue and low-cycle fatigue regions. In the high cycle region, life of the structure is assumed to be infinite if the maximum stress is kept below a certain limit called the endurance limit. The endurance limit depends on the material and geometric properties of the detail. Structures based on safe-life approach are designed to operate in this region. This implies low service repair or replacement costs, at the expense of a conservative structural design. Low cycle fatigue implies that the predominant maximum stresses the structure is subjected to will be greater than the fatigue limit strength at 10^5 cycles of the material. The main concept of low-cycle design criteria is that it is based on a short rather than an infinite acceptable lifetime of a structural detail. The S-N curves are based on laboratory tests carried out on unnotched specimens. To account for notches in real structures, these S-N curves are used along with a fatigue strength-reduction factor, K_f. In the absence of test data for the determination of K_f, the most widely used empirical relationship is suggested by Neuber [40], which accounts for the effect of size by means of the notch radius r, and of the differences between materials by the material constant, A, see equation (3.1).

$$9K_f = 1+\frac{K_t-1}{1+\sqrt{\frac{A}{r}}} \tag{3.1}$$

Figure 3-8 shows a plot of σ_u versus A for various types of steel. K_t is the stress concentration factor. It is to be noted that some of the applied loads at the notch root cause yielding which is not taken into account either in equation (3.1) or in the S-N diagrams. The fatigue process consists of three successive stages: crack initiation, crack propagation and fast fracture. Therefore, the number of cycles associated with failure, N_f, is the sum of the number of cycles spent in initiation, N_i, and the number spent in propagating the crack to fast fracture, N_p, i.e., $N_f = N_i + N_p$. In the high cycle regime, N_i is a large percentage of N_f. In such cases working stresses are low and it takes a long time for a crack to develop. In the low cycle regime, the situation is reversed, where N_i is a very small percentage of the total life, N_f, and most of the time is spent in propagation. This is illustrated in figure 3-9. Usually in fatigue based design, crack propagation is not considered. This is because structures are designed to operate below the endurance limit, i.e., in the high cycle regime where most of the fatigue life is spend in crack initiation. But for

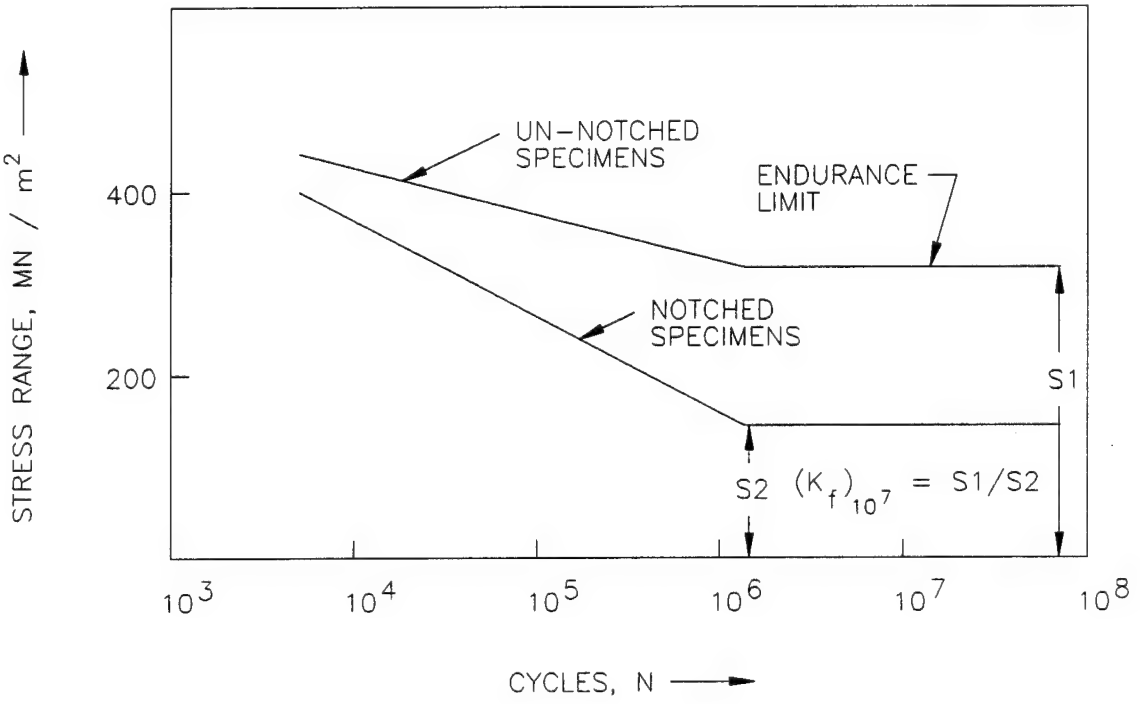

FIGURE 3.7 TYPICAL S–N DIAGRAMS FOR NOTCHED AND UNNOTCHED STEEL SPECIMENS

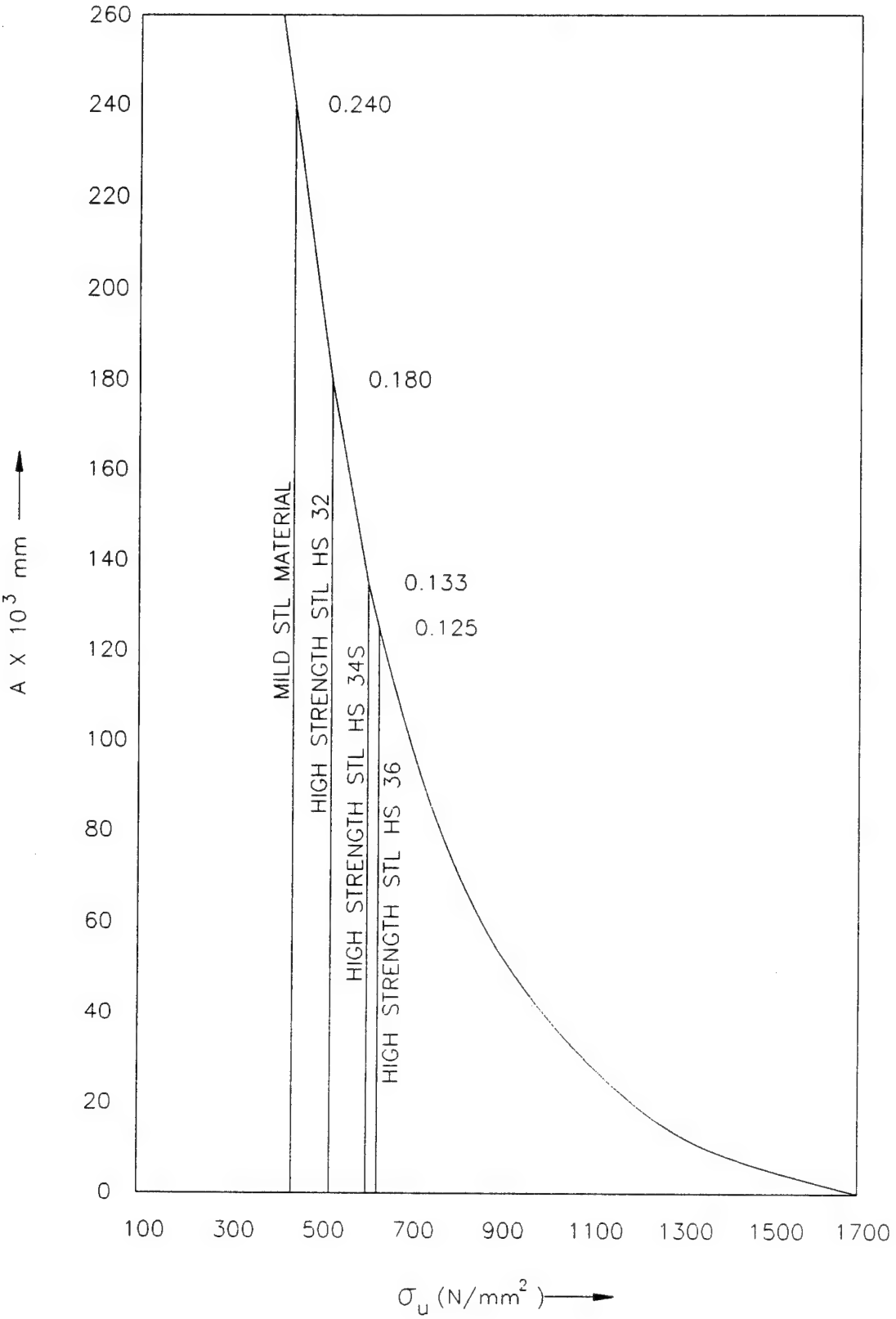

FIGURE 3.8 ULTIMATE STRENGTH VS 'A' (40)

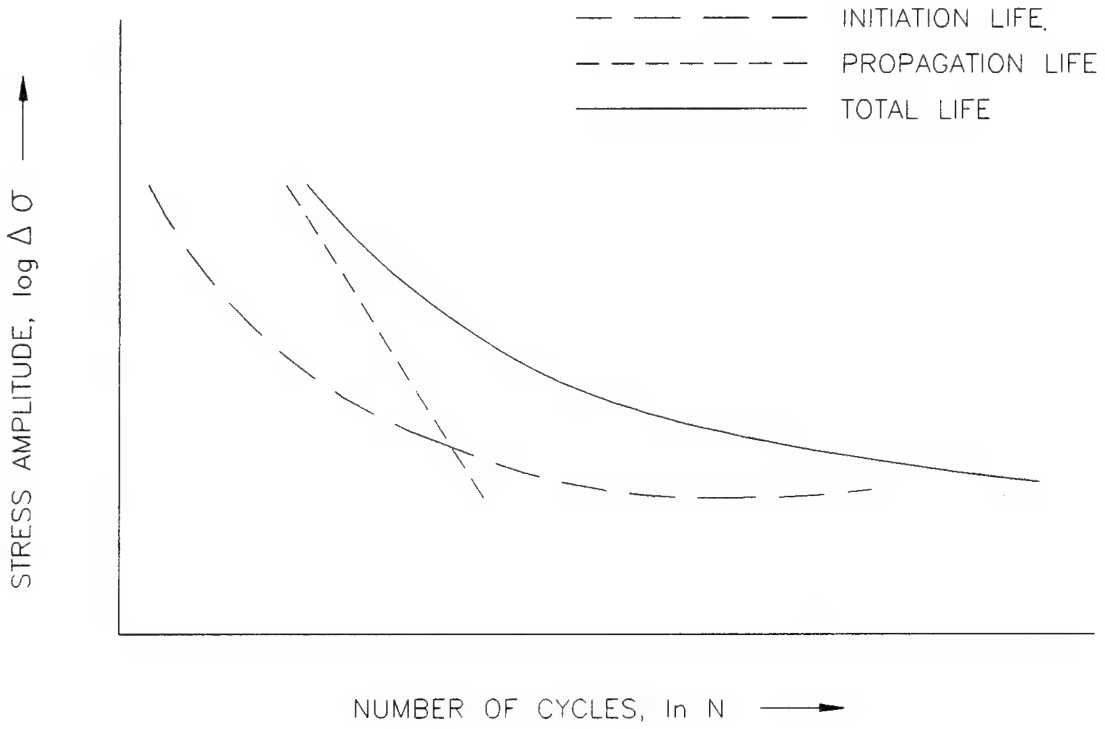

FIGURE 3.9 SCHEMATIC S–N CURVES OF INITIATION, PROPAGATION, AND TOTAL FATIGUE LIVES [15]

welded structures, flaws in the weld are assumed to exist and hence crack propagation controls the total life of the structure. Fracture mechanics takes into account crack propagation by providing a mathematical relationship based on the applied stress range and material properties. In the traditional method of fatigue assessment the criteria to prevent failure of a component under variable amplitude loading is calculated using linear Palmgren-Miner's hypothesis. In this concept it is assumed that n_i number of cycles of stress ranges S_i, use up n_i/N_i fraction of the total life where N_i is the fatigue limit for the stress range S_i. Hence the accumulated damage of a structure due to the application of "L" stress ranges is:

$$D = \sum_{L=1}^{L} \frac{n_i}{N_i} \tag{3.2}$$

Therefore, to prevent fatigue failure, "D" should never exceed 1. While in case of most ship structures, the value of "D" is chosen as 1, for offshore structures, depending on the criticality of the component as well as the possibility of access for inspection and repair, the value may vary from 0.1 to 1.0.

Table 3-2 gives some design fatigue factors which are the reciprocal of D, as suggested by the Norwegian Petroleum Directorate (NPD) [11]. In general fatigue failure criteria based on Miner's hypothesis are very conservative. The hypothesis is linear in nature, and therefore does not account for either the sequence of application of the stress range nor does it take into account interaction effects of various stress ranges which act together. Therefore, in summarizing, the conservatisms of traditional fatigue based assessment which make them inapplicable to the "fail-safe" approach are:

- does not take into account crack propagation.
- does not take into account plasticity at crack tips. Hence stresses are based on elasticity.

3.4.2.2 Fracture Mechanics

Fracture mechanics is a tool for examining crack propagation, stress intensities at tips of cracks, and residual static strength. It is generally used in the fail safe analysis of structures.

Generally there are two types of fracture mechanics concepts. The first, known as Linear Elastic Fracture Mechanics (LEFM), is applicable for stress levels up to 0.5 σ_y (the material tensile yield strength). The second, known as General Yield Fracture Mechanics (GYFM), is applicable for stress levels above 0.5 σ_y.

TABLE 3-2 DESIGN FATIGUE FACTORS (FATIGUE LIFE). NPD REGULATIONS

Classification of structural components	Access for inspection and repair		
	No access or in the splash zone	Accessible	
		Below the splash zone	Above the splash zone
Major importance for the structural integrity	10	3	2
Minor importance for the structural integrity	3	2	1

Linear Elastic Fracture Mechanics

The LEFM concept has been developed based on the assumption that the plastic zone which forms ahead of the crack tip is very small in comparison with the crack length. The LEFM approach is based on the stress intensity factor K. K gives a measure of the stress field ahead of a sharp crack and is related to the nominal stress in the member, the size of the crack, and the geometry of the structure. A crack in a solid can be stressed in three different modes, as illustrated in figure 3-10. There is a stress intensity factor that corresponds to each mode. For a crack under arbitrary loading, a combination of these three stress intensity factors are used. Mode I is the predominant form of cracking and hence discussions of stress intensity factors will be limited to this mode. The general form of the stress intensity factor for a finite size plate under tensile loading is:

$$K = Y \sigma \sqrt{\pi a} \tag{3.3}$$

where σ is the applied nominal stress, a is the semi-crack length of a through-the-thickness crack and Y is a parameter which depends on the geometry of the crack.

Unstable fracture occurs when the stress intensity factor at the crack tip reaches a critical value known as the critical stress intensity factor, K_{IC}. K_{IC} is a material property which represents the fracture toughness of the material. Critical stress intensity, K_{IC} is a function of the (1) thickness of the material (triaxiality effect), (2) temperature and (3) loading rate. These relations have been extensively discussed in [15, 16]. Figures 3-11, 3-12 and 3-13 illustrate the effect of thickness, temperature and loading rate on the critical stress intensity factor.

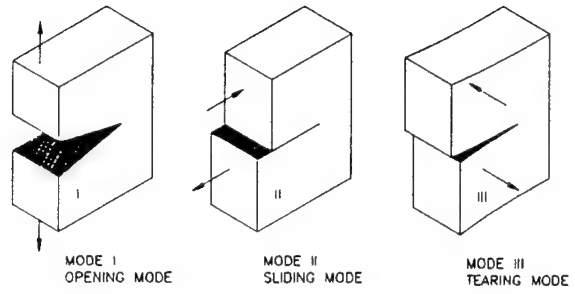

FIGURE 3.10 THREE MODES OF CRACKING

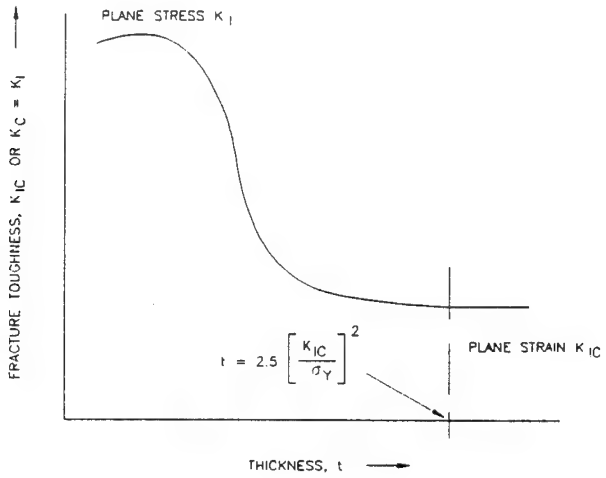

FIGURE 3.11 RELATIONSHIP BETWEEN THICKNESS AND FRACTURE TOUGHNESS [17]

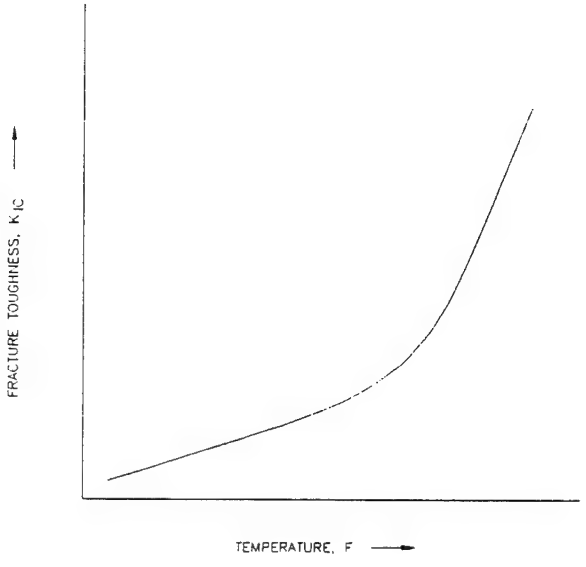

FIGURE 3.12 RELATIONSHIP BETWEEN TEMPERATURE AND FRACTURE TOUGHNESS [15]

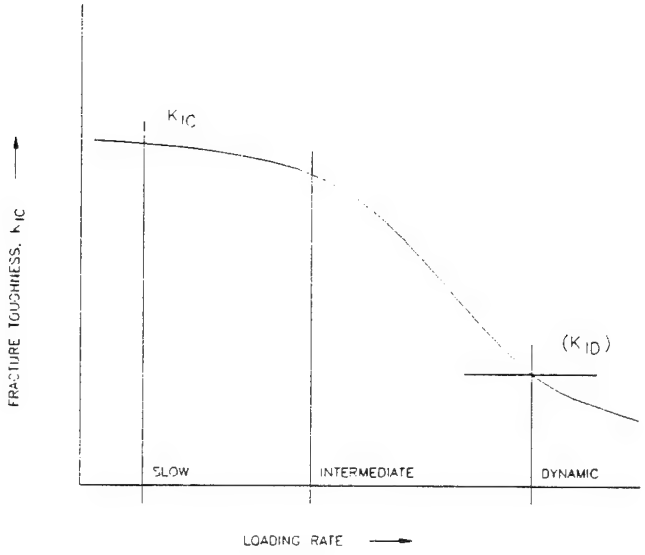

FIGURE 3.13 RELATIONSHIP BETWEEN LOADING RATE AND FRACTURE TOUGHNESS [15]

General Yield Fracture Mechanics

The techniques of linear elastic fracture mechanics give reproducible toughness values which may be used to calculate the critical defect sizes to avoid brittle failure. For sufficiently ductile materials, such as high strength steel, the LEFM theory breaks down when the extent of plasticity proceeding fracture becomes large. Three GYFM methods are discussed below. These three methods have wide applicability and are adequate to narrow the gap between the application of the linear elastic fracture mechanics and the general yielding fracture mechanics for special conditions, special cases and special geometries.

(1) Equivalent Elastic Crack Method:

The linear elastic fracture mechanics method, may be modified to provide more accuracy when a small plastic zone is present in front of the crack before the fast fracturing process commences. The modification takes into account the effect of the small amount of plastic yielding on the stresses and displacements ahead of a sharp crack. The plastic zone is assumed to extend a small distance, r_y, ahead of the crack tip. Within the plastic zone, the tensile stress is equal to the uniaxial yield stress σ_y (plane stress condition and assuming no work-hardening), as shown in figure 3-14. For the purpose of simplified stress analysis, the concept of a notional elastic, or equivalent elastic crack, is sometimes assumed to analyze the stress distribution ahead of the tip of a crack. The notional elastic crack is equivalent to the configuration of a real crack and plastic zone at moderately large distances. The equivalent crack tip is supposed to be located at the point r_y, where r_y is given by equation (3.4a):

$$r_y = \frac{K^2}{2\pi\sigma_y^2} \tag{3.4a}$$

From equation (3.3), we get

$$r_y = \frac{\sigma^2 a Y^2}{2\sigma_y^2} \tag{3.4b}$$

Therefore the equivalent crack length, a_1, is equal to $a + r_y$. The equivalent stress intensity factor, K_e, at the modified crack tip is

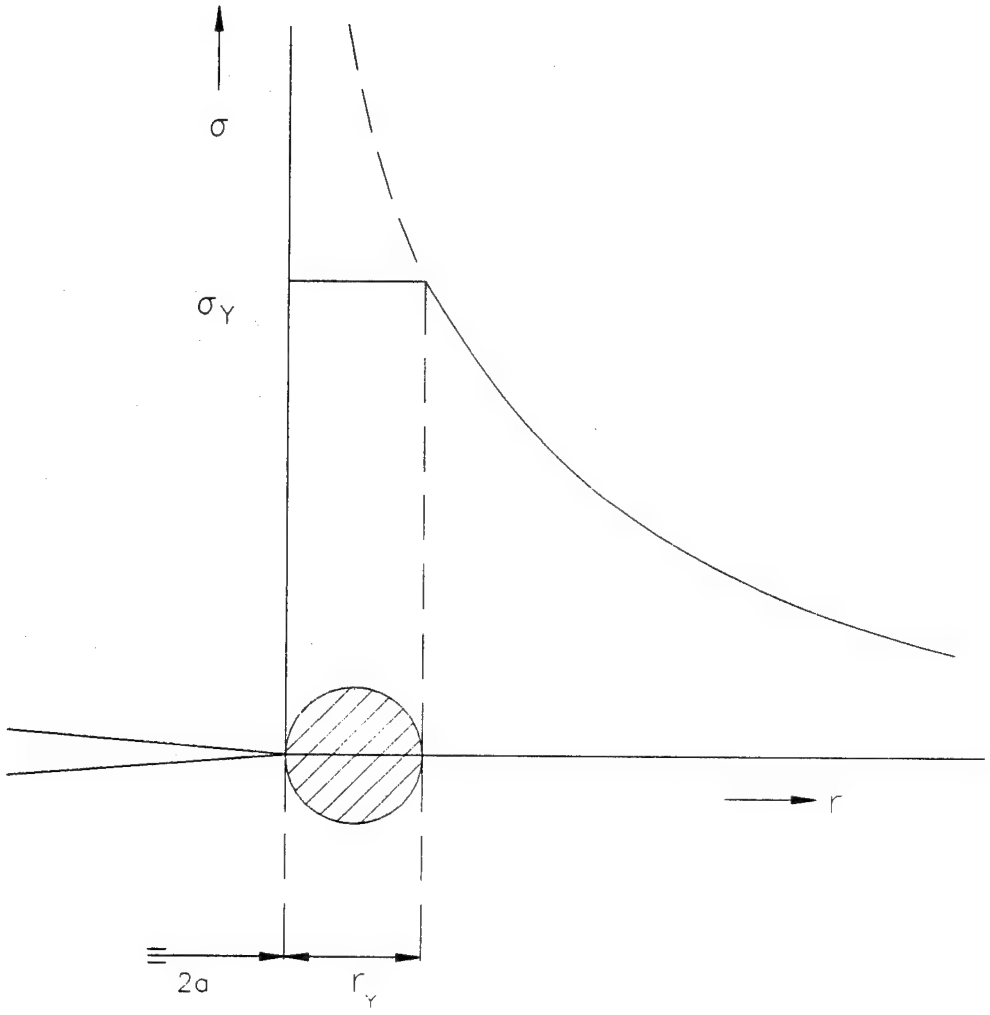

FIGURE 3.14 PLASTIC ZONE AT CRACK TIP

$$K_e = \sigma\sqrt{\pi(a+r_y)}Y_1 = \sigma\sqrt{\pi a_1}Y_1 \qquad (3.4c)$$

where Y_1 is the same as Y but at $a = a_1$.

The criteria to avoid brittle fracture is given by equation (3.5):

$$K_e \leq K_{IC} \qquad (3.5)$$

(2) Crack Opening Displacement Method:

The plastic zone at the tip of a crack enables the two faces to move apart at the crack tip without increasing the length of the actual crack. The magnitude of the separation at the crack tip has been termed the crack tip opening displacement (CTOD) and is denoted by δ_c. The model used in the CTOD approach is based on a real crack of length 2a in an infinite plate, subjected to a uniform tensile stress applied in the y-direction, normal to the crack length. The resultant plastic zone, at the tip of the real crack, extends to $x = \pm a_1$, or for the purpose of analysis, it is assumed that the crack length is $2a_1$. Eq. 3.6 expresses the relationship between the hypothetical crack, $2a_1$, and the real crack, 2a. The associated crack opening displacement at the tip of the real crack can be represented by equation 3.7:

$$\frac{a_1}{a} = \sec\left[\frac{\pi}{2}\,\frac{\sigma}{\sigma_y}\right] \qquad (3.6)$$

$$\delta_C = \frac{8\sigma_y a}{\pi E} \ln \operatorname{Sec}\left(\frac{\pi}{2}\,\frac{\sigma}{\sigma_y}\right) \qquad (3.7)$$

where E is Young's modulus of elasticity.

The value of δ_c becomes very sensitive to small changes in the ratio of σ/σ_y as this ratio approaches unity. Therefore, it is preferable to relate the δ_C value to the overall strain, ϵ, over a gauge length, 2y in equation (3.8).

Therefore:

$$\delta_c = \left(\frac{8}{\pi}\right)\epsilon_y a \ln \sec\left(\frac{\pi}{2}\,\frac{\epsilon}{\epsilon_y}\right) \tag{3.8}$$

The criteria to avoid fracture is given by:

$$\delta_c < \delta_{CR} \tag{3.9}$$

δ_{CR} is a material property which is dependent upon the service temperature and loading conditions.

(3) J-Integral Method:

The J-integral, which is another parameter that describes the condition near the crack tip, is an alternative failure criteria. It can be defined for any linear or non-linear stress-strain relationship with the reservation that it must be elastic (i.e., reversible) [17]. The J-integral is obtained by integrating the following expression along an arbitrary path around the tip of a crack (figure 3-15):

$$J = \int_{\Gamma}\left[W dy - T \cdot \frac{\partial u}{\partial x}\, ds\right] \tag{3.10}$$

where Γ is the path of integration, W is the strain energy density, T is the traction vector, u is the displacement vector, and ds is an increment along Γ. The coordinates x and y are as defined in figure 3-15. For non-linear elastic materials, Rice [18] showed that the value of J is independent of the integration path as long as the contour encloses the crack tip, as illustrated in figure 3-15.

For linearly elastic materials, the stress intensity factor is related to J by the following equation in the plane stress case:

$$K = \sqrt{JE} \tag{3.11}$$

In [19] it has been demonstrated that the J-integral method can be used in finite element analysis of cracked structure. A subroutine was developed, which was incorporated in a finite element program, to compute Rice's J-integral value and then to derive the stress intensity factor using equation (3.10).

The fracture criteria is that failure of the structure will occur once J approaches a critical value (J_C), i.e.

$$J \leq J_C \tag{3.12}$$

Fracture Criteria

In general the expected fracture behavior of a structure is related to three levels of fracture performance, plane strain, elastic-plastic or fully plastic. In an engineering sense, the ratio of critical plane-strain stress intensity factor, K_{IC}, and tensile yield strength, σ_y, is assumed to be a good relative index for measuring the level of fracture performance. Depending on the rate of loading, values of K_{IC} and σ_y measured under static or dynamic conditions are to be used. Slow or static loading is defined as a loading rate of approximately 10^{-5} in/in/sec. Dynamic, or impact loading is defined as a loading rate of approximately 10 in/in/sec. The three levels of performance are influenced by the service temperature and loading rate. This is shown schematically in figure 3-16. Based on the level of fracture performance of the structure, different fracture criteria are to be applied. The three levels of fracture performances are defined below:

1. Plane-Strain Behavior:

Structures, whose toughness and thickness are such that:

$$\frac{K_{IC}}{\sigma_y} < \sqrt{\frac{t}{2.5}}$$

exhibit plane-strain behavior. They fracture under elastic stress, generally in a brittle manner. Since brittle fracture can lead to catastrophic failure, usually structures are chosen to be of such toughness so as to avoid plane-strain behavior at service temperature and service loading rate. However, very thick plates, or plates used to form complex geometries where the constraint can be very high, may be susceptible to brittle fractures even though the notch toughness, as measured by small-scale laboratory tests, appears satisfactory. Structures performing at this level are assessed using LEFM criteria.

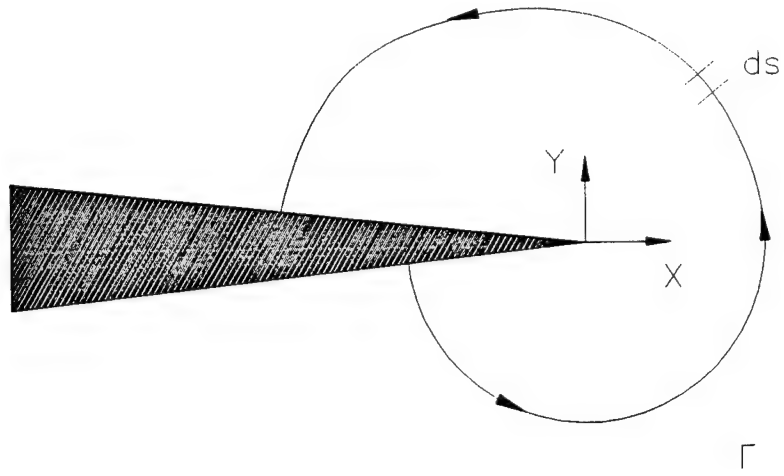

FIGURE 3.15 ARBITRARY CONTOUR AROUND A CRACK TIP

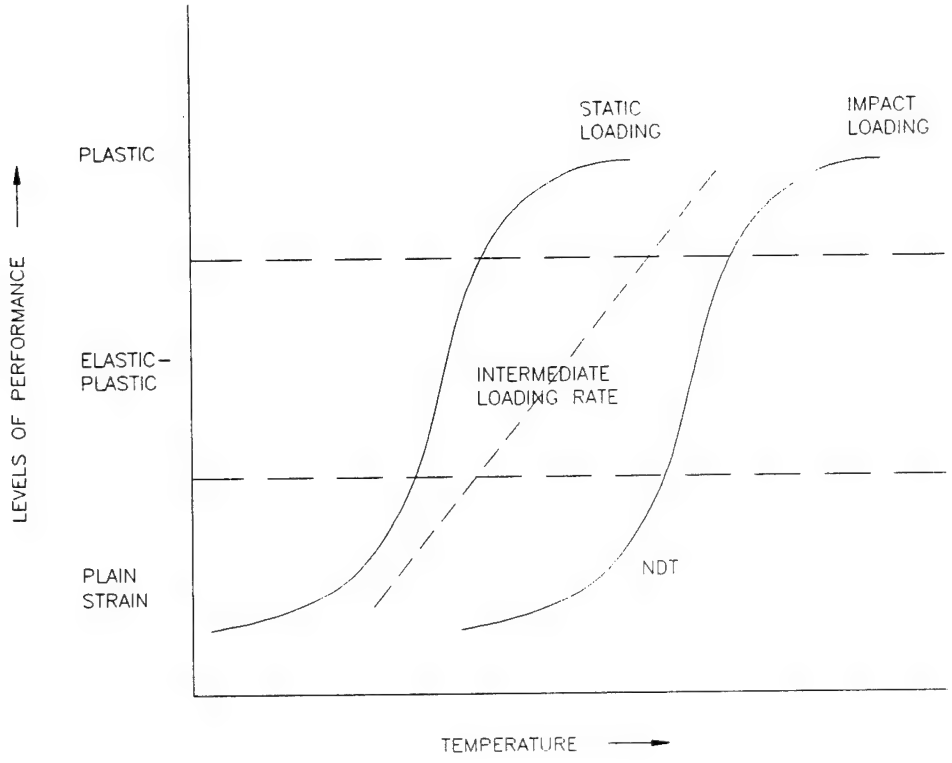

FIGURE 3.16 SCHEMATIC SHOWING RELATION BETWEEN NOTCH–TOUGHNESS TEST RESULTS AND LEVELS OF FRACTURE PERFORMANCE FOR VARIOUS LOADING RATES [15]

2. Elastic-Plastic (Mixed - mode) Behavior:

Structures, whose ratio of

$$\frac{K_{IC}}{\sigma_y} < \alpha\sqrt{t},$$

where α can be as high as 2 or 3, exhibit elastic-plastic fractures with varying amount of yielding prior to fracture. Fracture is usually preceded by the formation of large plastic zones ahead of the crack, therefore the tolerable flaw sizes at fracture can be fairly large. Ship structures usually perform at this level. The biggest drawback of structures performing at this level is the difficulty in obtaining correct K_{IC} values with small laboratory specimens. To overcome this problem CTOD based fracture criteria are used.

3. Plastic (General Yielding) Behavior:

Structures, whose ratio of

$$\frac{K_{IC}}{\sigma_y} > \alpha\sqrt{t},$$

where α can be as high as 2 or 3, exhibit ductile plastic fractures preceded by large deformation. Hence, tolerable flaw sizes are very large. Normally structures are not designed to perform at this level since it would be economically unfeasible, except in certain cases in the nuclear power industry where the reactors operate at very high temperatures.

For structures performing at the plane-strain level, cracks can be assessed by comparing the stress intensity factor at the crack tip with the critical plain-strain intensity factor K_{IC}. For structures exhibiting either elastic-plastic or plastic behavior, an interaction curve must be used. These interaction curves, also known in the industry as "design-curves" or "failure assessment diagrams", have been developed considering the interaction of two failure modes, namely brittle failure and plasticity. For practical application of these diagrams, engineering procedures have been outlined in the British Standard Institute, BSI, published document, PD 6493:1991 [20]. Relevant portions of PD 6493 for present use are discussed in section 4.2. The underlying theory behind the development of the failure assessment diagrams, including the assumptions and modifications, can be found in [20, 21].

The fracture performance of a conventional marine structure operating under normal service conditions is the elastic-plastic level. Fracture assessment at this level is usually performed using a fracture assessment diagram based on CTOD methods [19] or its modifications [20-25]. Fracture toughness parameters to be used at this level are based on either the stress intensity factor method, K_{IC} or the CTOD method δ_{CR}. K_{IC} values are measured from laboratory specimens under plane-strain conditions without any plastic zone formation. Unfortunately, the laboratory conditions hardly simulate reality. Measurements for δ_{CR} can be made even when there is considerable plastic flow ahead of a crack. These factors should be taken into account when analyzing cracked ship structures, otherwise assessment made solely on K_{IC} values may yield very conservative results.

Fatigue Crack Growth

Besides providing for criteria to assess cracks, fracture mechanics also provides an analytical tool to study fatigue crack propagation. It provides a basis for determining crack growth history given the loading and the material properties. The basis of most crack growth principals is the empirical relationship put forward by Paris in 1963, which is

$$\frac{da}{dN} = C\,(\Delta K_I)^m \tag{3.13}$$

where

a is the characteristic crack dimension.

N is the number of cycles.

ΔK_I is the stress intensity factor range based on the maximum and minimum applied stress.

C,m are material properties depending on the operating environment.

As shown in figure 3-17, the crack growth curve is sigmoidal in shape and can be split into three regions, each corresponding to the three periods in the life of a fatigue curve, namely crack initiation, propagation and unstable fracture. Region I is characterized by a "fatigue-threshold" cyclic stress-intensity factor fluctuation, ΔK_{th}. Below the threshold, cracks do not propagate. It has been observed that the threshold value ΔK_{th} is influenced strongly by the environment and the stress ratio R, which is the ratio of the minimum stress to maximum stress. Increasing R, decreases the threshold while increasing the growth

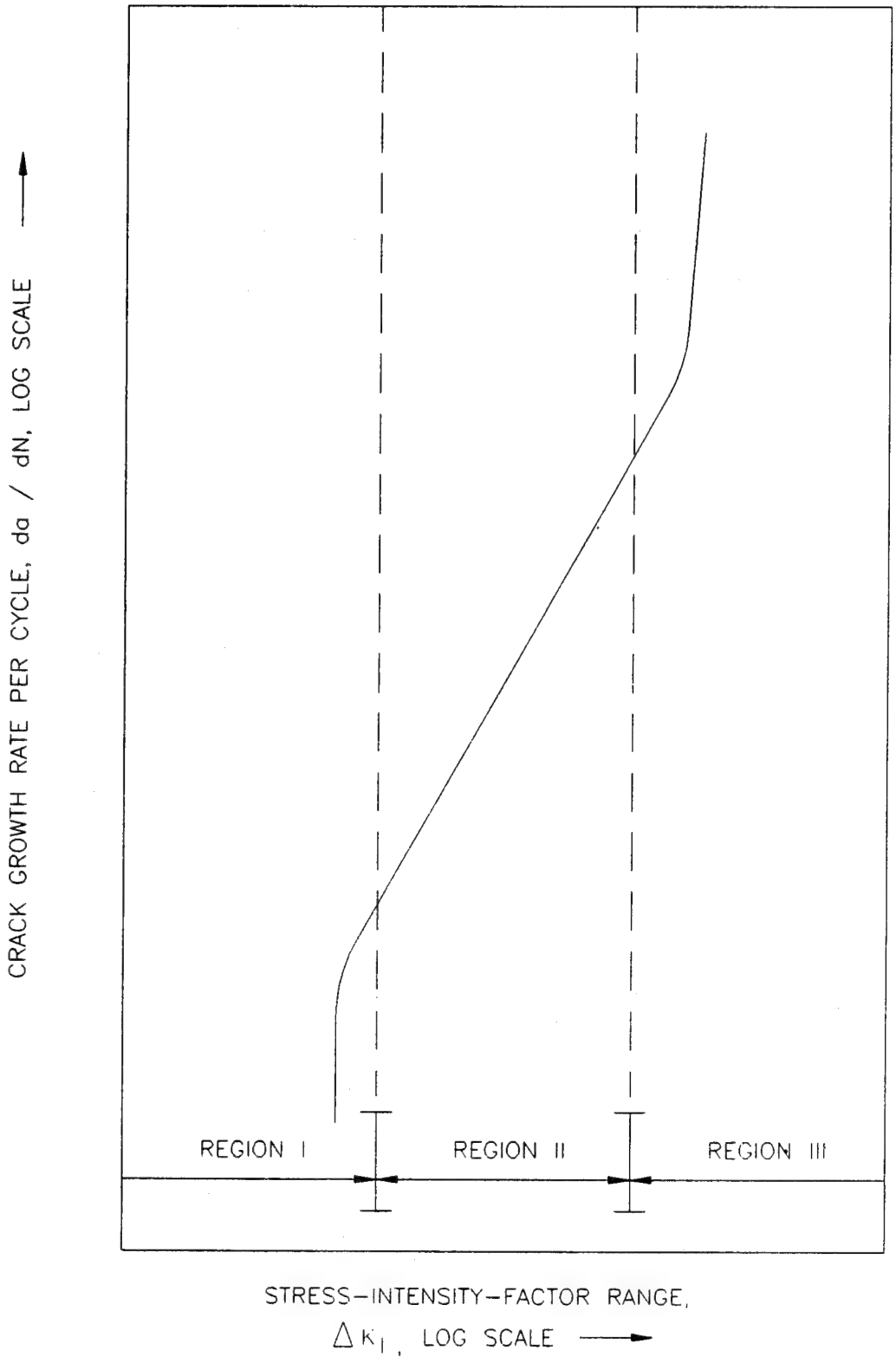

FIGURE 3.17 SCHEMATIC REPRESENTATION OF FATIGUE–CRACK GROWTH

rate in the vicinity. The threshold is independent of other material properties. Analysis of published data for carbon or carbon manganese steels in air and sea-water [26] indicates that for 97.7% probability of survival, ΔK_{th} (in $N/mm^{3/2}$) is as follows:

$$\Delta K_{th} = 63 \qquad \text{for } R > 0.5$$

or

$$\Delta K_{th} = 170 - 214R \qquad \text{for } 0 \leq R \leq 0.5 \qquad (3.14)$$

or

$$\Delta K_{th} = 170 \qquad \text{for } R < 0$$

The shape of the crack propagation curve in the low-crack growth region can be approximated in many ways [27], but a conservative approach is to extrapolate the Region 2 Paris curve to the threshold. A modification to Paris' equation of crack growth was proposed by Forman, et al. [28] which takes account of the fact that da/dn becomes infinite when the crack reaches a critical size, i.e., when K_{max} reaches K_{IC}. They arrived at:

$$\frac{da}{dN} = \frac{C\,\Delta K_I^m}{(1 - R)K_{IC} - \Delta K_I} \qquad (3.15)$$

While the application of the crack growth principals are straight forward in the case of constant amplitude loading, real structures like ships are subjected to variable amplitude loadings. Unfortunately, the effects of variable-amplitude loading on fatigue life are presently not well established, although models presented by Barsom [29, 30, 31] and by Wei and Shih [32] appear to be promising. The model advocated by Wei and Shih is a superposition model where the delay cycles caused by a change in stress magnitude are superimposed on the cycles obtained under constant-amplitude loading assuming no load interactions. The delay cycles in this model must be estimated from experimental data. The model advanced by Barsom [26] relates fatigue-crack-growth rate per cycle to an effective stress-intensity factor that is characteristic of the probability-density curve. The development of this model, which was designated the rms (root-mean-square) model, and the supporting experimental data can be found in [15]. In [15], it is shown that within the limits of experimental work, the average fatigue-crack-growth rate per cycle, da/dn, under variable amplitude random-sequence stress spectra can be represented by:

$$\frac{da}{dN} = C(\Delta K_{rms})^m \qquad (3.16)$$

where,

$$\Delta K_{rms} = \sqrt{\frac{\sum_{i=1}^{L} \Delta K_i^2}{L}}$$

L is the number of stress ranges and is independent of the order of occurrence of the cycle load fluctuation as shown in figure 3-18. The actual relationship between crack length and the life of the structure is obtained by integrating the crack growth between the initial and the final size. The integration is usually performed numerically. The final crack size is the tolerable crack size which is based on the consideration of unstable fracture or the loss of effectiveness of the local structure. Figure 3-19 illustrates the result of this integration in terms of number of cycles of load application, N, expended to reach a crack of length a.

3.5 Role of Inspection

Background

One of the premises on which residual strength assessment is based, is the availability of information regarding damage. The best source of such information is inspection records. Traditionally, inspections of marine structures have been based more on heuristics and experience rather than on a rational basis, the latter being impossible due to lack of theoretical knowledge. At times, such an approach could lead to subjective inspection results depending on the qualification of the inspectors and the scope of inspection.

Ship structural design is based on a combination of safe-life and fail-safe approaches because it would be uneconomical and infeasible to build ship using only the safe-life approach which assume the ship will last a lifetime in as-built conditions. The fail safe approach calls for early detection and monitoring of damage and provision for the capability to continue to carry load in a damaged condition - in other words, presence of structural redundancy. Such an approach, modeled after those employed in the aerospace industry, in conjunction with classification society requirements of periodical ("Special") detailed surveys every 5 years, supplemented by annual docking surveys and visual surveys

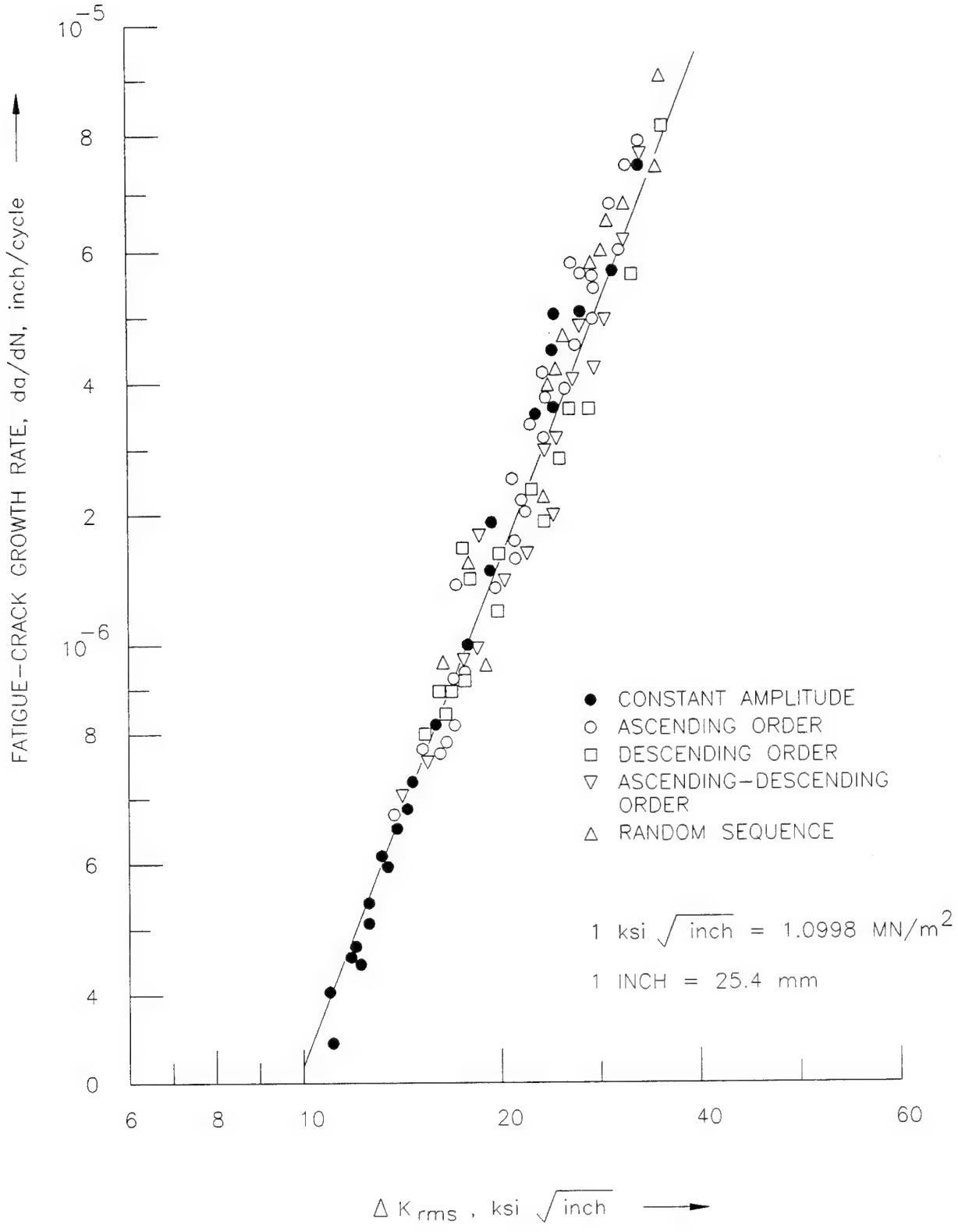

FIGURE 3.18 SUMMARY OF CRACK GROWTH RATE DATA UNDER RANDOM-SEQUENCE AND ORDERED-SEQUENCE LOAD FLUCTUATIONS.[15]

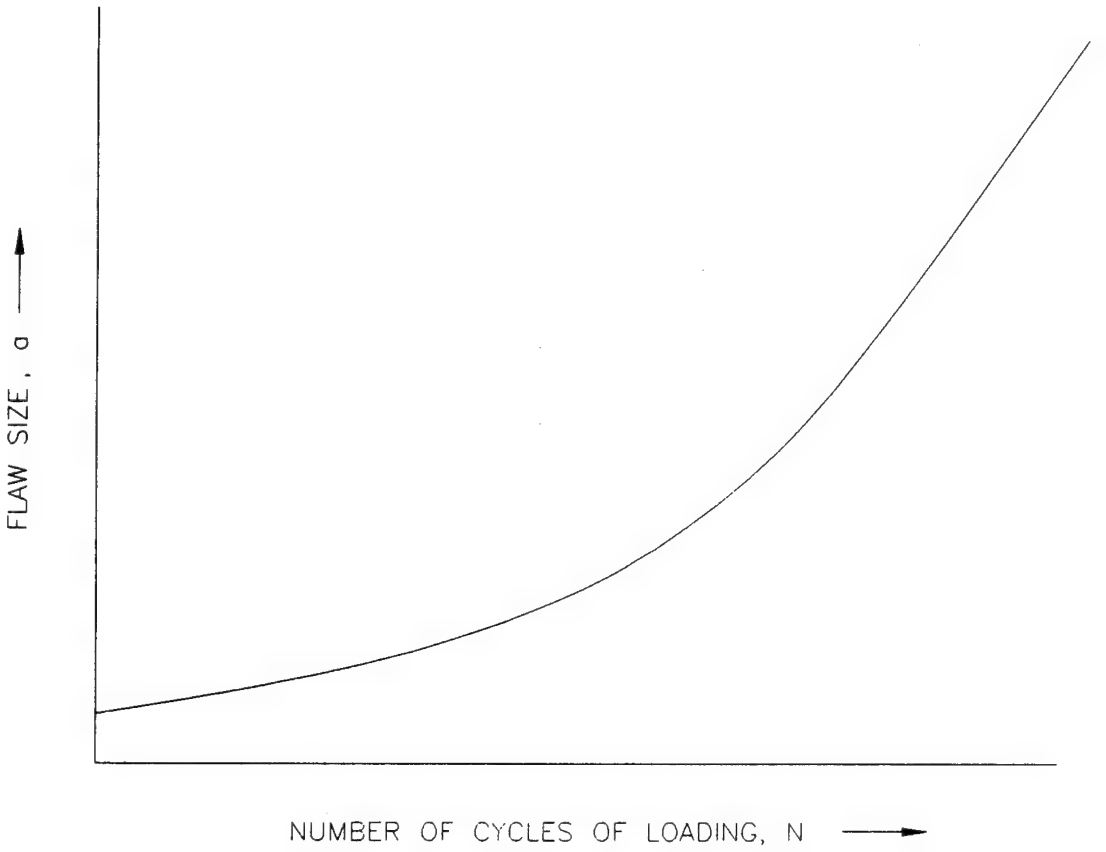

FIGURE 3.19 HISTORY OF FATIGUE-CRACK GROWTH

carried out by the owners, has worked quite well as evidenced by statistics on the decreasing number of damages to ship structures over the years. But certain critical differences between the two industries, and new trends in the marine industry, call for a reevaluation of the role of inspection in the context of safety and durability of marine structures.

Primary differences between marine structures (ships or offshore platforms) and aircraft are:

- Marine structures operate in a much harsher environment. Any predictions involving loading, degradation in strength or the physical condition of the structure are fraught with uncertainties.

- As mentioned in [33], due to the conditions and the extent of inspection required for marine structures any attempt should be considered "heroic". While aircraft inspections are conducted under the controlled atmosphere of a hangar, ship inspections are held in conditions of darkness, water, dirt, humidity and limited accessibility. Depending on the size of the ship, the extent of inspection could be about 2000 miles of welding and 100-200 acres of steel surface, which is typical of VLCC or ULCC.

- Extremely high downtime cost. Typically a ship costs about $40,000 per day and the biggest North Sea platforms about $20,000,000 per day of lost production.

New trends in the marine industry have been:

- Due to OPA 90, increased subdivision of tankers results in more numbers of compartments and surface area for inspection.

- Minimization of structural weight and thickness. According to [34] in the two periods from 1953 to 1965 and from 1965 to 1985 steel weight reduction was about 25% and 15% respectively.

- Development of structures like offshore platforms and SWATH, with very limited service-life experience.

Modern Practices:

One of the major problems facing inspection procedures is where to look for what kind of damage. Such information is absolutely necessary for huge structures like VLCC's, where critical examination of all details or joints is practically impossible. Selected critical details to be inspected could be based on service-life experience and analytical evaluations. Analytical evaluations can be carried out using well established methods in structural analysis, fatigue assessment, crack-growth prediction and risk analysis methods. Examples of the application of these types of theoretical tools for inspection procedures can be found in the aerospace industry [35, 36] where they have presented information on inspection intervals for critical components of aircraft structures based on analytical evaluation. Recent efforts in this direction in the marine industry have been initiated by the Tanker Structure Co-operative Forum, TSCF [37] and the International Association of Classification Societies, IACS for bulk carriers.

Besides periodic inspections, structural monitoring techniques to provide a continuous review of the integrity of marine structures must be implemented. Feedback from such monitoring devices can be helpful to evaluate performance for unique structural details for which previous service experience may not be available. Such devices could also help in assessment of remote or inaccessible areas. Few instances of the application of such monitoring systems can be found in the shipping industry [38] or the offshore industry [39].

Another significant area of development to aid in the inspection procedure is the development of computerized data bases for typical occurrences of damage and inspection results. A step in this direction has been taken by CHEVRON in the development and implementation of CATSIR (Computer Aided Tanker Structures Inspection and Repair) [40].

3.6 References

1. Lloyd, J.R. and Clawson, W.C., "Reserve and Residual Strength of Pile Founded Offshore Platforms", The Role of Design, Inspection and Redundancy in Marine Structural Reliability, Proceedings, National Academy Press, Washington, D.C., 1984.

2. de Oliveria, J.G. and Zimmer, R.A., "Redundancy Consideration in the Structural Design and Floating Offshore Platforms", The Role of Design, Inspection and Redundancy in Marine Structural Reliability, Proceedings, National Academy Press, Washington, D.C., 1984.

3. Nikolaidis, E. and Kapania, R.K., "System Reliability and Redundancy of Marine Structures: A Review of the State of the Art", Journal of Ship Research, Vol. 34, No. 1, March 1990.

4. Paliou, C., Shinozuka, M., and Chen, Y.N., "Reliability Analysis of Offshore Structures", Marine Structural Reliability Symposium, SNAME, 1987.

5. Nordal, H., Cornell, C.A. and Karamchandani, A., "A Structural System Reliability Case Study of an Eight-Leg Steel Jacket Offshore Production Platform", Marine Structural Reliability Symposium, SNAME, 1987.

6. Klingmuller, O. "Redundancy of Structures and Probability of Failure", 3rd. Int. Conference on Structural Safety and Reliability, ICOSSAR 1981, Norway.

7. Das, P.K. and Garside, J.F., "Structural Redundancy for Continuous and Discrete Systems", SSC-354, December 1991.

8. Stainsen, S.G., "Interrelation Between Design, Inspection and Redundancy in Marine Structures", The Role of Design, Inspection and Redundancy in Marine Structural Reliability, Proceedings, National Academy Press, Washington, D.C., 1984.

9. Brockenbrough, R.L. and Johnston, B.G., "U.S. Steel Design Manual", published by U.S. Steel, 1981.

10. Faulkner, D., "A Review of Effective Plating for Use in the Analysis of Stiffened Plating in Bending and Compression", Journal of Ships Research, Vol. 19, No. 1, Mardi, 1975.

11. Jennings, E., et al., "Inelastic Deformation of Plate Panels", Ship Structure Committee (SSC-364), 1991.

12. Smith, C.S. and Dow, R.S., "Residual Strength of Damaged Steel Ships and Offshore Structures", Journal of Constructional Steel Research, Vol. 1, No. 4, September 1981.

13. Dowling, P.J. and Dier, A.F., "Strength of Ships' Plating under Combined Lateral Loading and Biaxial Pressure", CESLIC Report SP6, Imperial College, London, September 1978.

14. "Ductile Collapse", "Fatigue and Fracture", Vol. 1, Proceedings of the 10th International Ship and Offshore Structures, Congress, 1988, Denmark.

15. Rolfe, S.T. and Barsom, J.M., "Fracture and Fatigue Control in Structures - Applications of Fracture Mechanics", Published by Prentice - Hall, Inc., 1977, New Jersey.

16. Thayamballi, A., Chen, Y.K. and Liu, D., "Fracture Mechanics based Assessment of Fatigue Reliability in Ship Structures", presented at Ship Structure Symposium, October 1984, Arlington, VA.

17. "Ship Design Manual - Marine Structures", Chapter 6, Part 8, Published by British Ship Research Association (BSRA).

18. Rice, J.R. "A Path-Independent Integral and the Approximate Analysis of Strain Concentration by Notches and Cracks", Journal of Applied Mechanics, Vol. 35, 1968.

19. Sharples, J.K., "Finite Element Methods Applied to Two Fracture Tests Specimens", National Engineering Laboratory, NEL Report No. 675, June 1981.

20. British Standard Institute, "Guidance on Methods for Assessing the Acceptability of Flaws in Fusion Welded Structures", PD 6493: 1991.

21. Anderson, T.L. "Elastic-Plastic Fracture Mechanics - A Critical Review", SSC-345 - Part 1, April 1990.

22. Burdekin, F.M. and Dawes, M.G. "Practical Use of Linear Elastic and Yielding Fracture Mechanics with Particular Reference to Pressure Vessels", Proceedings of the Institute of Mechanical Engineers Conference, London, May 1971.

23. Harrison, R.P., Loosemore, K., Milne, I., and Dowling, A.R., "Assessment of the Integrity of Structures Containing Defects", Central Electricity Generating Board Report R/H/R6-Rev 2, April 1980.

24. Garwood, S.J., "A Crack Tip Opening Displacement (CTOD) Method for the Analysis of Ductile Materials", ASTM STP 945, June 1985.

25. Milne, I., Ainsworth, R.A., Dowling, A.R. and Stewart, A.T., "Assessment of the Integrity of Structures Containing Defects", Central Electricity Generating Board Document R/H/R6 - Revision 3, May 1986.

26. Austen, I.M., "Measurement of Fatigue Crack Growth Threshold Values for use in Design", BSC Report No. SH/EN/9708/2/83/B, British Steel Corporation, January 1983.

27. Burnside, O.H. and Hudak, Jr. S.J., "Long-Term Corrosion Fatigue of Welded Marine Steels", presented at Ship Structure Symposium, Arlington, VA, October 1984.

28. Forman, R.G., Kearney, V.E. and Engle, R.M., "Numerical Analysis of Crack Propagation in a Cyclic-Loaded Structure", ASME Trans. J. Basic Eng. 89D, 1967.

29. J.M. Barsom, "Fatigue-Crack Growth Under Variable-Amplitude Loading in ASTM A514 Grade B Steel", ASTM STP 536, American Society for Testing and Materials, 1973, Philadelphia.

30. "NCHRP Project 12-12: Interim Report", U.S. Steel Research Laboratory Report 76.019-001, National Cooperative Highway Research Program-National Academy of Sciences, Oct. 1972, Washington, D.C.

31. J.M. Barsom and S.R. Novak, "NCHRP Project 12-14: Subcritical Crack Growth in Steel Bridge Members", U.S. Steel Research, Final Report for Highway Research Board, National Cooperative Highway Research Program, Sept. 1974, Washington, D.C.

32. R.P. Wei and T.T. Shih, "Delay in Fatigue Crack Growth", International Journal of Fracture, 10, No. 1, March 1974.

33. Bea, R.G., "Marine Structural Integrity Program (MSIP)", SSC-365, October 1991.

34. K.T. Skaar, S. Valsgard, P.E. Koheler, C. Murer, "How Low Can Steel Weight Go With Safety and Economy?", Trans. 3rd Int. Symposium on Practical Design of Ships and Mobile Units, PRADS '87, 1987, Norway.

35. Warren, D.S., "Design and Inspection Interrelation of Commercial Jet Transport Structure", Proceedings of International Symposium on the Role of Design, Inspection and Redundancy in Marine Structural Reliability, Committee on Marine Structures, Marine Board, National Research Council, National Academy Press, 1983, Washington, D.C.

36. Santos, D., "Fatigue Management for the A-7P", Fatigue Management: 72nd Meeting of the AGARD Structures and Materials Panels, April-May 1991, UK.

37. "Guidance Manual for the Inspection and Condition Assessment of Tanker Structures", produced by Tanker Structure Cooperative Forum (TSCF) and published by Witherby & Co. Ltd., 1992, U.K.

38. Melitz, D.T., Robertson, E.J. and Davison, N.J., "Structural Performance Management of VLCCS - An Owner's Approach", Marine Technology, Vol. 29, No. 4, Oct. 1992.

39. Dunn, F.P., "Offshore Platform Inspection", Proceedings of the International Symposium on the Role of the Design, Inspection and Redundancy in Marine Structural Reliability, November 1983, Washington, D.C.

40. Tikka, K, and Donnelly, J.W., "CATSIR Computer Aided Tanker Structures Inspection and Repair Planning", paper presented at the Marine Structural Inspection, Maintenance and Monitoring Symposium, March 1991, Arlington, VA.

4.0 METHODS TO EVALUATE RESIDUAL STRENGTH OF DAMAGED MARINE STRUCTURES

4.1 Indirect Method

The indirect method is an approximate step-by-step procedure to assess the residual strength of damaged marine structures. This simple procedure, utilizes service life experience and semi-empirical assessment criteria for local damage and uses simple computer programs, like ULTSTR [1], to determine the ultimate strength. Thus a practicing engineer can make a quick assessment of residual strength without having to perform complex 3-dimensional finite element analysis. Figure 4-1 is a flowchart of the procedure, which basically involves three steps. The first step is the identification of the critical locations and applicable failure criteria for damages at these locations. The next step is the local analysis to determine the extent of damage based on the applied load and the mode of failure. The last step is determination of the ultimate strength of the structure taking into consideration the damage components. Each of these steps is discussed in the following sections.

4.1.1 Service Life Experience

One of the primary roles of evaluation of service life experience is providing information on critical damage locations on marine structures. Critical locations are those locations where either the consequences of damage or the likelihood of damage or both are very high. Analytically, a finite element analysis of the global structure can be performed to identify critical locations where either the margin between static demand and capacity is minimum or there is a stress gradient (stress concentration). But such an effort is expensive and requires high level of technical expertise. For conventional marine structures like tankers, bulk carriers, etc., relevant information available from service life experience exists which can be used in an indirect or approximate evaluation of residual strength of marine structures. The other purpose of service life experience is to provide critical criteria for assessing residual strength or determining inspection and repair intervals with respect to failure consequences.

Although classification societies have collected a large amount of structural damage data, relevant service life experience data or statistics are rarely published. Analysis of service life experience gathered by ship owners and yards is considered proprietary. In recent years, due to efforts by various agencies and some ship owners, relevant information on service life experience has been made available. Interesting information may be found in references [2-11].

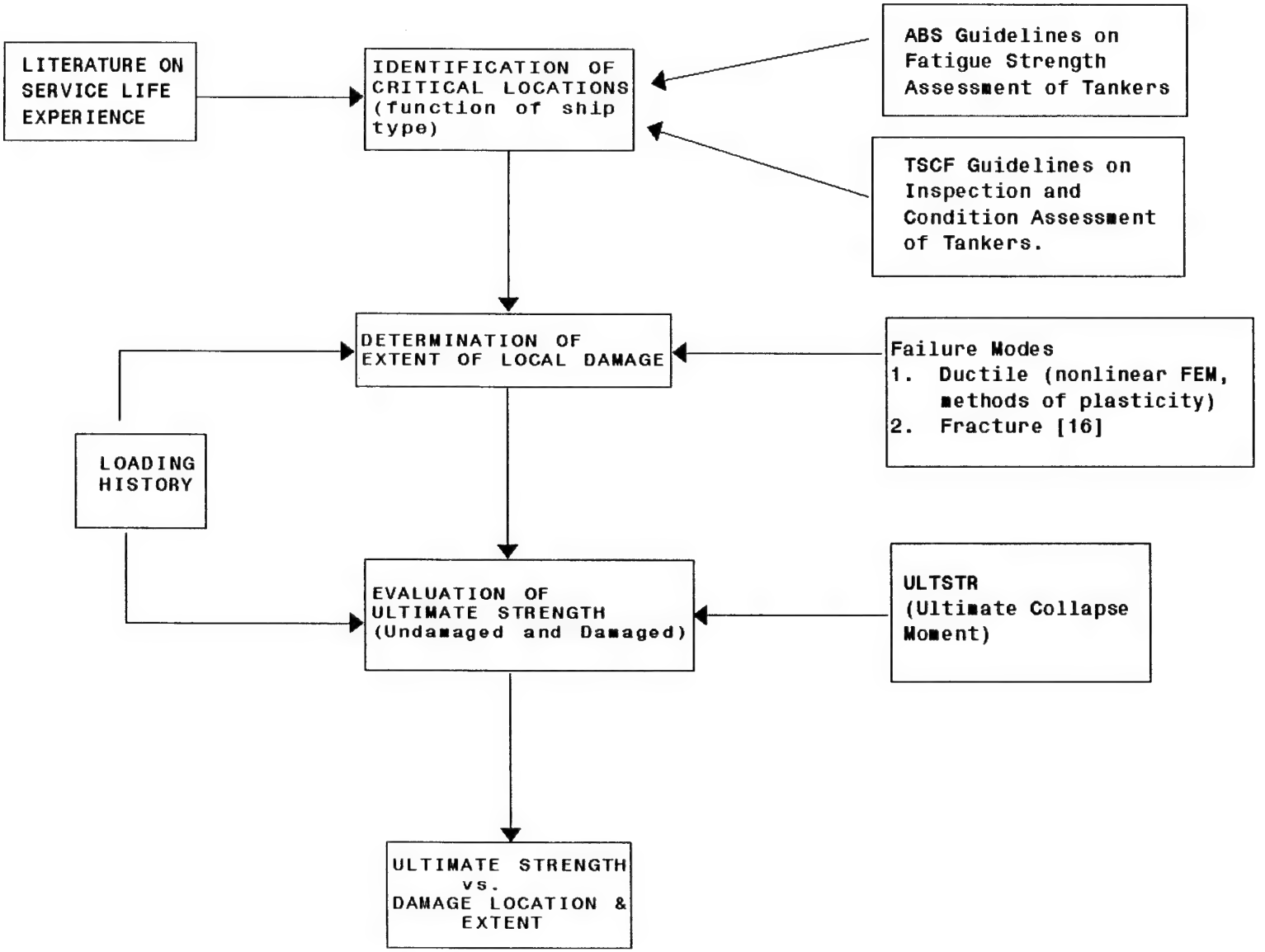

FIGURE 4.1 INTEGRATED APPROACH FOR RESIDUAL STRENGTH ASSESSMENT

As an example of the role of service life experience, investigations have recently been conducted by the Ship Structure Committee, to develop allowable permanent deformation criteria based on both in-service experience and analytical methods. The information presented in [12] determined that existing ship plate deformation criteria fall into the following two categories:

1. new construction tolerances
2. in-service allowances

A summary of the new construction deformation allowances presented in [12] is provided in table 4-1.

Authors in [12], could obtain only two useful in-service plate deformation criteria from the survey department of the DnV office at New Jersey, which were as follows:

- For shell plating located in the 0 to 0.25L (where L = overall ship length) and in the 0.75L to 1.0L portion of the hull, the maximum possible indent is 0.05 times the minimum span length between stiffeners (or b/20, where b equals the stiffener span).

- For midbody plating (0.25L to 0.75L), if the observed deformation is 10 mm to 30 mm in depth the ship owner is notified and the damage is recorded, if the observed deformation is greater than 30 mm (about 1-3/16 inches) the surveyor will recommend repair or replacement of the plating.

Furthermore they concluded through interviews with surveyors, that there are no analytical guidelines for maximum in service allowable plate deformation. It would appear that surveyors are trained by other experienced surveyors to accept or reject a deformed plate based on a "rule of thumb" guideline and not upon comparison of measured deflections with established deflection criteria. Tables 4-2 and 4-3 also taken from [12], present the results of the in service plate deformation data. Table 4-2 summarizes the principle characteristics of the ships surveyed and table 4-3 presents the survey results.

While criteria to prevent local failure like beam-column buckling, lateral-torsional instability (tripping) and plate buckling are well established, criteria for fracture are hard to come by. Reference [2] gives a very conservative criteria for treatment of fracture. It suggests "any fractures found are normally to be repaired by part renewal of material or by welding". The U.S. Coast Guard, in COMDTINST M16000.7, Marine Safety Manual (MSM), Volume II, suggests some repair guidelines for fracture based on experience. These are:

TABLE 4-1 NEW CONSTRUCTION PLATE DEFORMATION LIMITS[12]

	AGENCY							
	Ishikawajima-Harima Heavy Industries (JAPAN)		Japanese Shipbuilding Quality Standard - SNAJ (JAPAN)		German Shipbuilding Industry (GERMANY)		Noggrannhet vid Skrovbyggnad (SWEDEN)	
SHIP COMPONENT	Location	Allow-able Limit	Location	Allow-able Limit	Location	Allow-able Limit	Location	Allow-able Limit
Side shell and bottom shell	1. Parts within 0.6L* midbody 2. Fore and Aft	6 mm 7 mm	1. Parallel part, side and bottom 2. Fore and aft	6 mm 7 mm	1. Above water-line 2. Below water-line	15 mm 18 mm	-	Per SIS 21 11 12
Double bottom	1. Tank top 2. Floor	6 mm 8 mm	1. Tank Top 2. Floor	6 mm 8 mm	Inner bottom	18 mm	-	Per SIS 21 11 12
Bulkheads	1. Longitudinal 2. Transverse 3. Swash	8 mm 8 mm 8 mm	1. Longitudinal 2. Transverse 3. Swash	8 mm 8 mm 8 mm	-	18 mm	-	Per SIS 21 11 12
Main structural decks	1. Exposed part within 0.6L* midbody 2. Exposed part fore and aft 3. Enclosed part	6 mm 9 mm 9 mm	1. Exposed part within 0.6L* midbody 2. Exposed part fore and aft 3. Enclosed part	6 mm 9 mm 9 mm	Topside decks	15 mm	-	Per SIS 21 11 12
Second deck	1. Exposed part 2. Enclosed part	8 mm 9 mm	1. Exposed part 2. Enclosed part	8 mm 9 mm	-	-	-	-
Super-structure decks and wall	1. Exposed part 2. Enclosed part	6 mm 9 mm	1. Exposed part 2. Enclosed part	6 mm 9 mm	-	15 mm	Covered	15 mm
Web of girder and transverse	-	7 mm	-	7 mm	-	-	-	Per SIS 21 11 12
Cross deck	-		-	7 mm	-	-	-	-
Forecastle and poop decks	-		1. Bare part 2. Covered part	6 mm 9 mm	-	-	Covered	15 mm
House wall	-		1. Outside 2. Inside 3. Covered part	6 mm 6 mm 9 mm	-	15 mm	1. Uncovered 2. Inside 3. Covered	10 mm 8 mm 15 mm
Sheer strake	-		-	-	-	15 mm	-	-

* L = Overall length of ship

TABLE 4-2A PRINCIPAL CHARACTERISTICS OF SHIPS SURVEYED[12]

Ship	U.S. Navy Designation	Ship Type	Length Overall (m)	Full Load Displacement (Long Tons)
USS Kitty Hawk	CV-63	Aircraft Carrier	319	81,773
USS Detroit	AOE-4	Fast Combat Support Ship	242	53,600
USS Kidd	DDG-993	Guided Missile Destroyer	172	9,574
USS Kennedy	CV-67	Aircraft Carrier	319	80,941
USS Dahlgren	DDG-43	Guided Missile Destroyer	156	6,150
USNS Denebola	T-AKR 289	Vehicle Cargo Ship	288	55,355
USNS Vega	T-AK-286	Cargo Ship	147	15,404
Commercial Ship	-	Passenger Ship	189	30,325
Commercial Ship	-	Passenger Ship	-	-
USS King	DDG-41	Guided Missile Destroyer	156	6,150
USS Conyngham	DDG-17	Guided Missile Destroyer	133	4,825
USS Hayler	DD-997	Destroyer	172	8,040
USS Roosevelt	CVN-71	Aircraft Carrier	333	96,400

TABLE 4-2B SHIP SURVEY PLATE PANEL LOCATION[12]

Measurement	Ship	Survey Date	Plate Location
1	USS Kitty Hawk, CV-63	3-22-89	Port side shell, bow, about 12 ft above waterline
2	USS Kitty Hawk, CV-63	3-22-89	Port sponson shell, fwd panel, about 6 ft below deck
3	USS Detroit, AOE-4	3-22-89	Port side shell, stern, at waterline
4	USS Detroit, AOE-4	3-22-89	Port side shell, stern, at waterline
5	USS Kidd, DDG-993	3-22-89	Port side, fwd amidships at frame 103, 6 ft above waterline
6	USS Kidd, DDG-993	3-22-89	Weather deck centerline, bow, at frame 15
7	USS Kennedy, CV-67	5-10-89	Starboard shell, 20 ft fwd of stern, 10 ft above waterline
8	USS Kennedy, CV-67	5-10-89	Port shell, underside of aft elevator fairing, 10 ft above waterline
9	USS Dahlgren, DDG-43	5-10-89	Port shell, fwd of frame 43, 20 ft above
10	USS Dahlgren, DDG-43	5-10-89	Port shell, stern, at waterline
11	USNS Denebola, T-AKR 289	5-11-89	Starboard storage deck 2, near frame 228
12	USNS Vega, T-AK 286	5-11-89	Port side shell, amidships, frame 149, at waterline
13	USNS Vega, T-AK 286	5-11-89	Port side shell, stern, frame 176, below waterline
14	Commercial Passenger Ship	9-11-89	Starboard bottom shell, amidships
15	Commercial Passenger Ship	9-11-89	Port side shell, bow, 6 ft about waterline
16	Commercial Passenger Ship	9-11-89	Port side shell, bow, 6 ft above waterline
17	USS King, DDG-41	9-12-89	Starboard side shell, bow, at waterline
18	USS King, DDG-41	9-12-89	Port side shell, bow, at waterline
19	USS Conyngham, DDG-17	9-12-89	Starboard side shell, bow, 1 ft above waterline
20	USS Hayler, DDG-997	9-12-89	Port side shell, amidships, 1 ft above waterline
21	USS Conyngham, DDG-17	9-13-89	Starboard side shell, stern, frame 193, 5 ft above waterline
22	USS Hayler, DD-997	9-13-89	Starboard side shell, bow 1 ft above waterline
23	USS Roosevelt, CVN-71	9-13-89	Starboard elevator, underside sponson shell

TABLE 4-3 SHIP SURVEY PLATE PANEL DEFORMATIONS[12]

Measurement	a	b	a/b	t	Steel Type	Maximum Deflection	Deformation Type
1	144"	64"	2.25"	0.799"	HSS	2.0"	Impact
2	60"	24"	2.5"	0.350"	HSS	0.444"	Wave Slap/Impact
3	120"	30"	4.0"	0.591"	**	0.812"	Impact
4	64"	30"	2.13"	0.598"	**	4.25"	Impact
5	28"	27"	1.0"	0.433"	MIL-S-22698	0.295"	Wave Slap
6	21"	15"	1.4"	0.433"	MIL-S-22698	0.048"	Wave Slap
7	48"	48"	1.0"	0.600"	**	3.469"	Impact
8	24"	16"	1.5"	0.380"	**	1.245"	Impact
9	32"	28"	1.14"	0.437"	HY-80	0.484"	Wave Slap/Impact
10	42"	30"	1.4"	0.45"	HSS	1.094"	Impact
11	24"	18"	1.33"	0.875"	ABS Grade A	0.064"	Wheel Load
12	32"	30"	1.07"	0.725"	ABS Grade A	2.594"	Impact
13	32"	26"	1.25"	0.583"	ABS Grade A	1.125"	Impact
14	100"	32"	3.13"	0.95"	**	1.031"	Hull Grounding
15	36"	16"	2.25"	**	**	1.938"	Impact
16	26"	24"	1.08"	0.638"	**	1.016"	Impact
17	30"	24"	1.25"	0.438"	HY-80	1.016"	Impact
18	60"	38"	1.58"	0.46"	HSS	1.188"	Impact
19	48"	18"	2.67"	0.409"	HSS	0.622"	Wave Slap/Impact
20	48"	18"	2.67"	0.488"	MIL-S-22698	0.969"	Impact
21	52"	29"	1.8"	0.50"	HSS	1.031"	Impact
22	30"	24"	1.25"	0.438"	MIL-S-22698	2.109"	Impact
23	39"	24"	1.63"	0.331"	**	0.219"	Wave Slap

* See table 4-2 for ship and plate location
** Not available

(1) Side shell longitudinal with a fracture whose length is more than one-half the width of the longitudinal should be cropped out and renewed in kind.

(2) Side shell longitudinal with a fracture whose length is less than one-half the width of the longitudinal may be gouged out and rewelded.

(3) Bottom and side shell plate that experiences a fracture, generally, must be inserted. "Postage stamp" inserts are discouraged. Inserts of at least 18 inches are considered a minimum. Gouging out and rewelding of bottom and side shell plate fractures are allowable on a case by case basis if the fracture is relatively small and does not exceed one-half the plate thickness. However, if there is more than one fracture in a two foot area, then an insert is required.

Although information available from service life experience can be used as a starting point for residual strength assessment, its application has limited scope. In many cases, areas identified as prone to damage from service life experience were not critical, i.e. the damage would not result in a catastrophic failure. Secondly the criteria for allowable limits, which are based on service life experience, have been developed to prevent local failure. The limits are very conservative since they do not account for redundancy which is inherently present in continuous structures like ships. The limits have been based on the premise that any local failure can be the cause of global failure and hence incorporate a high factor of safety.

4.1.2 Engineering Procedures for Permanent Deformation Assessment

Assessing the impact of permanent deformation requires an understanding of the total load deflection relationship. Figure 4-2 presents a typical load deflection relationship characteristic of a plate panel subjected to lateral loads. Evaluating the behavior of a stiffened plate structure subjected to lateral loads, beyond the elastic limit, requires the calculation of the large deflection response (maximum structural strain) and the ultimate strength response (limiting fracture strain). Methods for calculating the limiting fracture strain are discussed in section 4.1.3. Elastic theory is available but has limited applications because loads severe enough to cause large deflections also cause yielding. Figure 4-3, taken from [12], presents a typical flow diagram for assessing allowable panel deformations that shows the relationship between the predicted maximum structural strain (ϵ_{max}) and the critical fracture strain ($\epsilon_{fracture}$). In the case of evaluating permanent deformations due to lateral loadings, the measure of residual strength can be taken as the following:

$$\epsilon_{fracture} / \epsilon_{max}(\text{damage}) > 1$$

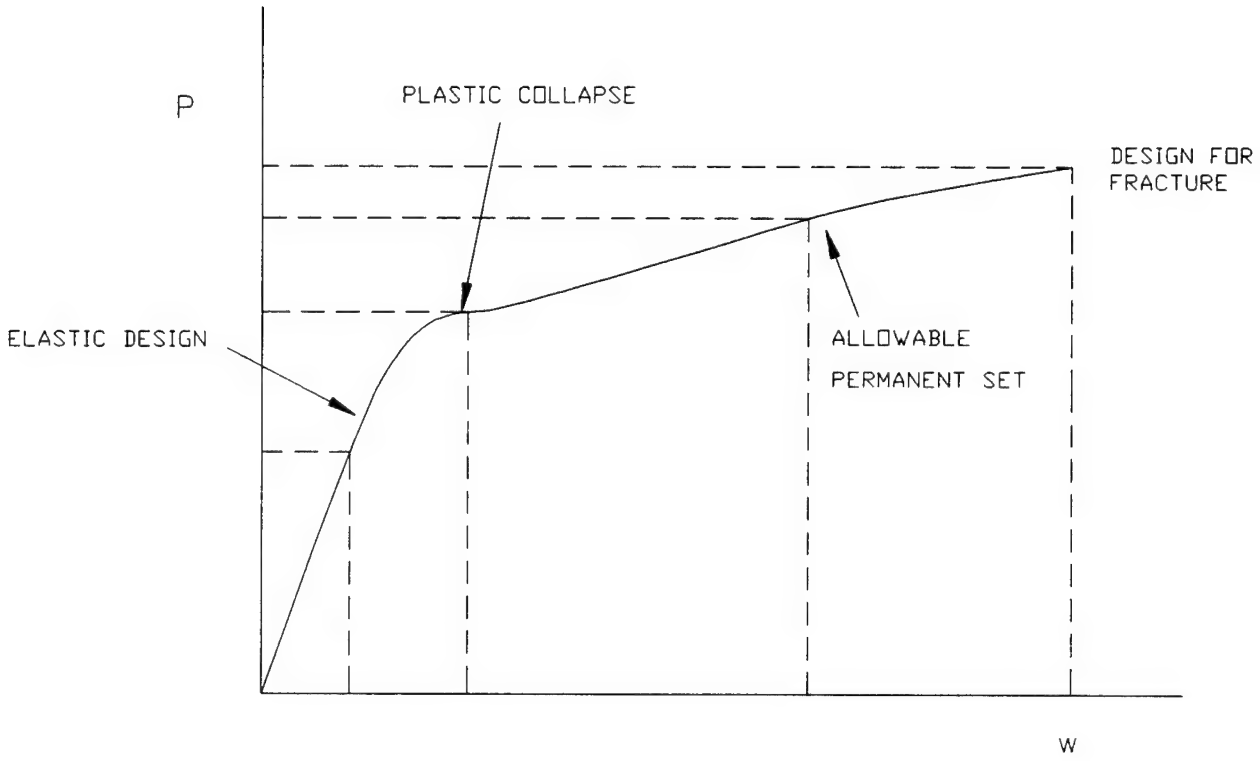

FIGURE 4.2 LOAD–DEFLECTION CURVE OF A PLATE PANEL UNDER LATERAL LOAD

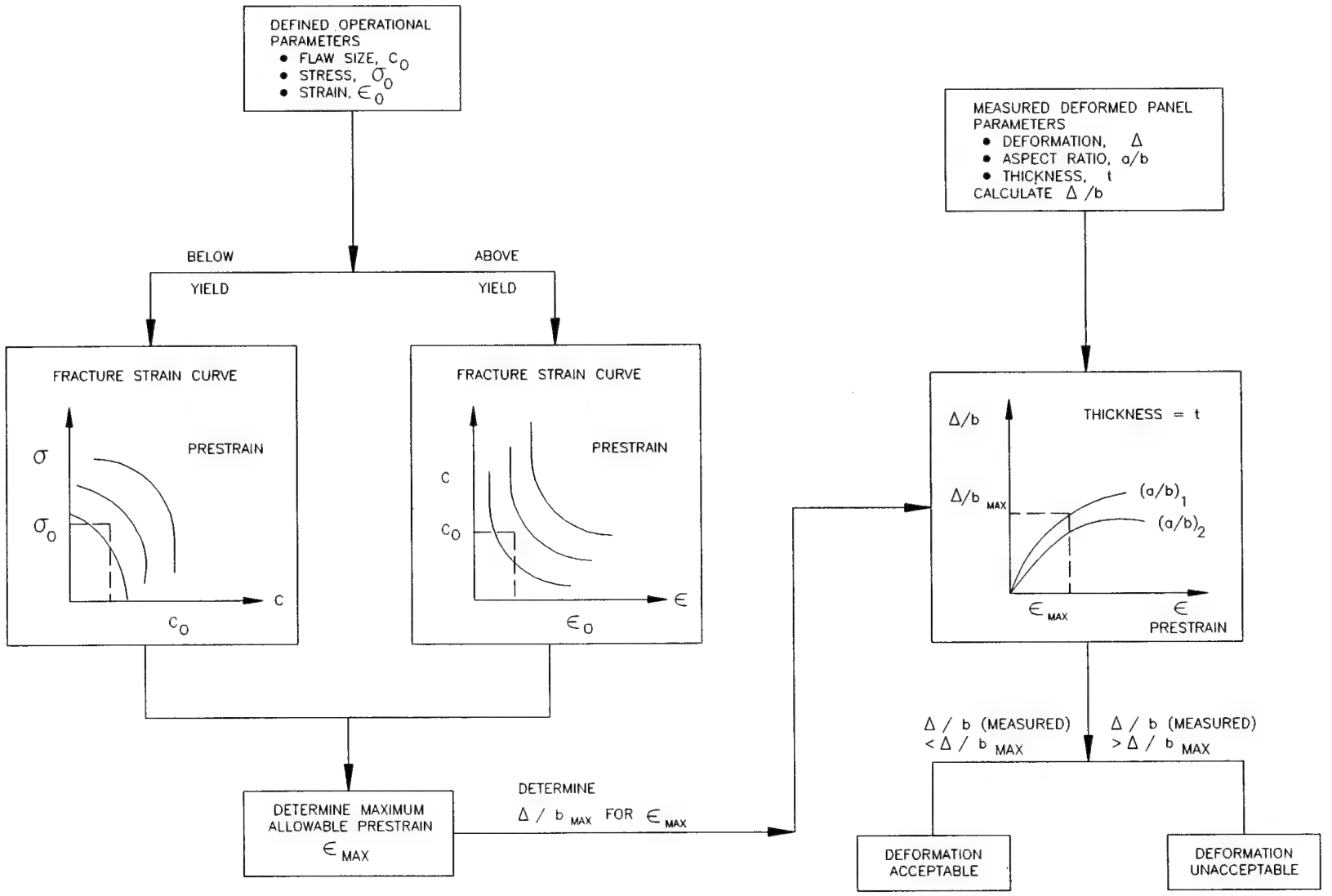

FIGURE 4.3 FLOW DIAGRAM FOR ASSESSING ALLOWABLE PANEL DEFORMATION (BASED ON FRACTURE MECHANICS) [12]

The development of $\epsilon_{fracture}$ is based on fracture mechanics and is further described in subsection 4.3.1, example 4. The development of ϵ_{max} is based on non-linear methods of analysis and a function of the allowable permanent deformation. These methods fall into two distinct categories:

1. approximate methods of plastic analysis
2. non linear finite element analysis

Application of plastic analysis is an industry recognized method to evaluate the residual strength of ductile damaged structure due to lateral loads [13]. One of the attractive features of plastic analysis is that it is often possible to obtain reasonable predictions for the plastic behavior of structures with much less effort than is required for a corresponding non-linear finite element analysis.

For residual strength assessment, the solutions of stiffened plate panel structure are obtained from the investigation of energy dissipation in the analysis of kinematically admissible deformation fields. The equations developed to approximately predict either the collapse load or the resulting structural strain for a given permanent deformation are based on the following assumptions:

1. Rigid plastic material idealization assumes elastic deformations are small compared with plastic deformations.

2. The assumed collapse deformation (based on yield line theory) gives an upper bound solution. At collapse the yield or hinge lines are developed at the location of maximum moments. Along the yield lines constant ultimate moments and axial forces are developed. Yield lines are straight.

3. Equating the external energy due to the applied load with the internal energy dissipated due to the formation of the hinge lines provides a minimum upper bound solution.

For a beam, equating the external energy due to the applied load and assumed deformation field with the rate of internal energy dissipated of the hinge gives the following:

$$\int_0^1 p\dot{w}\, dx = \sum_{i=1}^{n} M_Y \dot{\theta}_i + \int_0^1 P_Y \dot{\epsilon}_i\, dx \qquad (4.1)$$

For a stiffened panel this relationship becomes:

$$\int_A p\dot{w}\, dA = \sum_{i=1}^{n} \left(M_Y \dot{\theta}_i + P_Y \dot{\epsilon}_i \right) l_i \qquad (4.2)$$

where, for equations (4.1) and (4.2)

p = uniform lateral pressure

l = length of the beam

A = area of plate

l_i = length of the ith hinge line

$\dot{\epsilon}_i$ = concentrated rate of elongation along hinge line

$\dot{\theta}_i$ = concentrated rate of rotation along hinge line

M_Y = fully plastic bending moment

P_Y = fully plastic axial force

$\dot{w}$ = velocity field associated with the assumed displacement field

It is important to note that in the analysis of beams or stiffened plates, in which only the bending stresses are considered, the failure mechanism takes the form of a plastic hinge or hinge line pattern. In this case "failure" implied the first deformation of plating under the load assuming a rigidly perfectly plastic material idealization. This resulted in a collapse load prediction. When membrane forces are introduced the word failure becomes a misnomer. Instead of a single collapse load prediction there is a load deflection relationship with the definition of failure becoming the designer's decision in determining that the permanent deflection is permissible.

[13] presents a general load deflection relationship for beam, which is:

$$\frac{w_o}{Sd} = \frac{1}{2}\left(\frac{P}{P_c} - 1 \right) \qquad (4.3)$$

where

S = non-dimensional shape factor given by $(4M_Y/HP_Y)$

d = depth of the beam

P = line load acting on the beam which is obtained by multiplying the pressure times the spacing it acts on

P_c = static collapse load of a beam given as $16M_Y/l^2$

l = length of the beam

w_0 = permanent set associated with the loading.

[14] presents a general load deflection relationship for a stiffened panel:

$$p = \frac{M_{Yx}}{b_e A^2 \left(3\frac{b}{a} - 1\right)} \left[48 \frac{b}{a} + 6 \left(\frac{w_o}{H_x}\right)^2\right] \tag{4.4}$$

where,

p = design pressure

A = area of panel

a = plating length in stiffened direction

b = plating length in unstiffened direction

b_e = effective breadth of material

M_{Yx} = yield moment in the stiffened direction of plate-beam section (function of b_e)

w_0 = permanent deflection of entire ship panel

H_x = equivalent half thickness in the stiffened direction.

The full plastic bending moment (yield moment), M_{Yx}, and the full plastic yield force, P_{Yx} are defined below:

$$M_{Yx} = \sigma_y H_x^2$$

$$P_{Yx} = 2\sigma_y K_x H_x$$

The equivalent thickness (2H) has been based on the equivalent plating providing the same yield moment. The resulting section area, if fully effective would give too high a value for P_{yx} for the equivalent plate. The factor "K_x" then gives the fraction of the

equivalent thickness based on bending which is to be effective for carrying the plastic axial force.

4.1.3 Engineering Procedures for Crack Assessment

For large structures, subjected to low stresses, it is appropriate to apply well established Linear Elastic Fracture Mechanics (LEFM) procedures. If stresses are above approximately half the yield strength, plasticity effects can be significant and the LEFM method will be extremely non-conservative. If the LEFM analysis does not contain some type of plasticity correction, it gives no warning when the linear elastic assumptions become suspect. It is perhaps better, as suggested in [15], to apply elastic-plastic criteria to all problems; then, the appropriate plasticity corrections are accounted for. As pointed out in [15], available U.S. technology in elastic-plastic fracture mechanics either can't be translated to ordinary welded steel structures like ships, because they have been developed in the nuclear power industry where reactors operate at several hundred degrees above room temperature, or they are scattered throughout published literature. The British Standards Institute's (BSI) published document, "Guidance on Methods for Assessing the Acceptability of Fusion Welded Structures - PD 6493:1991", (PD 6493), [16] was found to be the most up-to-date published document containing procedures and criteria to determine the acceptability of cracks and flaws in welded structure.

4.1.3.1 Description of PD 6493

1. Levels of Assessment

PD 6493 offers alternatives for the treatment of fractures at three levels of complexity. The choice of a particular level is governed by the input data available and the degree of complexity the user is prepared to adopt. A thorough discussion on the background and theory behind each level of assessment can be found in [15] and in references quoted in PD 6493. At each level, failure assessment diagrams are presented. These are interaction curves, accounting for failure in the fracture and collapse mode. At any of these levels the treatment may be carried out either using LEFM procedures - stress intensity factor, K or the crack tip opening displacement procedure - CTOD. A brief account of the differences in the three levels of assessment are mentioned below:

Level 1: The assessment at this level is based on the Crack Tip Opening Displacement (CTOD) design curve developed in the early 1970's which utilized fracture mechanics theory where available and relied on empirical correlations and conservative assumptions where theory was unavailable, specifically in the elastic-plastic and fully plastic regimes. This level does not explicitly address plastic collapse but implicitly seeks to avoid plastic collapse through checks on net section yielding. The original curve was modified in the mid-1970's to account for stress concentration

effects, residual stresses and flaws that do not extend entirely through the thickness of the plate. This is meant to be an initial screening level and hence the results are very conservative.

Level 2: Also referred to as the normal level in PD 6493. It is based on the Central Electricity Generating Board (CEGB), UK approach known as the R-6 method. This method assumes an elastic-perfectly plastic material behavior and explicitly considers the interaction between fracture and collapse failure modes. This method utilizes a strip yield model due to Heald et al. [17]. This treatment gives improved accuracy over level 1 with respect to flaws in stress gradients and residual stress effects. It also allows the user the opportunity to assess the safety margins required rather than use the variable safety factor inherent in level 1.

Level 3: This is an advanced level of assessment which is not normally necessary for general structural steel applications like ships. It provides greater accuracy but involves greater complexity and requires more material data. It is particularly appropriate for materials of high strain hardening capacity, or where analysis for stable tearing fracture is required. For further details on the use of this level of assessment, readers are referred to PD 6493.

2. Information Required for Assessment

The relevant data for fracture mechanics analysis of structures containing flaws are discussed below: Flaws, as classified in PD 6493 are: (a) planar flaws like cracks, (b) non-planar flaws like cavities and solid inclusions, and (c) shape imperfections like misalignment or imperfect profile. In this work we will be dealing with crack-like planar flaws only.

(a) Stresses: Three kinds of stresses are considered in PD 6493. Ways of combining these stresses depend on the level of assessment. The three kinds of stresses are: (a) primary stresses which include membrane, P_m, and bending, P_b, components, (b) secondary stresses, Q, and (c) peak stress, F. Schematically, they are shown in figure 4-4.

The membrane component of the primary stress, P_m, is the stress due to the imposed loading which is uniformly distributed across the cross-section. The bending component, P_b, varies across the thickness. In PD 6493, P_b is superimposed upon P_m. Secondary stresses, Q, are self equilibrating stresses, like thermal and residual stresses which, according to PD 6493, do not cause plastic collapse, since they arise from strain/displacement limited phenomena, but contribute to severity of local conditions at a crack tip. For fracture assessment at level 2, the secondary stresses may be divided into membrane (Q_m) and bending (Q_b)

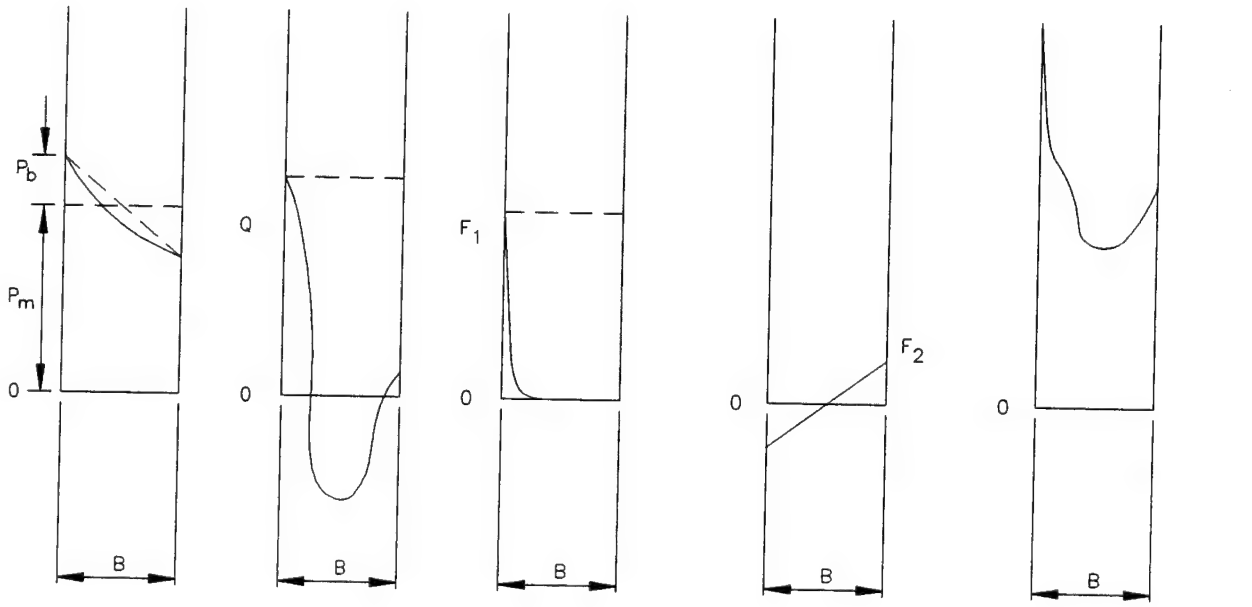

FIGURE 4.4 SCHEMATIC REPRESENTATION OF STRESS DISTRIBUTIONS ACROSS SECTION[16]

components. Peak stresses, F, are the stresses due to concentrations at local discontinuities. They have a peak value usually at the surface near the discontinuity which decays rapidly to zero through the thickness. In level 1 assessment, the maximum tensile stress, σ_1, is taken to be uniform and equal to the maximum sum of the values of the stress components ($P_m + P_b + Q + F$) as defined above. In level 2, actual stress distributions are used if known. If a partial safety factor approach is being used the stresses should be multiplied by the appropriate factors which are described later. The peak stress, F, is not required at level 2 because peak stresses are included in the stress intensity magnification factors or the stress concentration factors.

In level 1 assessment, the document recommends a tensile residual stress value in the as welded condition, equal to the yield strength of the parent material. For stress relieved weldments, the estimated residual stress can be reduced. In level 2 assessment, where actual distribution of the residual stress is known, the document suggests using that, otherwise a uniform distribution of magnitude equal to the yield strength is assumed. The document also allows for the reduction of the residual stress value, σ_R to the lower of σ_y or $(1.4 - \sigma_n/\sigma_f)\ \sigma_y$ where, σ_y is the yield strength of the material, σ_n is the effective net section stress and σ_f is the flow strength of the material which is assumed to be the average of yield strength and tensile strength. Some typical distribution of residual stresses at welds can be found in PD 6493.

(b) Flaw Description: Normally, flaws are assumed to be elliptical in shape. The document recommends that planar flaws be idealized by the height and length of their containment rectangle. These dimensions, 2a for through flaws, a and 2c for surface flaws and 2a and 2c for embedded flaws are shown in figure 4-5. If the partial safety factor approach is adopted in level 2, these dimensions are to be multiplied by appropriate factors which are discussed later.

(c) Material Properties:

(i) Fracture Toughness: PD 6493 allows the use of fracture toughness data which could be based on K-methods, including conversion from J-methods, or on CTOD methods, but requires a consistent use of data throughout the assessment process. The document does not permit conversion of CTOD toughness data to equivalent K data. The representative toughness values used in the document for the assessment are termed K_{mat} for K-methods and δ_{mat} for CTOD methods. The document emphasizes the desirability of having accurate toughness data and suggests the use of established standardized testing technique in their derivation. The procedure for these testing techniques are discussed in detail in the document. If valid K_{IC} values for K_{mat} are not available, the

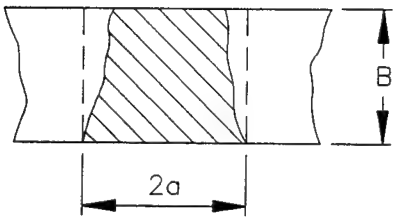

(a) THROUGH THICKNESS FLAW
REQUIRED DIMENSIONS: 2a, B

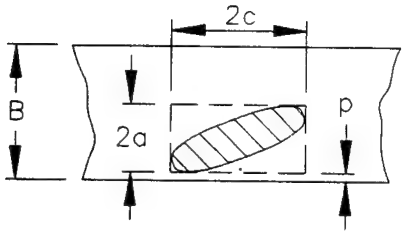

(b) EMBEDDED FLAW
REQUIRED DIMENSIONS: 2a, B, 2c, p

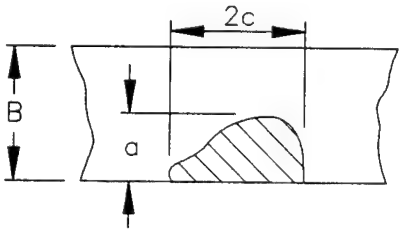

(b) SURFACE FLAW
REQUIRED DIMENSIONS: a, B, 2c

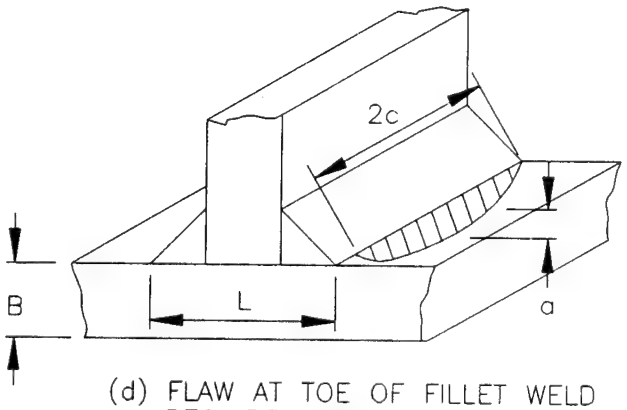

(d) FLAW AT TOE OF FILLET WELD
REQUIRED DIMENSIONS: a, B, 2c

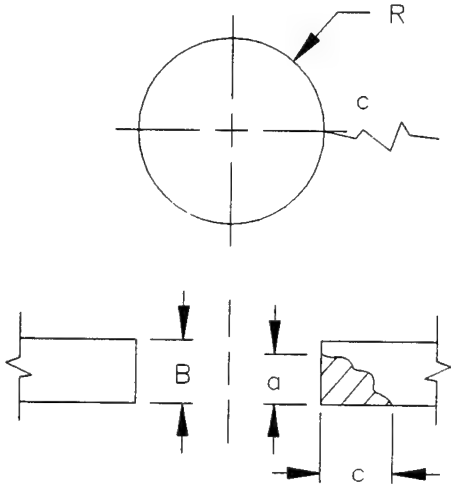

(e) FLAW AT HOLE
REQUIRED DIMENSIONS: a, B, c

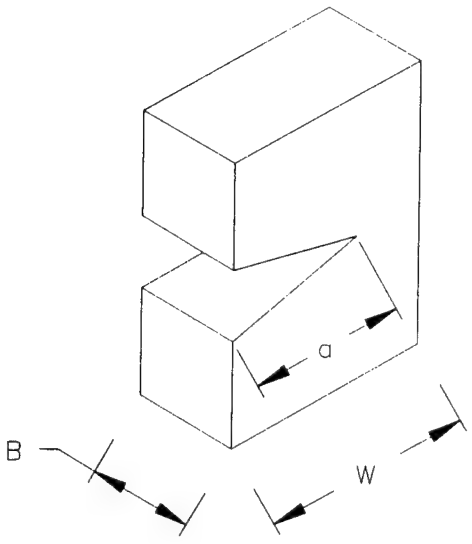

(f) SURFACE EDGE CRACK
REQUIRED DIMENSIONS: a, B, W

(16)

FIGURE 4.5 FLAW DESCRIPTION FOR CRACK ASSESSMENT

document suggests either using CTOD assessment routes or to derive equivalent K_{mat} values from J-integral based methods of fracture toughness testing. The J_{mat} value obtained from testing may be converted to an equivalent K_{mat} value using:

$$K_{mat}^2 = \frac{EJ_{mat}}{(1 - \nu^2)} \tag{4.5}$$

The toughness values should be divided by the appropriate factors, if partial safety factor approach is used in level 2 assessment.

(ii) Tensile Properties: For both level 1 and level 2 assessment methods, the material yield strength (σ_y), tensile strength (σ_u) and modulus of elasticity (E) at the appropriate temperature and obtained from standard sources should be used.

3. Partial Safety Factors on Stress, Flaw Size and Toughness

The partial safety factors are based on acceptable level of probability of failure which in turn depends on the consequences of the failure of the component. Two types of failure consequences are defined, moderate and severe. The following table gives the definition of these consequences.

Failure consequences	Structural effect
Moderate	Local failure which would not cause complete structural collapse (e.g., redundant member)
Severe	Risk of complete structural collapse or severe hazard

For the two types of failure consequences, recommendations in the document for partial safety factors to be applied to the best estimate (mean) values of maximum tensile stresses and flaw sizes and to the characteristic value of fracture toughness are given in table 4-4.

TABLE 4-4 PARTIAL SAFETY FACTORS FOR ASSESSMENTS AT LEVEL 2

Data variable	Partial factors for failure consequences	
	Moderate	Severe
Stress (known accurately measured) (COV 5%) γ_s	1.1	1.4
Stress (estimated) (COV 30%) γ_s	1.2	1.6
Flaw size (SD 2 mm to 5 mm) γ_a	1.0	1.2
Flaw size (SD 10 mm) γ_a	1.1	1.4
Toughness expressed as K_{mat} (minimum of three results) γ_t	1.0	1.2
Toughness expressed as δ_{mat} (minimum of three results) γ_t	1.0	1.4

Note: SD is the standard deviation.

4. Parameters Required for Assessment:

(a) Stress Intensity Factor, K_I:

For the assessment level 1, the document provides two formulae, depending on the type of flaw, for computing the stress intensity factor.

(i) for through thickness flaws,

$$K_I = \sigma_1\sqrt{\pi a} \qquad (4.6)$$

where,

σ_1 is the maximum tensile stress ($P_m + P_b + Q + F$)

2a is the flaw length

(ii) for partial thickness flaws,

$$K_I = \frac{M_m}{\Phi} \sigma_1 \sqrt{\pi a} \tag{4.7}$$

where,

Φ is the elliptic integral, which can be approximated as:

$\Phi = \{ 1.0 + 1.464(a/c)^{1.65} \}^{0.5}$ for $a/c \leq 1$

$\Phi = \{ 1.0 + 1.464(c/a)^{1.65} \}^{0.5}$ for $1 < a/c \leq 2$

M_m is the flaw shape factor for flaws under axial tension.

In the level 2 approach the document suggests using either:

(i) handbook solutions [18, 19], finite element analysis or weight function techniques, as described in reference [20] for calculating values of stress intensity factor, or

(ii) using the general equation

$$K_I = (Y\sigma)\sqrt{\pi a} \tag{4.8}$$

where a is half flaw length for through thickness flaws and full flaw height for surface flaws;

and $Y\sigma = (1/\Phi) \{M_m(M_{km}P_m + Q_m) + M_b(M_{kb}P_b + Q_b)\}$ (4.9)

where, M_m and M_b, known as flaw shape factors for flaws under axial tension and bending respectively, are the correction functions, dependent on crack size and shape, proximity of the crack tip to free surfaces and loading.

M_{km} & M_{kb} are the stress concentration factors due to local structural discontinuities to be applied to the membrane and bending components of the primary stress.

Some parametric formulae and figures for M_m, M_b, M_{km} and M_{kb} are presented in the document and can also be found in standard handbooks on fracture mechanics.

(b) Crack Tip Opening Displacements δ_I:

Using stress intensity factor K_I defined in the previous section, the applied CTOD δ_I is determined as:

For level 1,

$$\delta_I = \frac{K_I^2}{\sigma_y E} \qquad \text{for } \frac{\sigma_1}{\sigma_y} \le 0.5 \tag{4.10}$$

$$\delta_I = \frac{K_I^2}{\sigma_y E}\left(\frac{\sigma_y}{\sigma_1}\right)^2\left(\frac{\sigma_1}{\sigma_y} - 0.25\right) \qquad \text{for } \frac{\sigma_1}{\sigma_y} > 0.5$$

where σ_y is the yield strength and E is the Young's Modulus;

For level 2,

$$\delta_I = \frac{(Y\sigma)^2 \pi a}{\sigma_y E} \tag{4.11}$$

(c) Parameter K_r, δ_r and S_r:

For using the failure assessment diagrams in any level of assessment, parameters K_r, δ_r and S_r are required. Parameter K_r is the ratio of the stress intensity factor K_I to the fracture toughness, K_{mat}. Similarly, δ_r is the ratio of δ_I to δ_{mat}. Where secondary stresses are present, in level 2 assessment, a plasticity correction factor, ρ, has to be used to allow for plasticity interaction of primary & secondary stress such that:

$$K_r = \frac{K_I}{K_{mat}} + \rho \tag{4.12}$$

$$\sqrt{\delta_r} = \sqrt{\left(\frac{\delta_I}{\delta_{mat}}\right)} + \rho \tag{4.13}$$

Figures for determining ρ, are given in PD 6493.

Parameter S_r is the plastic collapse ratio, and is defined as σ_n/σ_f, where σ_n is the net effective section stress. Formulas for σ_n for some simple configurations can be found in this document. References [21, 22] provide σ_n for more complex geometry. σ_f is the flow strength, whose value is assumed as the lesser of $1.2\sigma_y$ or the average of the yield and tensile strength.

5. Acceptability of Known Flaws:

For a known flaw, the parameters K_r or δ_r and S_r are calculated and the resulting point is plotted on the failure assessment diagrams shown in figure 4-6 for the two levels of assessment. If the point lies within the assessment curve, then the flaw is acceptable.

6. Estimation of Acceptable Flaw Size:

In the document, acceptable flaw size is defined in terms of an equivalent flaw parameter, $\bar{a}_m$, which is the half length of a through thickness flaw in an infinite plate subject to remote tension loading. This flaw parameter accounts for a variety of flaw shapes and sizes at the same level of severity. Equivalent part thickness flaws can be obtained from figures in PD 6493.

For assessment level 1, using K - methods, the following equation gives the acceptable flaw size $\bar{a}_m$:

$$\bar{a}_m = \frac{1}{2\pi}\left(\frac{K_{mat}}{\sigma_1}\right)^2 \tag{4.14}$$

Using CTOD - method,

$$\bar{a}_m = \frac{\delta_{mat} E}{2\pi\left(\frac{\sigma_1}{\sigma_y}\right)^2 \sigma_y} \qquad \text{for } \frac{\sigma_1}{\sigma_y} \le 0.5 \tag{4.15}$$

$$\bar{a}_m = \frac{\delta_{mat} E}{2\pi\left(\frac{\sigma_1}{\sigma_y} - 0.25\right)\sigma_y} \qquad \text{for } \frac{\sigma_1}{\sigma_y} > 0.5$$

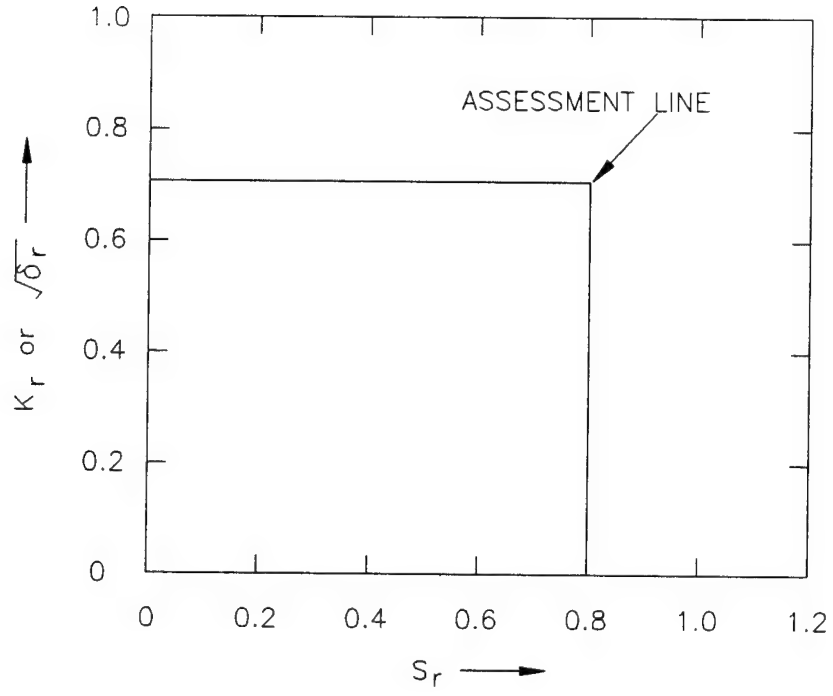

(A) – LEVEL 1 FAILURE ASSESSMENT DIAGRAM

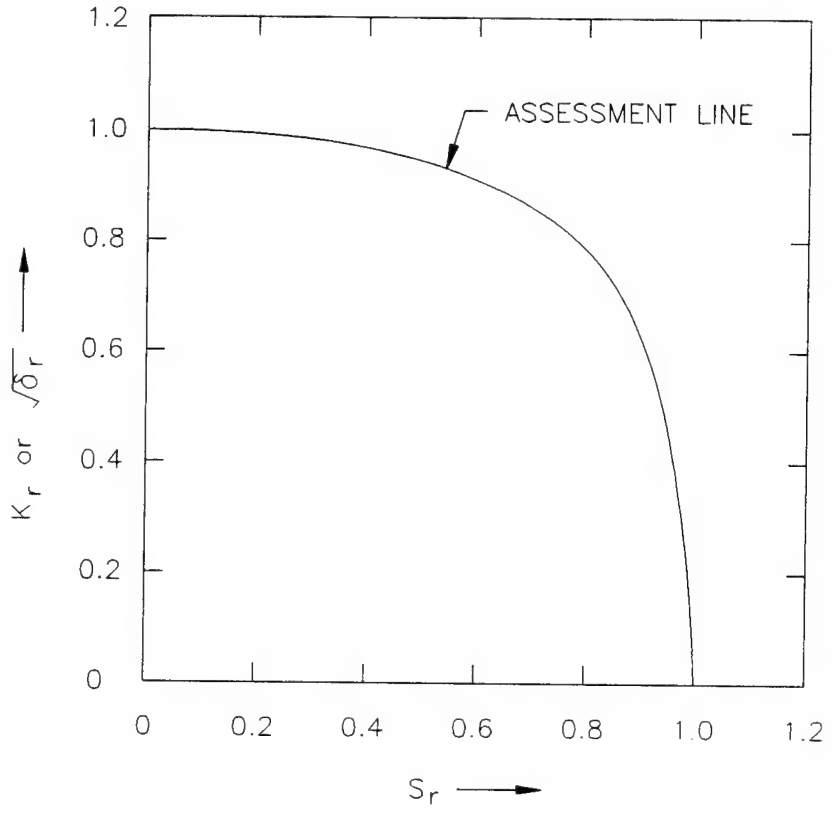

(B) – LEVEL 2 FAILURE ASSESSMENT DIAGRAM

(16)

FIGURE 4.6 FAILURE ASSESSMENT DIAGRAMS

The resulting flaw dimension has to be checked for plastic collapse by computing the associated S_r value. If S_r is less than 0.8, the flaw is acceptable, if it is greater, then the flaw dimensions have to be reduced to give an S_r less than 0.8. In the above equation, the stress ratio, σ_1/σ_Y, can be replaced by an applied strain ratio ϵ_1/ϵ_Y up to a limit of 2. For strain ratio exceeding 2, elastic-plastic finite element analysis is to be used to obtain strain information. In level 2, failure due to plastic collapse is explicitly taken care of in the derivation of the failure assessment curves, hence no implicit check is required on S_r. The acceptable flaw size is determined iteratively such that the resulting flaw size satisfies the following equation:

$$\bar{a}_m = \frac{E\sigma_y\delta_{mat}\left(\left[S_r\left\{\frac{8}{\pi^2}\ln\sec\left(\frac{\pi}{2}S_r\right)\right\}^{-0.5}\right]-\rho\right)^2}{\pi(Y\sigma)^2} \qquad (4.16)$$

A flow chart for crack assessment based on the steps discussed above is presented in figure 4-7.

4.1.4 Two Dimensional Methods for Ultimate Strength Assessment

This section provides a summary of the 2-dimensional methods available to determine the ultimate strength of ship structures. These methods are based on the "component" approach. The general idea of the component approach was first presented by Caldwell in 1965 in his paper entitled "Ultimate Longitudinal Strength" [23]. In this approach, hull girder strength is calculated on the basis of individual strength behavior of the components making up the hull girder. Since Caldwell's paper, parallel efforts based on the component approach were undertaken by both the U.S. [1, 24] and UK Navies [25]. These efforts led to the development of two computer programs, ULTSTR by Adamchak at David Taylor Research Center (DTRC) and a similar program by C. Smith and associates at the Admiralty Research Establishment (ARE) in the UK.

In the component approach, the hull cross-section is discretized into either gross-panel elements or hard corner elements and curvature in small finite increments is applied to it. The gross-panels could be single longitudinal stiffener with the associated plating (plate-beam combinations) or a stiffened panel made up of a number of plate-beam combinations. A hard corner is a particular structural detail which is assumed to resist any form of buckling under compressive loads. Hard corners are usually intersections of major plate elements e.g., decks/bulkheads to shell plates, etc. Wide plates which are longitudinally unstiffened, as found in transversely framed ships, are considered in both the ARE and

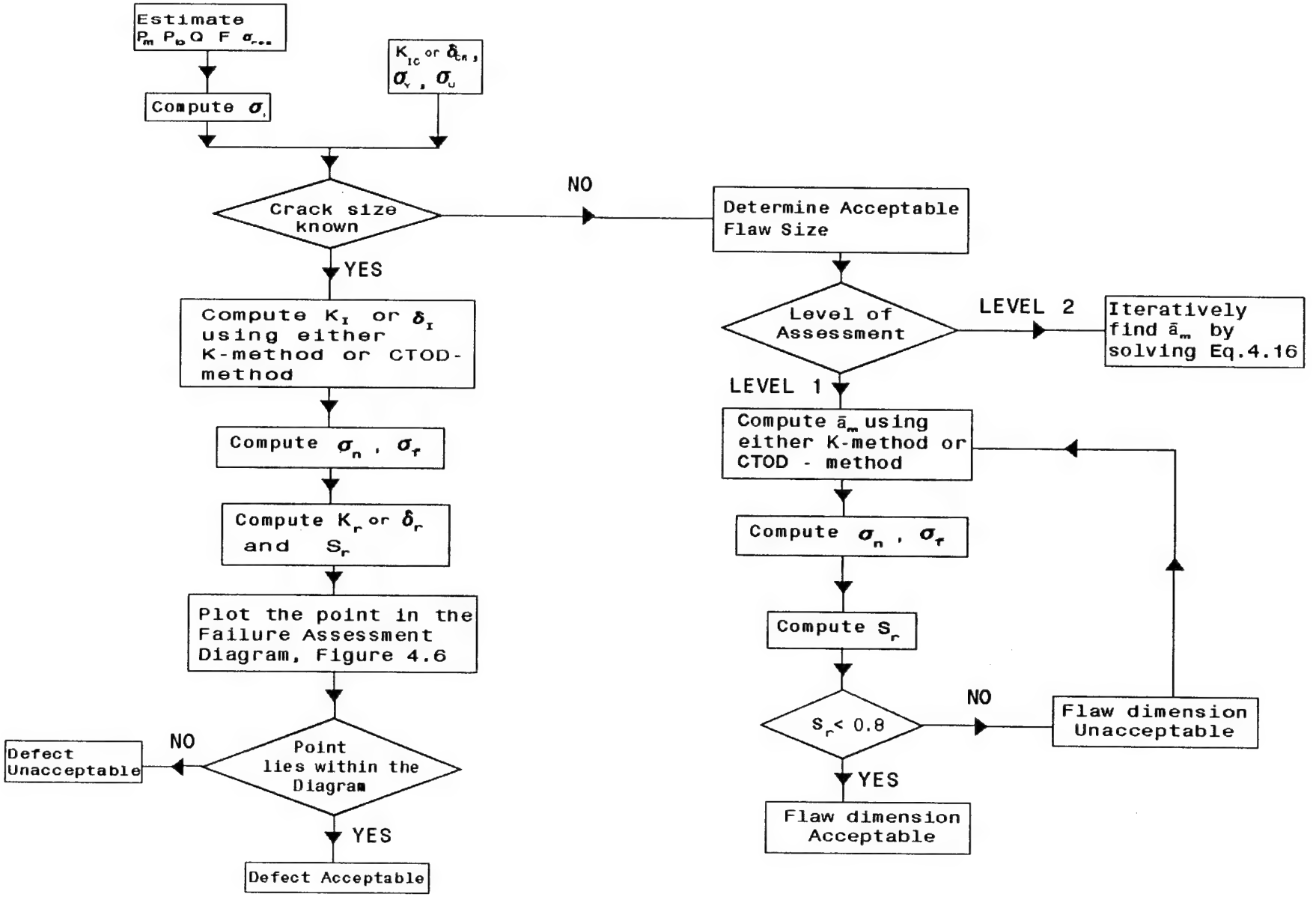

FIGURE 4.7 PROCEDURE FOR ASSESSMENT OF CRACKS

(DEVELOPED FROM REFERENCE 12)

ULTSTR programs. Each increment of curvature is assumed to produce a linear strain distribution through the depth of the cross-section. The location of zero strain corresponds to the "instantaneous" or "incremental" neutral axis. At each value of curvature, the program evaluates the equilibrium state of each gross panel and hard corner element relative to its state of stress and stability corresponding to its particular value of strain. It then computes the total moment on the cross-section by summing the moment contributions (stress x effective area x lever arm) of all of the elements that make up the section. In this manner a moment-curvature relationship is defined. Since the stress distribution, unlike that of strain, is not necessarily linear across the depth of the section, the location of the instantaneous neutral axis must be determined in an iterative fashion from the condition that the net axial force on the cross-section must be zero. This force is computed in the same fashion as the bending moment, that is, by summing the contributions of all the elements of the cross-section.

Besides structural yielding other common forms of ductile failure modes of gross panel elements are:

(1) Inelastic flexural column buckling of stiffeners and attached plating.

(2) Lateral-torsional buckling (tripping) of stiffeners.

(3) Overall grillage buckling involving bending of transverse frames - this form of failure is normally avoided by provision of stiff transverse frames and intermediate support from bulkheads & pillars.

Plate buckling is not included as an explicit failure mode but is incorporated through effective width. In the ARE method and in ULTSTR, regardless of the specific type of failure mode, the general nature of an element's behavior is described in terms of "load-shortening" curves, although the approach to deriving the curves are different.

In ULTSTR, failure by beam-column buckling can be of two types. Type I is characterized by all lateral deformations occurring in the same direction and Type II is characterized by an alternating buckling pattern. Load shortening curves for these two failure modes are derived analytically based on the respective failure theories taking into consideration the effect of plasticity. The curves for tripping failure are derived in a similar fashion but ignore plasticity effects. During the derivation, an initial sinusoidal distortion was assumed and other imperfections like fabrication induced residual stress was accounted for by incorporating a semi-empirical residual strength reduction factor in the calculation of effective width of associated plating. Since the effective width of plating is assumed to be load dependent, it is computed iteratively. Two shortcomings of the method are the

gross approximations and educated guesses made in modeling the post-buckling behavior and lack of consideration of tripping failure mode in the elasto-plastic range.

In the ARE method, the load-shortening curves for beam-column components were obtained using a large-displacement incremental finite element analysis applied to a beam - column idealization as illustrated in figure 4-8. The idealized structure is, in each case, subdivided along its length into elements as shown in figure 4-8a, elements being further subdivided over their depth into "fibers" as shown in figure 4-8b. The tangent stiffness of the plating was estimated from the slopes of stress-strain curves, as shown in figure 4-9, which were represented numerically in the computer. Two adjacent interframe spans, each having a central plane of symmetry, were modeled with a simple support condition at transverse frames. This idealization accounted for the important "continuous beam" interactions between adjacent spans and correctly represented the progressive shift in neutral axis of the cross-section caused by yielding and local buckling of the plating.

In figure 4-9, for various values of plate slenderness, where $\beta = (b/t)\sqrt{(\sigma_y/E)}$, effective stress-strain curves have been derived which account for buckling, yielding and effects of either mean or severe imperfection. These curves were derived numerically [26, 27]. Similar curves have been derived for plates in transverse compression [28-31], biaxial load [28, 29, 32] and for the case of combined inplane stress and lateral pressure [33, 34]; for plates under combined direct and shear stresses, effective stress-strain curves have been based on theoretical studies [35]. The main limitation in the ARE method outlined above is that, it does not take into account elasto-plastic tripping of stiffeners in the post collapse range.

Two important assumptions in the ultimate strength programs developed based on the component approach are:

(1) Collapse of the hull girder results from a sequence of failure of local structural components rather than from an overall simultaneous instability of the complete cross-section. Thus it is assumed that the buckling loads are widely separated and there is no interaction between various local failure modes.

(2) The hull-girder is treated as a beam such that when an incremental curvature is applied to the hull, as is done in the component approach, a linear strain distribution is assumed to exist across the depth of the section. While this is a perfectly sound assumption which is sufficiently valid for stress level below the so called design value, it ignores the two dimensional state of stress that exists due to the presence of transverse shear in the hull.

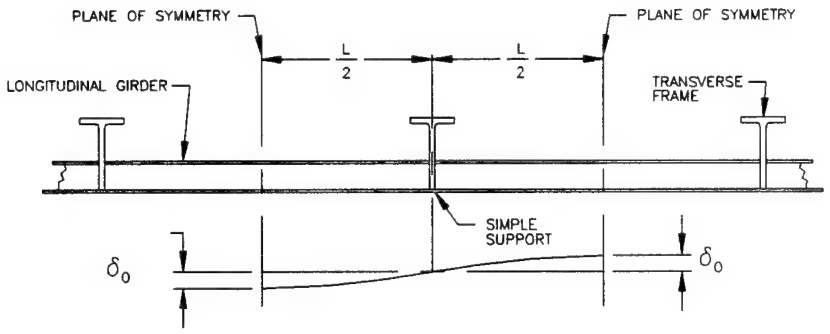

(a) SUBDIVISION OF STIFFENED PANEL INTO ELEMENTS SHOWING ASSUMED INITIAL DEFORMATION

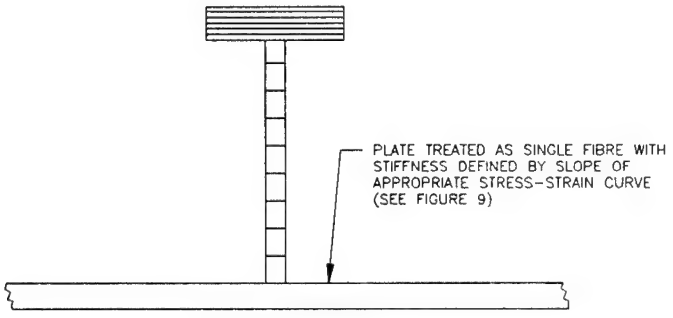

(b) SUBDIVISION OF CROSS SECTION INTO "FIBRES"

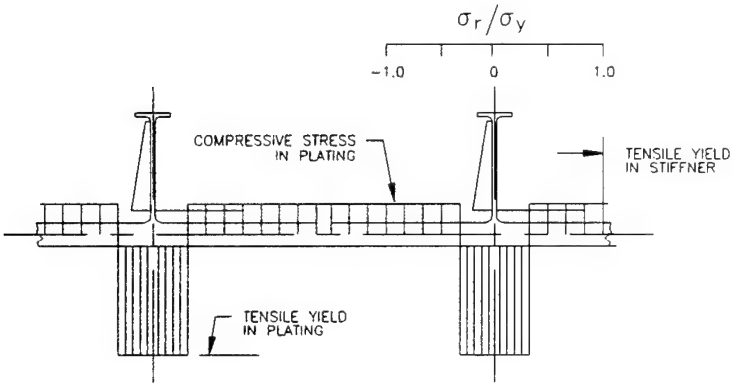

(c) ASSUMED RESIDUAL STRESS DISTRIBUTION

FIGURE 4.8 BEAM-COLUMN IDEALIZATION OF STIFFENED PANELS [25]

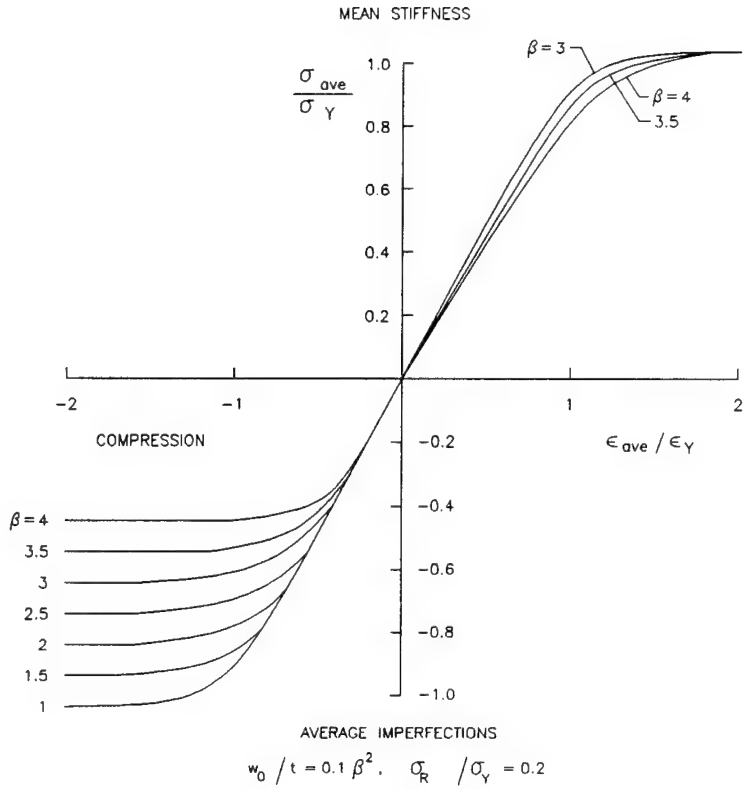

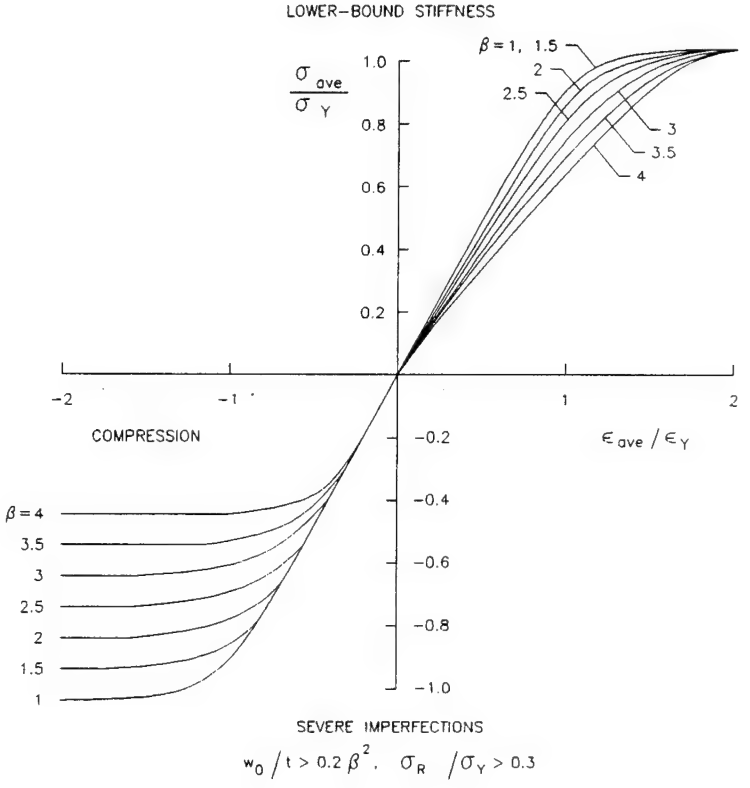

FIGURE 4.9 STRESS–STRAIN CURVES FOR PLATE ELEMENTS UNDER LONGITUDINAL TENSION AND COMPRESSION (25)

To predict residual strength and life of damaged marine structures, it is important that ultimate strength programs be capable of incorporating the effects of damage and their growth, like the growth of fatigue cracks. Consequences of damage are loss of stiffness and strength of the local component which results in the overall reduction of ultimate hull girder strength. For severe damage, like holing or gross deformation where it can be assumed that the damaged structure is fully ineffective in carrying any further load, it would be quite appropriate to model the whole structure minus the affected area. This approach can also be adopted during a "worst-case scenario" study since the results are bound to be conservative. Where damage is less severe, like that arising from a badly executed drydocking resulting in lateral interframe deformation, deletion of the affected area may be too severe and too conservative. For such cases, a realistic assessment of residual stiffness and strength is obtained by imposing a predetermined amount of lateral deformation in the elements in the affected area.

For programs based on the "component approach", like ULTSTR, which only allows modeling of the longitudinal components making up the cross-section, the effect of damage in transverse members cannot be simulated. Only in cases where damage to transverse members is so severe that it affects the longitudinal strength by increasing the length of an unsupported stiffener or panel, can the effect of a damaged transverse member be determined. Similarly, ULTSTR would not be able to give a true picture of structural redundancy for certain damaged hull configurations, for example double hull tankers which have potential for stress redistribution in their transverse strength members.

For certain time dependant damage, like fatigue cracking, the residual strength changes over time. Hence to determine inspection intervals, or to predict the effect of an existing crack at a future time, crack growth analysis must be carried out. None of the existing ultimate strength programs have any provisions for crack growth analysis. Service life experience has indicated that (1) most of the fatigue cracks occur in secondary structural members, (2) very rarely have these cracks resulted in catastrophic failure due to brittle fracture. Hence, in an indirect approach, the best way to consider such damage is a two step procedure. In the first step, for each cracked local structure, a fracture mechanics based assessment is carried out to determine the acceptability of the crack based on certain criterion like PD 6493 [16]. The second step would be ultimate strength analysis of the whole structure where, depending on the residual strength of the damaged component, it is either modeled in its original form or completely discarded.

In summary the indirect method is based on numerous assumptions and is very conservative. Specific limitations of the indirect method are:

1. It is based on the assumption that the location and form of local damage will be available from service life experience. While this is true for conventional ship structures, it may not be true for structures like offshore platforms or other unique structures which lack data on service life experience.

2. Linear beam theory assumptions are made which assume that the longitudinal components making up the section is under uniaxial state of stress. But in reality, due to transverse shear over the depth of a section and twisting over the length of the structure, components are under a bi-axial state of stress.

3. No explicit consideration for transverse strength members like transverse bulkheads and hence loss of structural redundancy at times of potential load distribution.

4. Damages like cracks are modeled by removing damaged portions without any consideration for the residual stiffness or strength the member still possess.

5. Interaction of failure modes are not allowed for.

4.2 Direct Methods

Key steps involved in the direct method of analysis are: identification of potentially critical locations, determination of the type and extent of damage at these locations and the ultimate strength analysis of the global structure. Because of the limitations of the indirect method, conservative assumptions have to be made at each step with regard to the stress field, extent of damage, etc. These assumptions take into account discontinuity in the passage of data and information between the steps. In the direct method these steps are integrated and performed using linear and non-linear 3-dimensional finite element analysis. The finite element analysis is carried out at both the local and global level in an iterative fashion. Results of linear global stress analysis are utilized at the local level for non-linear fracture analysis. Output of the fracture analysis is integrated into the non-linear ultimate strength assessment of the global structure.

Usually ships are designed to have sufficient strength margin. Nevertheless in a rational procedure for residual strength assessment, high stressed areas have to be identified for possibilities of failure at these locations. Therefore a 3-D linear finite element analysis of the whole structure is performed. Loadings for these analyses consist of quasi-static still water bending moments under various cargo loading conditions and allowable wave bending moments. As observed in section 2.0, ship structural components are well designed against local ductile failure like buckling or tripping of stiffeners. Fatigue cracking was found to be a dominant form of damage in ship structures. To

identify locations susceptible to fatigue cracking, ship motions and loads programs are used in conjunction with finite element programs. This has been demonstrated by Hughes et al. in [36] where, a linear, 3-dimensional ship motions and load program called Small Amplitude Motion Program (SAMP), was incorporated in MAESTRO to compute the fatigue inducing loads due to the sea way. MAESTRO, is a finite element based structural analysis program tailored for full scale, 3-dimensional modeling of ships.

Having determined locations prone to cracking, calculations are performed to determine the time taken by the cracks to cause failure of the component and the extent of cracking. Various computer programs are available which can predict crack propagation in structural components under variable amplitude spectral loadings [37-39]. These programs either use the Paris equation for calculating crack growth rate or its modifications like the Forman's equation. These programs require as input, stress intensity factors of the cracked structure. Fracture mechanics based finite elements can be used in these locations for the determination of the stress intensity factor, K_I. Various types of these elements of varying complexity and ease of use [40-43] have been developed in non-marine industry. They can be applied for cracks in thin sheet material as well as for cracks in complex 3-dimensional configuration involving mixed mode loading and material non-linearity. To determine the extent of the crack, a sufficiently detailed 3-dimensional finite element analysis of the region has to be performed. Depending on the location of the crack, the local analysis should include effects of local stress raisers like structural discontinuities and misalignment. The extent of the local region should include all areas which are stressed as much or higher than the area in which the crack is situated. This is done to preclude any chances of the crack propagating into a higher stressed area and leading to unstable fracture. Boundary conditions for this local analysis is obtained from the global finite element analysis. Determination of critical crack length can be based on codes like PD 6493 [16]. Depending on the magnitude of the stress and the material type, if extensive yielding occurs in the vicinity of the crack, non-linear finite element analysis should be performed to compute strains to determine critical crack lengths.

To integrate the effect of local failure upward to the global structural level and ensure that correct load transfer paths and internal load distributions are calculated, a full 3-dimensional non-linear finite element analysis is carried out. This is done in conjunction with the local failure analysis in an iterative manner. A full 3-dimensional non-linear analysis allows an assessment of the simultaneous effect of different modes of failure at various locations (longitudinal and transverse) on the overall strength of the structure. Non-linear finite element programs, developed in the marine industry, specifically for ultimate strength assessment

of ship structures are available. These ultimate strength programs are based on the "unified" approach. Under the unified approach, methods to evaluate ultimate strength are primarily based on standard finite-element procedures which allows for the interaction of local and global failure modes, geometric and material non-linearities, imperfections due to fabrication and residual stress effects and three dimensional effects of the hull girder. Three such programs, Ultimate Strength Analysis of Structure (USAS) by ABS [44, 45], Finite Element Non-linear Collapse/collision (FENCOL), by DnV [46, 47] and Idealized Structural Unit Method (ISUM) by Ueda & Rashed in Japan [48] are discussed here.

The Ultimate Strength Analysis of Structures, USAS, developed by the American Bureau of Shipping (ABS) [44], is a finite element based program which takes into account non-linearities in geometry and material. It has three kinds of elements which the user can use to model the ship structure, beams, isotropic plates and orthotopic plate elements. The constitutive relationships for the elements were derived taking into account elasto-plastic behavior with provision for strain hardening, moderately large rotations in the structural elements, local and overall buckling of structural elements and their post-buckling strength and transverse shear. Besides static analyses, it can also be used for dynamic analysis. No a priori assumptions are made regarding load distribution and boundary conditions. Imperfections in the structure, like initial deformations, can be modeled explicitly, but the program does not take into account residual stresses due to fabrication. Applications of USAS can be found in [45] where, the authors have used USAS to evaluate the ultimate strength of various ship configurations and discuss modeling techniques for efficient non-linear finite element analysis.

FENCOL (Finite Element Non-linear Collapse/Collision) is a special version of the general purpose non-linear program FENRIS. Elements available are two-noded bar, two noded beam and four noded quadrilateral membrane elements. In FENCOL, the element's response is based on the "load characteristic" curves which are similar to the "load shortening" curves used in the component approach. These load-characteristic curves developed as a result of extensive parametric studies [49], for different kinds of loading take into account local buckling and imperfections. Strength criteria used are those normally given in the design codes. The buckling failure criteria used are those from CN30.1 [50] and generalization of interaction formulae in reference [51]. For the post-collapse strength of stiffened plate panels, information from DnV [52, 53] and Cambridge University are used. FENCOL considers a tension-tearing rupture mode of failure. It describes tension-tearing with a Crack Tip Opening Displacement (CTOD) criterion [54]. Tension tearing rupture occurs when a defect, like a through thickness crack, in the tension flange of the hull is of a size such that the critical rupture strain is in the order of the yield strain. FENCOL allows two kinds of models. Small models, also known as

one-frame models, the longitudinal extent of which is one element and large models which are basically full 3-dimensional models with a number of elements in the longitudinal as well as transverse direction. The 3-dimensional models can be used in those cases where there is a high possibility of stress redistribution in the longitudinal as well as transverse strength members, as in the case of double bottom structures, and hence provide a better picture of structural redundancy.

The Idealized Structural Unit Method (ISUM) is a numerical method proposed by Ueda and Rashed [48] to model non-linear behavior of large sized redundant structure reliably and accurately in much less time than a conventional non-linear finite element analysis. In this method, the structure to be analyzed is modeled using very large size elements named "idealized structural units". Usually, each basic structural member for example a girder (beam) between two vertical web stiffeners or a stiffened panel bounded by four primary supporting members, is chosen as an idealized structural unit. Geometric and material non-linear behavior of components of the structural unit, such as buckling of plate elements, collapse of flanges of stiffeners, imperfections, etc., is idealized and described in concise forms related to forces and displacements of a limited number of nodal points at the boundaries of the structural unit. These concise forms are a set of failure interaction surfaces and a set of stiffness matrices expressing the behavior of the unit before and after failure. ISUM has been applied to various types of steel structures such as transverse rings [55, 56], upper decks, [57, 58], double bottom structures [59-61], hull girder [62-64] and tubular offshore structures [65-72].

In summary, the direct method is the most rational and complete procedure for residual strength assessment. Except for the assumptions inherent in finite element procedures, it is based on very few assumptions. Theoretically, it overcomes all limitations of the indirect method and the accuracy of the results are limited by the level of sophistication adopted in the analysis. While theoretically the direct method is very sound, a few practical drawbacks of the method are:

1. It is a time-consuming and computationally intensive procedure;

2. It requires a considerable amount of technical expertise to determine the level of sophistication required in modeling the structure to extract the desired information;

3. Because of (1) and (2) above, it cannot be used as a quick assessment procedure and has limited application.

4.3 Summary of Current Industry Practice

This section provides an overview of typical methods and tools currently used by both the marine and non-marine industries to quantify the effect of local damage on the global strength of structures. Representative case studies from the following segments of industry:

- Ship structure - 4 examples
- Offshore structure - 2 examples
- Aircraft structure - 2 examples

were chosen to illustrate current practice.

4.3.1 Ship Structure

Historically the marine industry has adopted very conservative design and maintenance practices due to the uncertainties in seaway induced loads and the lack of proper analytical and computational tools. The development of fracture mechanics and finite element analysis techniques accompanied by the availability of powerful computers has allowed the development of analysis techniques to evaluate residual strength and the risk of structural failures of complex structures such as ships. Therefore, most of the relevant information on residual strength assessment has been obtained in the last 10-15 years.

Example 1

Although many experimental studies have been conducted to correlate the performance of structural components under various loading using theoretical and numerical analyses, there is a shortage of full scale tests to study the ultimate strength of marine structures. Also incidence of ships "breaking their backs" are either very low or sufficient information for analysis is not available. Hence very few comparisons exists to evaluate the performance of the existing ultimate strength programs. The failure of a VLCC, ENERGY CONCENTRATION in 1980 provided a rare opportunity for validating existing ultimate strength techniques since the loading condition at failure was well defined.

The ENERGY CONCENTRATION collapsed due to incorrect cargo handling during discharge which caused an excessive hogging moment. The actual still water bending moment at the time of collapse was estimated at 17,940 MNm. The vessel was judged to be in good condition with limited corrosion. Valsgaard & Steen in [47] used a special version of the program FENRIS, named FENCOL (Finite Element Non-linear Collapse/Collision) for estimating the ultimate strength of the ship. Valsgaard & Steen determined a residual

strength index, B_c, which they refer to as the "cross-section margin", and define as:

$$B_c = \frac{M_u}{M_{CR}}$$

M_u is the ultimate collapse moment computed by FENCOL. M_{CR} is the collapse moment derived from the strength of the panel in the compression flange that governs the onset of final collapse of a ship's cross-section. M_{CR} is defined as the panel strength (σ_u) times the section modulus (SM). This quantification of residual strength is different from the usual definition of residual strength index, which is the ratio of the ultimate collapse moment to the allowable design moment. In this case, the governing failure mechanism is identified as the collapse of the bottom panels and subsequent reserve strength comes from redistribution of the load in the remaining cross-section.

Six cases were run varying the strength formulation, yield stress, imperfection level and corrosion. The results of these runs are shown in table 4-5. The panel strength formulation used in FENCOL is based on criteria from CN30.1, reference [50]. The uncertainty of the formulation is approximated by a mean value and a standard deviation as follows:

Mean value (m):

$$E\left[\frac{\sigma_u}{\sigma_y}\right] = 0.795\left[\frac{\sigma_u}{\sigma_y}\right] + 0.270$$

Standard deviation (s):

$$S\left[\frac{\sigma_u}{\sigma_y}\right] = 0.116 - 0.034\left[\frac{\sigma_u}{\sigma_y}\right]$$

Based on an in-house study at DnV, on the variability of yield strength of plate material delivered from Japanese steel mills, a mean value of 400 MPa with a COV = 0.066, was used for NV-32 steel (σ_y = 315 MPa). Stiffener imperfection value used in FENCOL is the standard DnV offshore rule value which is one-sinusoidal half-wave with a maximum deviation of 0.0015L and a mean of 0.0008L where L is the frame spacing. Based on experience, a uniform 1 mm corrosion loss of plate thickness was assumed in cases 3 and 5.

TABLE 4-5 STRENGTH PREDICTIONS OF ENERGY CONCENTRATION[47]

Case No.	Strength[1] Model DnV CN30.1	Yield[2] σ_y [MPa]	Imperfection[3] Level	Corrosion	Moment Capacity M_u [MNm]	Panel σ_u [MPa]	Panel Moment Capacity M_{CR} [MNm]	Cross-Section Margin $B_c = M_U/M_{CR}$
6	E(RS)	(400)	(0.0008)	no	20670	263.3	18170	1.138
5	E(RS)	(400)	(0.0008)	1 mm	19103	256.8	16934	1.128
4	E(RS)	315	(0.0008)	no	18363	232.9	16072	1.143
3	E(RS)	315	(0.0008)	1 mm	16978	227.5	14993	1.132
2	(RS)	(400)	(0.0008)	no	14649	191.7	13229	1.107
1	(RS)	315	0.0015	no	13984	182.5	12594	1.110
Section modulus: SM = 69.009 m^3 (intact) 65.903 m^3 (corroded)							(mean) : 1.127 (std) : 0.013 (COV) : 0.011	

[1]E(RS) is the mean value of the basic CN30.1 panel strength formulation, ref. (50); RS is the nominal value.
[2]Values in parenthesis are the mean values of yield for NV-32 steel.
[3]Standard stiffener imperfection values from DnV offshore rule; Values in parenthesis are the mean values.

The case closest to the actual value of 17,940 MNm was number 4 which was 2.4% above the actual value.

Using similar assumptions on yield strength, corrosion and local imperfections, the ultimate strength of ENERGY CONCENTRATION was determined by Rutherford and Caldwell [73], using LLoyd's Register LRPASS Program No. 20202 and by Hughes using MAESTRO [74]. The predicted value of the ultimate moment in both the cases were very close to the actual value and is shown in figure 4-10.

Example 2

To effectively control the risk of structural failure, the authors in [75] presented a structural management strategy based on simple risk analysis procedures. This approach was developed for a class of VLCC's that their company operates. Key steps identified for the successful implementation of the strategy were: development of an analytical database, development of focussed criterion for structural inspection/maintenance and obtaining feedback concerning ship's structural performance.

Setting up the analytical database consisted of identifying critical locations based on: (i) the stress distribution in the ship structure under various loading conditions: quasi-static, springing and slamming; and (ii) fatigue durability. The critical locations were determined using analytical methods developed to study vibration of hull girders in waves [76] and slamming effects [77] along with finite element techniques. A two level fatigue durability assessment was performed. The first level was based on certain assumptions and comparison of fatigue calculations with known fractures. The second level, was based on fracture mechanics. Critical crack lengths and acceptability of cracks were determined according to procedures outlined in PD 6493. By modeling crack like defects using special fracture mechanics based elements in a finite element model, critical locations susceptible to rapid crack propagation were identified. The theoretical method to determine critical crack length to initiate brittle fracture included simplistic assessments of critical crack size determination based on plane strain stress intensity factor K_{IC}, figure 4-11. Based on this analyses the critical locations on the vessel were identified as; longitudinal connections, upper cross tie connection to side shell, longitudinal centerline girder brackets, transverse bulkhead stringer bracket toe and the upper deck.

A focused inspection criteria based on critical location, fatigue durability and structural monitoring was developed. A structural monitoring system, which includes onboard measurement devices and displays, was installed to provide feedback concerning the ship's

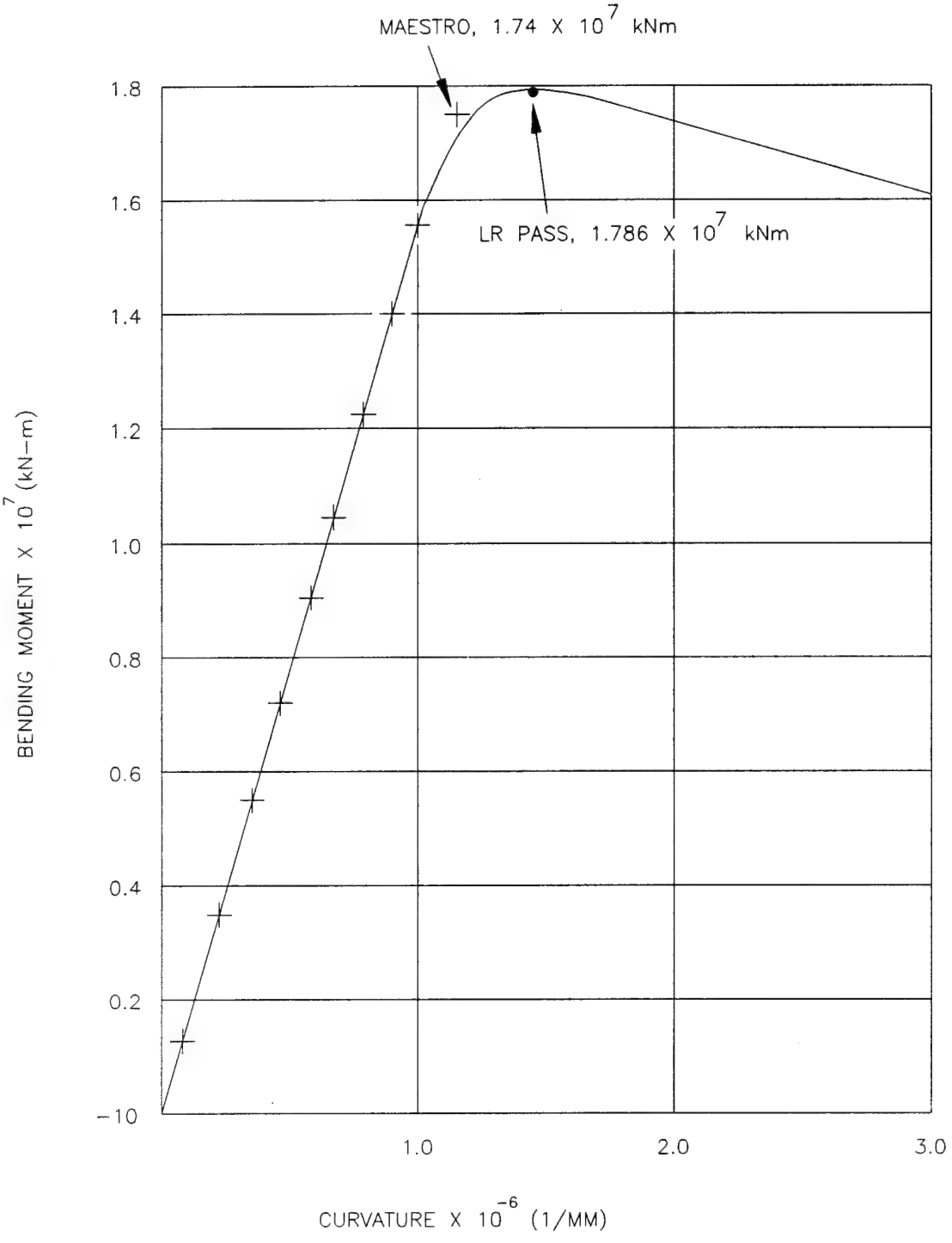

FIGURE 4.10 ULTIMATE STRENGTH OF 'ENERGY CONCENTRATION' – COMPARISON OF MAESTRO RESULTS WITH LLOYD'S LRPASS PROGRAM

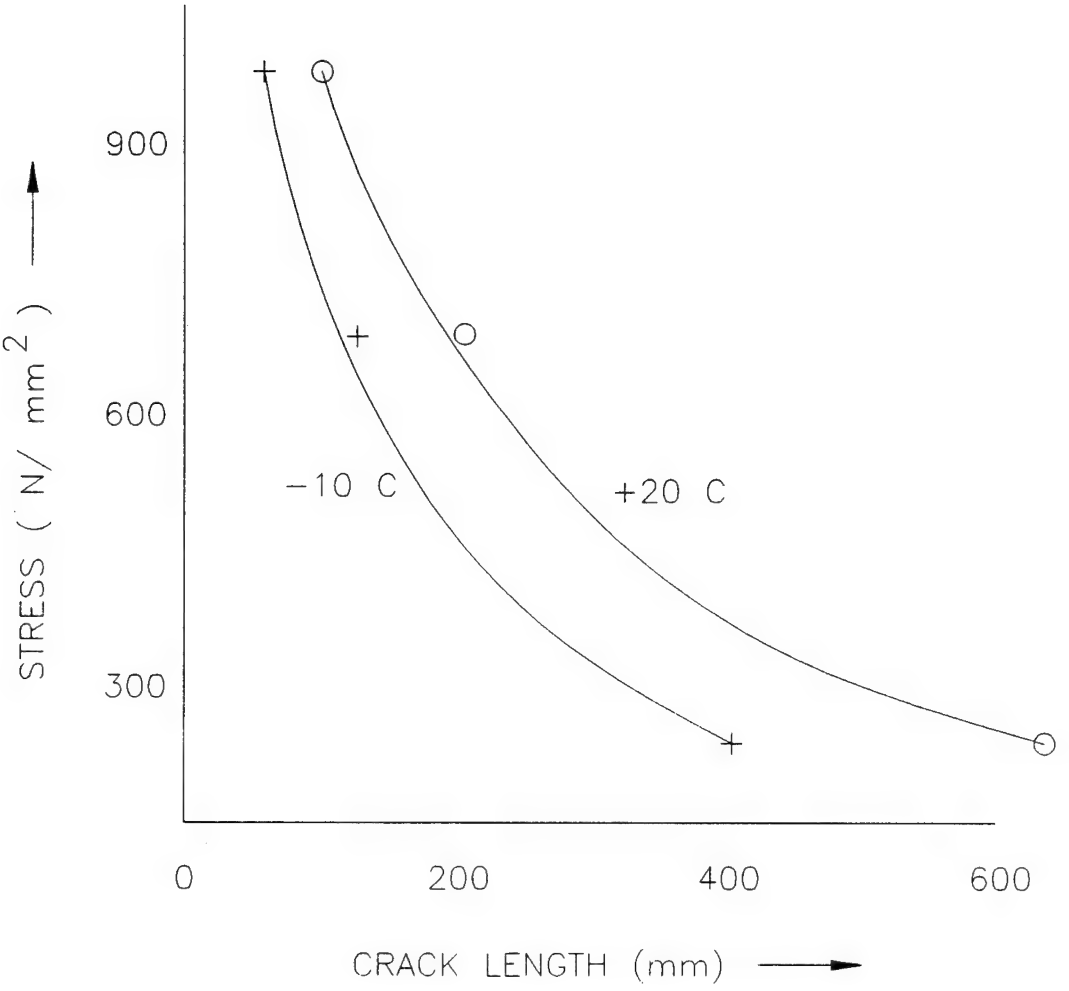

FIGURE 4.11 STRESS/TEMPERATURE EFFECT ON CRITICAL CRACK SIZE (75)

structural performance. The system performs the following functions: (i) to provide continuous guidance to the ship's staff with regard to limiting loading condition and speed, and (ii) record peak and cyclic environmental loading data to be used for analytical prediction.

Example 3

Recently, fracture mechanics techniques to assess the structural risk of failure were applied to the evaluation of a fine lined ship of low prismatic coefficient. This ship, henceforth referred to as ship A, developed cracks at the 01 Level and side shell, as shown in figure 4-12. A previous ship, referred to as ship B, which had a different structure but similar configuration at that area was in service for a longer time and had not developed any cracks. A series of engineering studies were carried out to quantify the service time required to initiate cracks similar to those found in ship A and grow them to their critical crack size.

To determine time required for crack initiation, cumulative fatigue damage was computed using Palmgren-Miner's rule. For loading, a 30 year North Atlantic stress exceedence curve based on lifetime bending moment at 50% operability was used. Cracks were assumed to initiate at a weld therefore S-N curves for welded specimen at stress ratio, R = -1 were used. Using these inputs, a fatigue comparison of ship A and ship B was carried out for locations at midship and at the actual location of the crack found in ship A. Results are shown in figure 4-13.

A similar study was conducted using the same stress spectrum and operating conditions to determine the time required for an existing surface crack, 6.4 mm long and 3.2 mm deep, to reach a critical length. Using high strength steel plate crack growth rate data in Paris' equation, a comparison of crack growth rate was made, for both ships. Results are shown in figure 4-14.

This study concluded that the use of fracture mechanics techniques and associated engineering assumptions could be applied to realistic operational scenarios and form the basis for quick response risk assessment decisions.

Example 4

This example illustrates the application of fracture mechanics techniques coupled with finite element analysis to analyze ductile fracture and tearing of a corrugated transverse bulkhead at the junction with the main deck. Reference [78], drawn from several case studies, demonstrates the application of techniques like fracture mechanics, impact analysis, sloshing load prediction, finite element methods and time-variant reliability analysis in the assessment of vulnerability of an in-service bulk carrier.

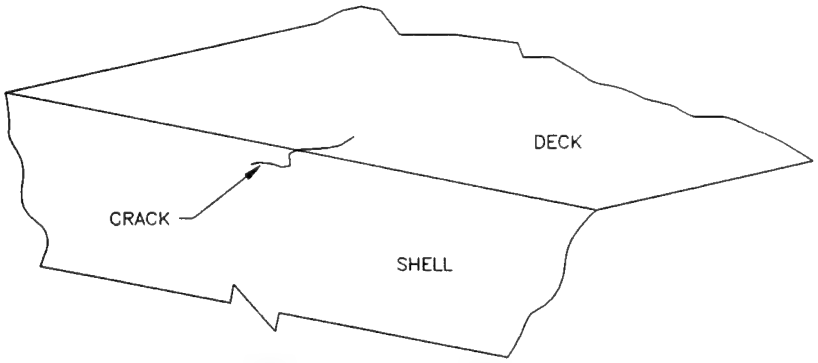

FIGURE 4.12 LOCATION OF THE CRACK ON SHIP A

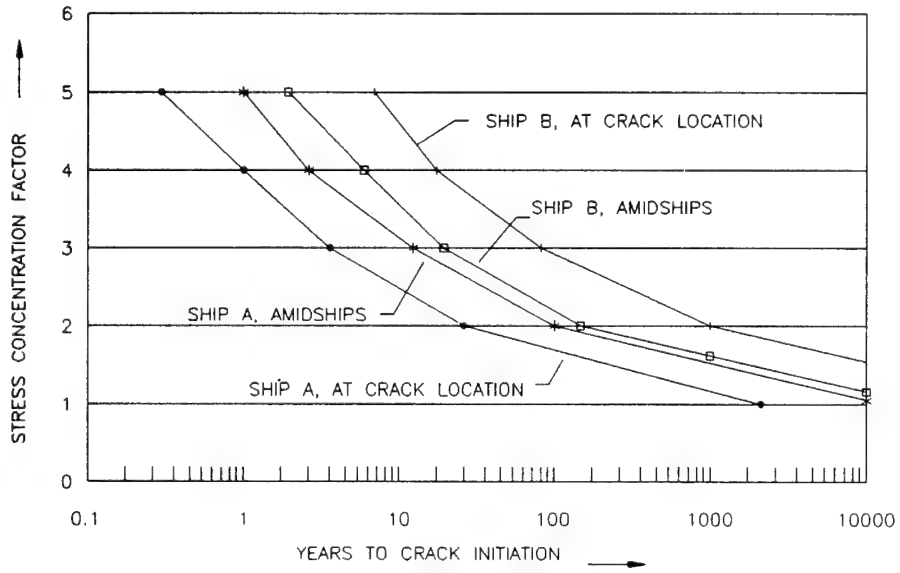

FIGURE 4.13 FATIGUE COMPARISON OF SHIPS A & B

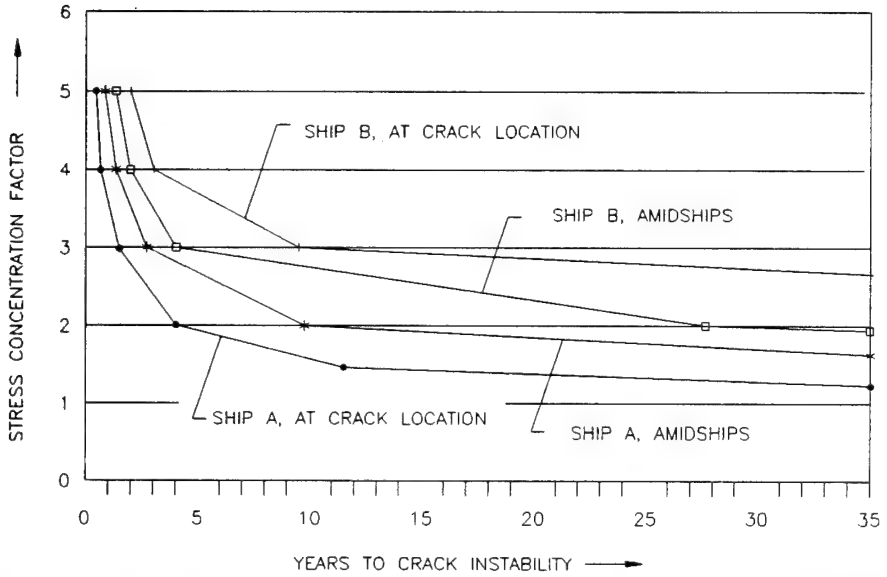

FIGURE 4.14 CRACK GROWTH COMPARISON OF SHIPS A & B

As mentioned earlier in chapter 2, the primary causes of failure of bulk-carriers are corrosion and fatigue cracking in side and transverse bulkhead structures. But recently it has been found that besides these factors, deficient operational and maintenance procedures have led to the loss of bulk carriers. For bulk carriers of single skin construction, with no effective cargo securing devices that are incorrectly loaded with high density solid cargo, there is the probability of side shell puncture due to impact of the solid cargo during heavy weather. Resulting ingress of water in the damaged cargo hold coupled with severe pitch motions, may lead to the fracture of transverse bulkhead at its junction with the upper deck and side wing tank due to excessive sloshing and hydrostatic pressure. Ultimately the loss of effectiveness of the transverse bulkhead may lead to hull girder collapse.

Reference [78] presented procedures for computing the energy absorption capability of side shell plating before rupture and the fracture strength of corrugated bulkhead under sloshing and hydrostatic loads. The energy absorption capability of side shell plating is estimated based on fracture (rupture) criteria. The rupture criteria is defined by the equivalent rupture strain and is strongly influenced by any defects embedded in a damaged structure. Figure 4-15 shows the relationship between the rupture strain near an internal defect and the size of the defect. The recommended equivalent rupture strain for welded structures is approximately 0.015 which represent 12.5 times the yield strain [79]. The stress value prior to the rupture of the side shell plate can be taken to be the yield stress.

The following table reproduced from [78], shows the variation of the energy absorption capacity with thickness of a 5.81m x 2.74m side shell plating which has a yield strength of 230 MN/m^2. E_{imp} is the static energy absorption capability while E_{dimp} is the modified E_{imp} to reflect the dynamic nature of impact.

t (mm)	E_{imp} (MJ)	E_{dimp} (MJ)
10.0	0.23	0.24
12.0	0.28	0.29
14.0	0.33	0.34
16.0	0.38	0.39
18.0	0.43	0.44
20.0	0.48	0.50
22.0	0.53	0.55

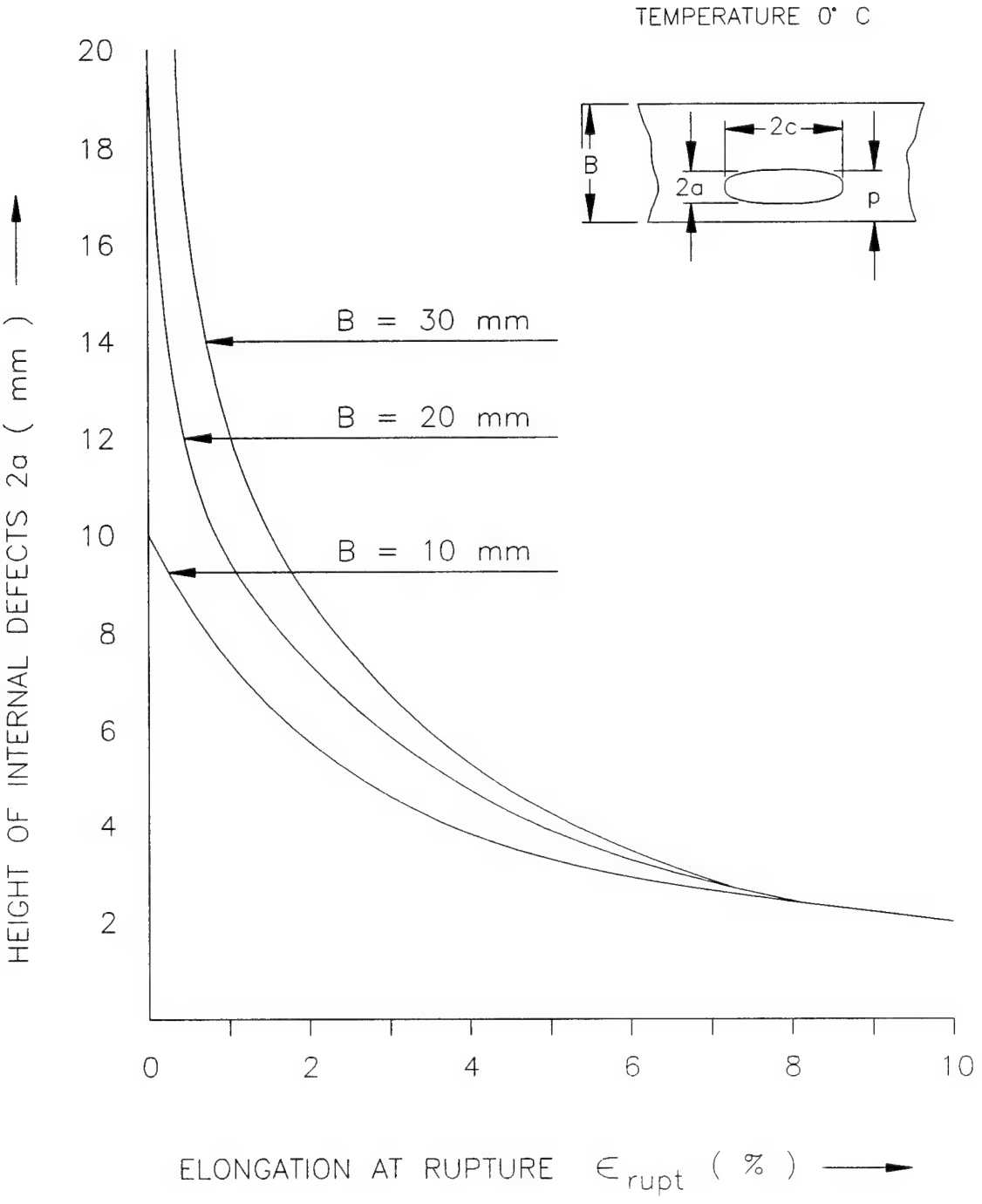

FIGURE 4.15 CRITICAL RUPTURE STRAIN AS A FUNCTION OF INTERNAL DEFECT SIZE (IN WELD) [79]

To evaluate the fracture strength of a corrugated bulkhead under sloshing and hydrostatic loads, a three-dimensional finite element model using shell elements to represent the corrugated bulkhead, cross deck strip, hatch coaming, hatch end beam and stiffeners attached to the bulkhead at the junction with the deck strip was used. The analysis predicted that moderate sloshing loads combined with stress concentrations due to structural discontinuities and residual weld stress, will cause large areas of the bulkhead at the junction with the upper wing tank and cross deck strip to undergo tensional stressing beyond the material yield strain. Therefore the fracture of mild steel bulkhead plating is usually not a brittle failure; extensive yielding occurs in the vicinity of critical fatigue cracks which induce the fracture. Using the value of strain obtained from the finite-element analysis, the author used the CTOD method and estimated a critical crack length of 40 mm for mild steel bulkhead plating having a critical CTOD, δ_{CR}, of 0.25 mm.

4.3.2 Offshore Structures

The lack of service life experience of offshore structures coupled with incidences of catastrophic failures, like the loss of "Alexander L. Kielland", has led to the development of the Norwegian Petroleum Directorate (NPD), safety criterion [80] for offshore structures. The most significant difference between the NPD regulations [80] and ship regulations such as ABS, DNV, etc., is the failure criterion applied in the former regulation. This criterion calls for an explicit check, during design, of the residual strength due to various assumed damaged conditions under normal operating conditions. Two instances of residual strength assessment, one on a mobile offshore platform [81] and the other on a fixed eight legged platform [82], are presented below.

Example 1

In [81], a non-linear finite element program based on "Idealized Structural Unit Method" (ISUM) is used to do an ultimate and residual strength assessment of a drilling rig of the Aker H3.2 type shown in figure 4-16. In the ISUM procedure, one finite element per structural element is used. Non-linear geometric and material behavior is included. Damage of tubular members, including permanent lateral deformation, dents and the effect of fire, are taken into account in the formulation. A number of explosion damage cases are simulated at critical locations. Two explosion damage cases in the mud room are considered. The first one is assumed to blow out one of the main walls in the mud room so that the oblique bracings are no longer effective. The second one assumes that the explosion has led to permanent deformation in the panels surrounding the mud room, in which case, the damage is modeled by reducing the shear area. Another explosion case occurs at the main leg and is simulated by its removal. Normalized load

versus displacement curves of the response of the platform to explosion damage in the mud room is shown in figure 4-17. Loads have been normalized to a design wave load due to a wave of length 88m and height of 9.5m, with a return period of 100 years. The displacements are normalized against the reference load pattern which is a combination of gravity loads and buoyancy forces. The results have been summarized in table 4-6.

Example 2

The ultimate and residual strength of a typical eight-legged, North Sea platform is computed in [82], using USFOS, an incremental, non-linear finite element program. USFOS is based on beam theory and accounts for large displacements and elasto-plastic material behavior. The platform shown in figure 4-18 is situated at a water depth of 70m. Its members have been sized according to the API-RP2A design code. Loading consists of the gravity load and environmental load. Three load cases were considered based on design waves with a return period of 100 years. They are:

- LC1: Waves 45° relative to the longitudinal axis (diagonal waves), Wave height = 26m.
- LC2: Waves along the longitudinal axis, Wave height = 27m.
- LC3: Waves perpendicular to the longitudinal axis, Wave height = 20.6m.

Four damage scenarios were studied. Two to simulate damage due to ship collision near the waterline and the other two to simulate damage at the lower ends of the jacket due to dropped objects. These four cases are:

- DC1: The complete cross-bracing at sea level is considered ineffective.
- DC2: A corner leg is assumed damaged at the sea level. The damage consisting of a dent of depth 0.35m (22% of the diameter) and a permanent lateral deformation of the neutral axis of 0.68m (3.2% of the leg length).
- DC3: Bottom, End row cross-bracing ineffective.
- DC4: Bottom, Front row cross-bracing ineffective.

Figure 4-19 is the response curve for the quartering sea case, LC1. The load is non-dimensionalized against the design wave load with a return period of 100 years. The displacement corresponds to a transverse displacement at the top corner node. Results of all calculations are summarized in table 4-7.

The study concluded the presence of tremendous reserve strength and redundancy in the jacket and the insignificant influence of relatively severe collision damages assumed at sea level.

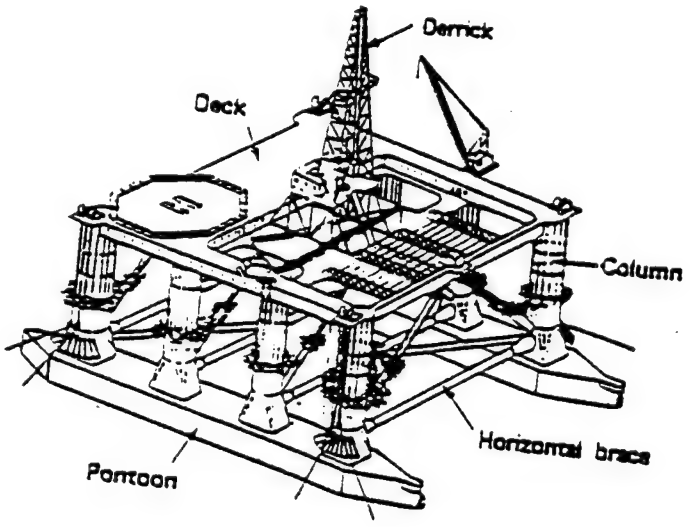

FIGURE 4.16 MOBILE OFFSHORE PLATFORM

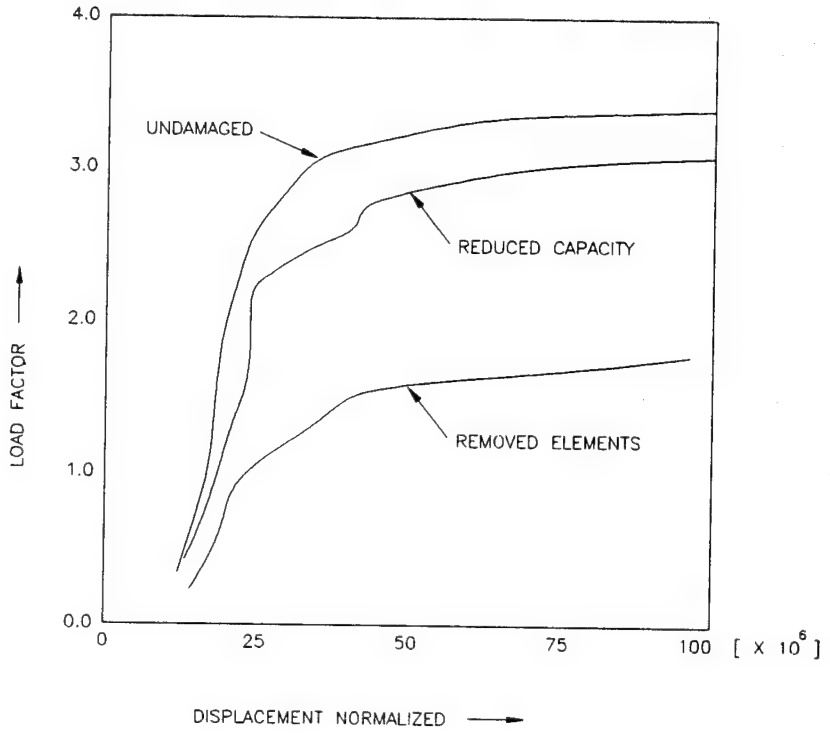

FIGURE 4.17 LOAD–NORMALIZED DISPLACEMENT FOR EXPLOSION IN MUD ROOM [81]

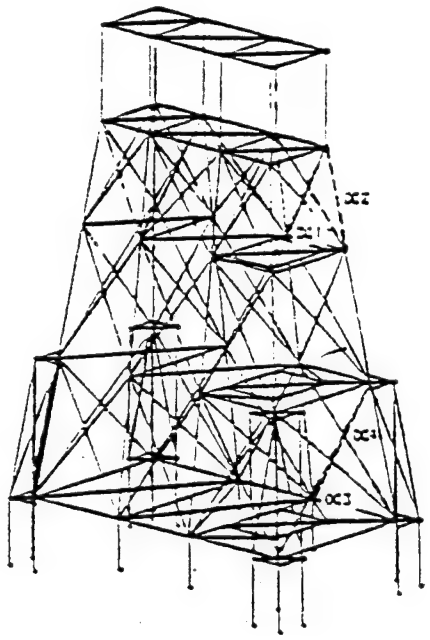

FIGURE 4.18 EIGHT LEGGED NORTH SEA PLATFORM

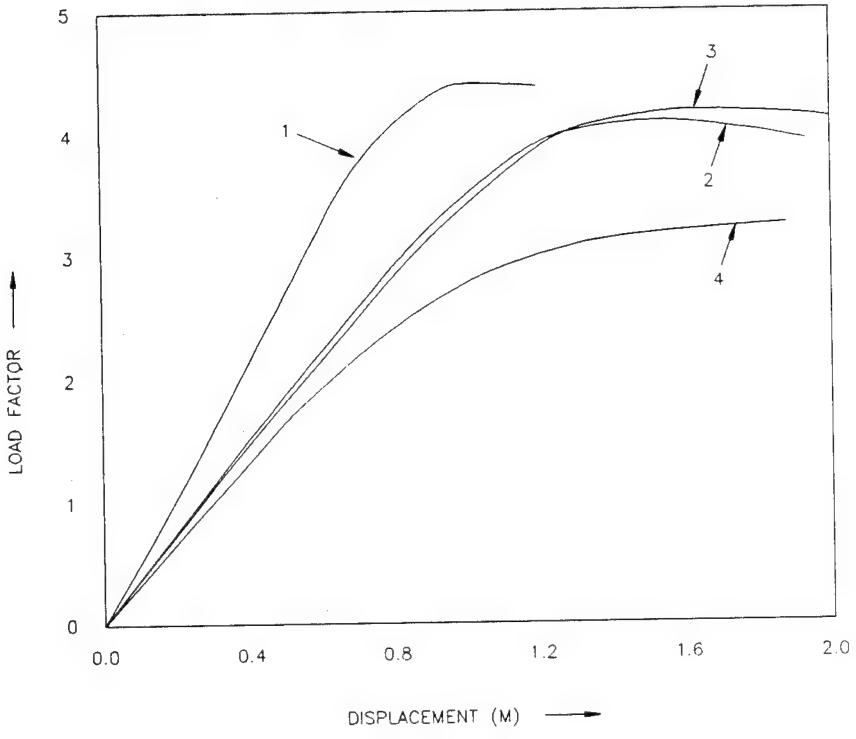

FIGURE 4.19 LOAD VERSUS TRANSVERSE DISPLACEMENT OF TOP CORNER NODE OF JACKET STRUCTURE.
(LC1-DIAGONAL WAVES) (82)

TABLE 4-6 RESULTS OF RESIDUAL STRENGTH ASSESSMENT OF A DRILLING RIG[81]. LOAD FACTORS ARE GIVEN IN MULTIPLES OF THE 100 YEAR WAVE LOAD.

Case	Condition	First yield	Ultimate	Reserve strength factor	Residual strength factor
1	Undamaged	1.28	3.76	3.76	
2	Explosion mud room Elements removed	0.18	1.86	-	0.49
3	Explosion mud room Reduced capacity	1.1	3.45	-	0.92
4	Explosion main leg	1.0	3.08	-	0.82

TABLE 4-7 RESULTS OF RESIDUAL STRENGTH ASSESSMENT OF A TYPICAL 8-LEGGED NORTH SEA PLATFORM[82]. LOAD FACTORS ARE GIVEN IN MULTIPLES OF THE 100 YEAR WAVE LOAD.

Case	Load Case	Damage Case	First yield	Ultimate	Reserve strength factor	Residual strength factor
1	LC1	Intact	2.60	4.39	4.39	-
2	LC1	DC1	2.64	4.10	-	0.93
3	LC1	DC2	2.52	4.25	-	0.97
4	LC1	DC3	2.00	3.15	-	0.72
5	LC2	Intact	2.49	3.71	3.71	-
6	LC2	DC4	1.82	3.38	-	0.91
7	LC3	Intact	2.99	4.32	4.32	-
8	LC3	DC3	2.19	3.39	-	0.78

LC1 = Diagonal Waves; LC2 = Longitudinal Waves; LC3 = Transverse Waves

DC1 = X-Bracing at sea level ineffective;
DC2 = Corner leg dented and laterally deformed;
DC3 = Bottom, end row X-Bracing ineffective;
DC4 = Bottom, front row X-Bracing ineffective.

4.3.3 Aircraft Structures

The principles and procedures of residual strength and life assessment of aging aerospace structure are embedded in the Aircraft Structural Integrity Program (ASIP). The ASIP program was initiated in 1958 by the USAF in response to fatigue failures on B-47 aircraft. A detailed history which led to the development of ASIP and the modifications which it underwent over time, can be found in [83-85].

In a general sense, aging aircraft are characterized by deteriorating strength and related problems such as crack development, loss of redundant features and the resulting increased maintenance cost. From a structural damage standpoint, [86] defines an aging aircraft as an aircraft that contains multiple site damage (MSD) characterized by the linkup of fatigue cracks. Since the inception of ASIP, USAF, commercial jet manufacturers and owners and NASA have been working in this interdisciplinary program on the maintenance of aging aircrafts. Issues related to maintenance are, safety and damage tolerance capability. Initially, damage tolerance analysis method used fracture mechanics in a deterministic manner. That is flaw growth was predicted using a fixed potential flaw size, a fixed da/dN versus ΔK relationship, and a stress spectrum derived from a predicted average usage. This is a conservative approach. In an aging fleet, structural damage is stochastic in nature. Hence presently stochastic procedures are being used to analyze initiation and growth of cracks and probability of fracture. A brief description of the research efforts under both these approaches - deterministic and probabilistic, and their practical applications in the military and commercial world are presented below, with a view to identify concepts and technologies which may be applicable to the marine industry.

Example 1: Deterministic Approach

Crack Growth Prediction: Crack growth predictions have been based on crack growth programs. These programs are automated procedures which predict the propagation of various flaw shapes in structural members under variable amplitude spectral loading environments. Figure 4-20 shows schematically the inputs and output of a crack growth program called "AGPF" used by the Douglas Aircraft Co. for their DC-10 Inspection Program [87]. A similar program called "EFFGRO" is used for the Fatigue Management of the A-7P Air Force aircraft [88]. They numerically integrate equations of crack growth rate to come up with a crack growth profile. EFFGRO utilizes Forman's equation (3.15).

From studying the influence of variable loading on crack growth rate, it has been found that peak overload blunts the crack tip and retards crack growth; EFFGRO uses the "Wheeler Retardation" model to mathematically represent this response. EFFGRO utilizes the

fracture toughness value (K_{IC}) for plane strain and critical stress intensity value (K_c) for plane stress failures given in [89, 90]. Crack tip stress intensity models for critical locations used in EFFGRO were developed and verified by coupon and/or component testing during the original A-7P ASIP [90] and during the testing phase of the program. For those which were not, closed form solutions for stress intensity factors were obtained using the computer program BTAB [91].

Inspection Interval: The outcome of damage tolerance analysis is to recommend inspection intervals and critical locations, to ensure the safety of the structure. This is done by determining the residual strength of the cracked structure. A schematic of the procedure taken from [87] for the DC-10 program is shown in figure 4-21. Combining the crack growth prediction results and residual strength results, shown schematically in figure 4-22, an inspection interval "L_n" in terms of flight hours is determined for a certain factor of safety. Recommendations based on such analysis are known as the Force Structural Maintenance Plan in the Air Force and MRB (Maintenance Review Board) Inspection Program, in the commercial world. Samples of Air Force Structural Maintenance Plan for the A7P taken from [88] and the DC-10 program taken from [87] are presented in tables 4-8 and 4-9.

Example 2: Probabilistic Approach

Burns, in [86] discusses a risk analysis computer code called PROF (PRobability Of Fracture) whose objective is to stochastically assess structural integrity. PROF was developed by the University of Dayton Research Institute under contract to the U.S. Air Force. PROF is a VAX-based computer program written in FORTRAN which is capable of determining the probability of fracture of an aircraft or fleet of aircraft subjected to a given usage. Inspection capabilities and intervals can be manipulated to yield the optimum inspection schedule for the specific aircraft or fleet. PROF accounts for cracking in the metallic aircraft structure, and accounts for a distribution of crack sizes that may exist in a structural detail. PROF does not account for any corrosion or multiple site damage (interaction) effects. A concise description of the principles behind the working of PROF and the output that can be obtained are provided below. Details can be obtained from [86].

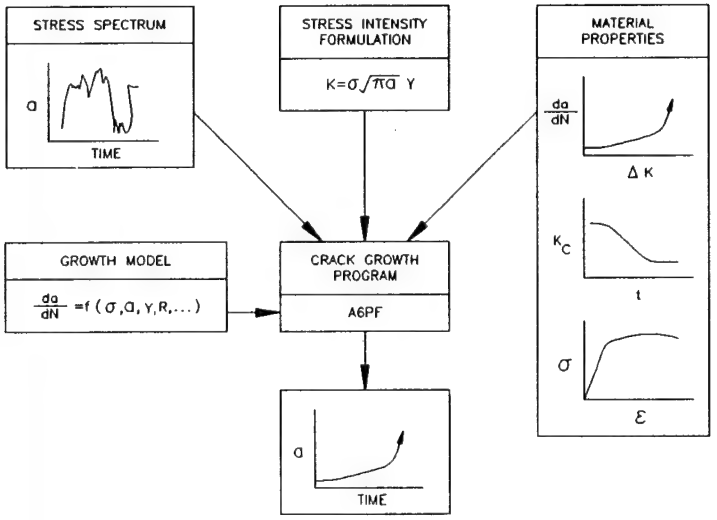

(87)

FIGURE 4.20 CRACK GROWTH PREDICTION

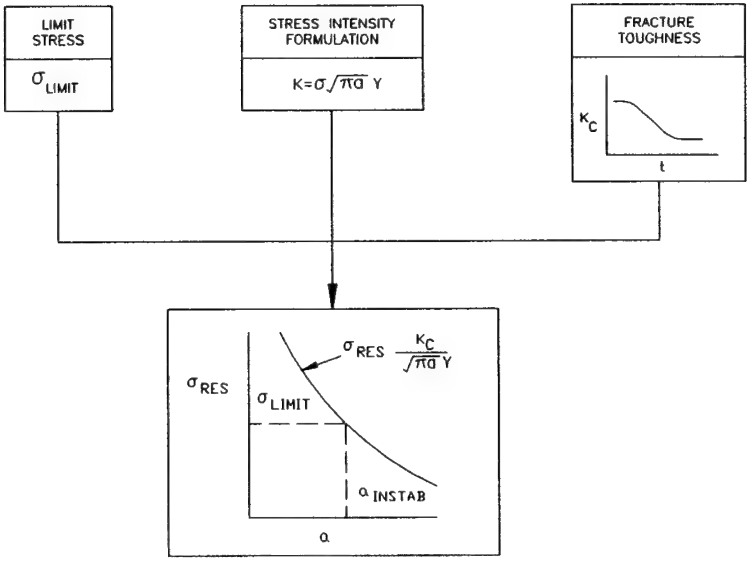

(87)

FIGURE 4.21 RESIDUAL STRENGTH PREDICTION

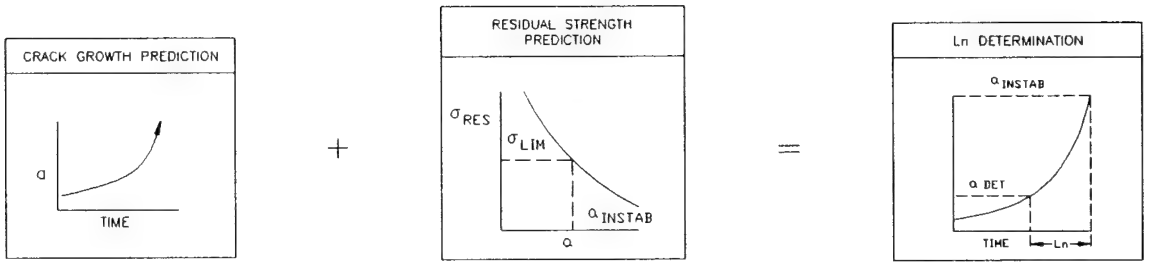

(87)

FIGURE 4.22 DAMAGE TOLERANCE EVALUATION BY ANALYSIS

TABLE 4-8 SAMPLE A-7P, CRITICAL LOCATIONS AND OPTIMUM INSPECTION INTERVALS[87]

CODE	DESCRIPTION	INSPECTION INTERVAL (FLIGHT HOURS) SEVERE ENVIRONMENT (SAFETY LIMIT/2)				CRITICAL SIZE
		INSPECTION PROCEDURES				
		IN-HOLE EDDY CURRENT		SURFACE EDDY CURRENT		C_{cr}** (IN.)
		PT	T	PT	T	
A1	LWS, WS24.6 @ 1st Intermediate Spar	6650	5690	3830	4670	4.00
A2	LWS, WS24.6 @ 2nd Intermediate Spar	3050	2180	1300	1700	1.55
A3	LWS, WS24.6 @ 3rd Intermediate Spar	3650	2385	1050	1725	1.47
A4	LWS, WS24.6 @ 4th Intermediate Spar	3350	2150	1050	1725	1.19
A5	LWS, WS24.6 @ 5th Intermediate Spar	3300	2100	975	1515	1.19
A6	LWS, Inb'd Pylon @ 2nd Intermediate Spar	5200	3650	1960	2840	2.82
A7	LWS, WS-53.7 @ Rear Spar (Dry hole)	1175	960	--	--	0.35
A8	LWS, WS-50.0 @ Rear Spar (Wet hole)	2350	1090	--	--	0.47
A9	LWS, WS-50.0 @ Rear Spar (Dry hole)	1210	1025	--	--	0.34
A10	Lower Spar Cap, WS-50.0 @ Rear Spar	1360*	1020*	--	--	0.47
A11	LWS, WS-32.2 @ 4th Intermediate Spar	3175	2060	925	1470	1.29
A12	LWS, Cntr Pylon @ 1st Intermediate Spar	6725	4560	2660	3800	2.74
A13	LWS, WS-32.2 @ 2nd Intermediate Spar	2950	2255	1185	1570	1.55
A14	LWS, WS-68.0 @ 4th Intermediate Spar	2850	2020	915	1400	1.29

* Does not include continuing damage
** Number in parenthesis is Part Through Critical flaw size
All others are Through Critical flaw size
-- Surface eddy current inspections do not apply
PT Part Through crack
T Through thickness crack

TABLE 4-9 SAMPLE DC-10, MAINTENANCE REVIEW BOARD (MRB) REPORT[86]

REFERENCE NO.	GENERIC STRUCTURAL ELEMENT	ZONES	SIGNIFICANT LOCATIONS	EXTERNAL HOURS	INTERNAL	
			DETAILS		HOURS	SAMPLES
541.13.021	Web, Stiffeners, and cutout doublers on upper face of spar	437,487	STA YN 266 to 342. Panels 437EL, 437FL, 487EL, and 487FL			1/5 or 20% (20,000)
541.14.025	Reverser door actuator support attach points and built-up hat section (applicable to - 10/10CF, - 30/30f/30cf Only)	415,416, 465,466	Fwd face of STA YN 222 bulkhead. Raise reverser door		4,000	
541.15.027	Bulkhead vertical caps and end fittings at lower ends	438,488	STA YN 286 aft face doors 438 AL, 438 AR, 488AL, and 488 AR	12,000		1/5 or 20% (20,000)

PROF is applicable to a population of structural elements. Population is defined as details which experiences essentially equivalent stress histories. Two main tasks performed by PROF are:

(i) Modeling the crack size distribution; which includes

(a) determination of growth of crack size distribution,
(b) maintenance effect on crack size distribution.

(ii) Determining the Probability of Fracture.

A flow chart of these tasks and subtasks is presented in figure 4-23.

Growth of Crack-Size Distribution Given an initial distribution of crack sizes at a reference time, T_R, the program estimates the distribution of crack sizes at $T_R + \Delta T$ flight hours by projecting the percentiles of the initial crack size distribution using the deterministic crack growth versus flight hours relation of the damage tolerance analysis. This calculation is performed in PROF by referring to data bases.

Maintenance Effect on Crack-Size Distribution Maintenance action will change the crack size distribution. This change is a function of the inspection capability and the quality of repair as shown in figure 4-23. Inspection capability is modeled in terms of the probability of detection as a function of crack size POD (a). Repair quality is expressed in terms of the equivalent repair crack size distribution, $f_r(a)$. Using these inputs the program determines a crack size distribution as a result of the maintenance action as shown in figure 4-23. The post-maintenance crack size distribution is then projected forward for the next interval of uninspected usage. The process is continued for as many inspection intervals as is desired.

Determination of Probability of Fracture Safety is quantified in terms of the probability of fracture (POF). POF is calculated as the probability that the maximum stress encountered in a flight will produce a stress intensity factor that exceeds the fracture toughness for a structural detail as shown in figure 4-23. This calculation is performed in two contexts. The single flight POF is the probability of fracture in the flight given that the detail has not fractured previously. The interval probability is the probability of fracture at any flight between the start of an analysis (reference time of zero or after a maintenance action) and the number of spectrum hours, T. This POF is useful in predicting the expected fractures in a fleet of aircraft in an interval and is required for the expected costs associated with a maintenance schedule. Using PROF, various kinds of parametric analyses can be performed like:

(i) Probability of panel fracture between inspections for selected inspection intervals.

(ii) Selecting the most optimum inspection interval based on cost.

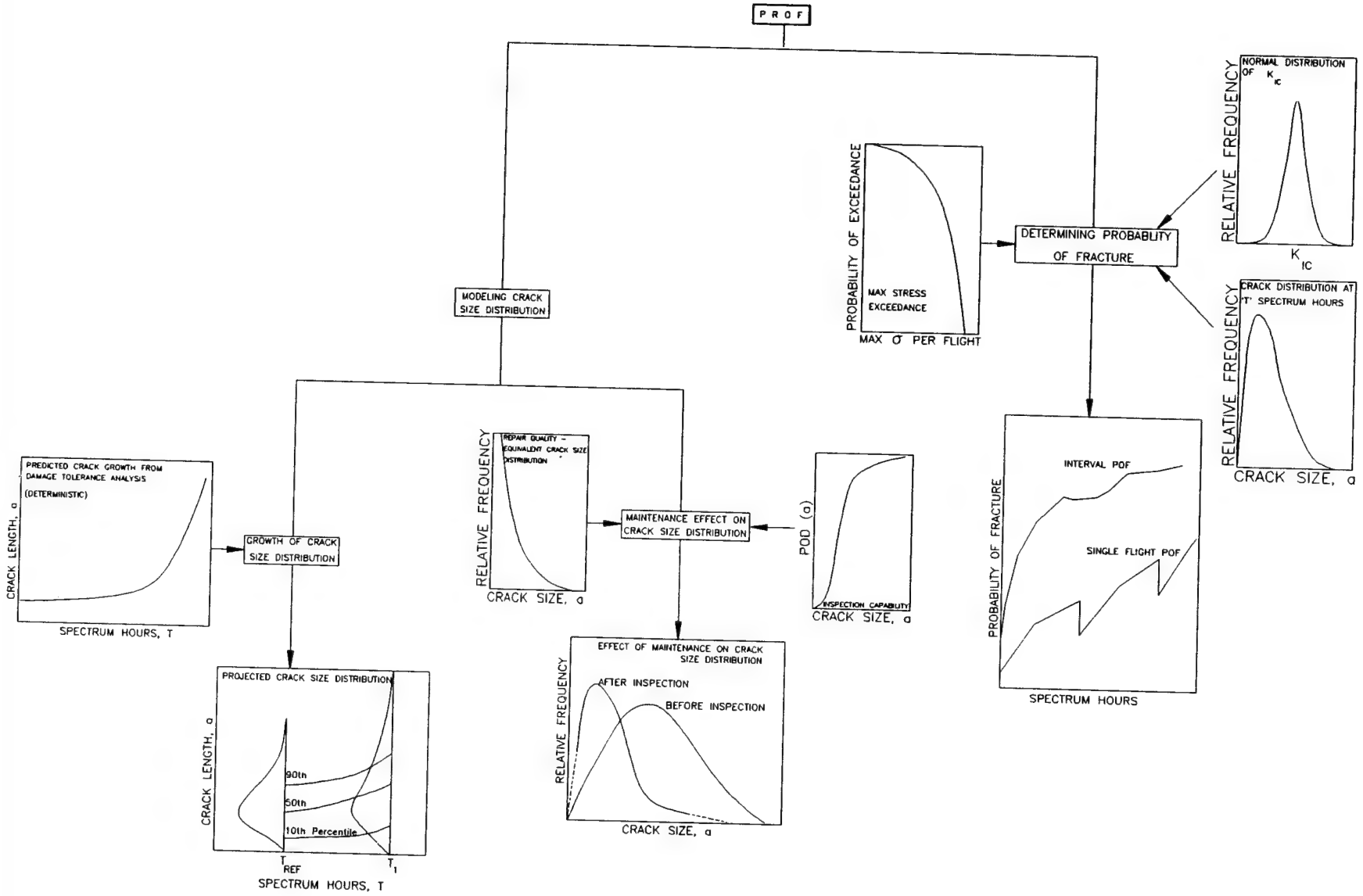

FIGURE 4.23 FLOW CHART SHOWING THE TASKS PERFORMED BY THE COMPUTER PROGRAM 'PROF'.[86]

4.4 References

1. Adamchak, J.C., "An Approximate Method for Estimating the Collapse of A Ship's Hull in Preliminary Design", Proceedings, Ship Structure Committee Ship Structure Symposium, Arlington, Va., October, 1984.

2. "Guidance Manual for the Inspection & Condition Assessment of Tanker Structures" produced by Tanker Structure Cooperative Forum (TSCF) and published by Witherby & Co. Ltd., U.K., 1992.

3. Weber, P.F., "Structural Surveys of Oil Tankers", Exxon paper presented at a joint meeting of the Institute of Marine Engineers & Royal Institution of Naval Architects, Trans I Mar E Vol. 96, 1984.

4. "Study Report on Bulk Carrier Loss", by Nippon Kaiji Kyokai (NKK), Japan, January 1992.

5. "Bulk Carriers: Guidance & Information to Shipowners and Operators", by International Association of Classification Societies (IACS), April 1992.

6. Y. Akita, "Lessons Learned from Failure & Damage of Ships", 8th International Ship Structures Congress, Gdansk, 1982.

7. C.A. Carlsen, et al., "Lessons Learned from Failure & Damage of Offshore Structures", 8th International Ship Structures Congress, Gdansk, 1982.

8. S. Hanzen & O. Nilsson, "Hull Damage in Large Ships", Lloyd's Register Technical Association Paper No. 1, Session 1972-73.

9. Proceedings of the 10th International Ship & Offshore Structures Congress, Vol. 2, Lyngby, August 1988.

10. C.R. Jordan and C.S. Cohran, "In-Service Performance of Structural Details", Ship Structure Committee (SSC-272), 1978.

11. C.R. Jordan and L.T. Knight, "Further Survey of In-Service Performance of Structural Detail", Ship Structure Committee (SSC-294), 1980.

12. Jennings, E., et al., "Inelastic Deformation of Plate Panels", Ship Structure Committee (SSC-364), 1991.

13. Wierzbicki, T., Chryssostomidis, C. and Wiernicki, C., "Rupture Analysis of Ship Plating due to Hydrodynamic Wave Impact", Ship Structure Symposium, October 15 - 16, 1984, Arlington, Virginia.

14. Wiernicki, C., "Damage of Ship Plating Due to Ice Impact Loads", SNAME, Marine Technology, January, 1986.

15. Anderson, T.L., "Elastic - Plastic Fracture Mechanics, A Critical Review (Part 1)", Ship Structure Committee (SSC-345), 1990.

16. "Guidance on the Methods for Assessing the Acceptability of Flaws in Fusion Welded Structures, PD 6493: 1991", Published by the British Standards Institution (BSI).

17. Heald, P.T., Spink, G.M. and Worthington, P.J., "Post Yield Fracture Mechanics", Materials Science and Engineering, Vol. 10, 1972.

18. Rouka, D.P. and Cartwright, D.J., "Compendium of Stress Intensity Factors", HMSO, London, 1976.

19. Tada, H., Parik, P. and Irvin, G., "The Stress Analysis of Cracks Handbook", Del Research Corporation, Hellertown, Massachusetts, 1973.

20. Oore, M. and Burns, D.J., "Estimation of Stress Intensity Factors for Irregular Cracks Subjected to Arbitrary Normal Stress Fields", Proceedings of 4th International Conference on Pressure Vessel Technology, London, Institution of Mechanical Engineers, Vol. 1, 1980.

21. Willoughby, A.A. and Davey, T.G., "Plastic Collapse at Part Wall Flaws in Plates", ASTM STP 1020, 1989.

22. Miller, A.G., "Review of Limit Loads of Structures Containing Defects", Central Electricity Generating Board Report TPRD/B/0093/N82 Rev. 1, December, 1984.

23. Caldwell, J.B., "Ultimate Longitudinal Strength", Transactions, RINA, 1965.

24. Ostapenko, A., "Strength of Ship Hull Girders under Moment, Shear and Torque", Proceedings, Ship Structure Committee Extreme Load Symposium, Arlington, Va., October, 1981.

25. Smith, C.S., and Dow, R.S., "Residual Strength of Damaged Steel Ships and Offshore Structures", Journal of Constructional Steel Research, Vol. 1, No. 4, September, 1981.

26. Frieze, P.A., et al. "Ultimate Load Behavior of Plates in Compression", Proceedings International Symposium on Steel Plated Structures, Crosby Lockwood Staples, London, 1977.

27. Little, G.H., "The Collapse of Rectangular Steel Plates Under Uniaxial Compression", Structural Engineer, Vol. 58b, No. 3, September, 1980.

28. Dowling, P.J., et al., "Plates in Biaxial Compression", CESLIC Report SP4, Imperial College, London, November, 1979.

29. Dier, A.F. and Dowling, P.J., "The Strength of Plates Subjected to Biaxial Forces", Proceedings of Conference on Behavior of Thin-Walled Structures, Glasgow, March 1983.

30. Valsgaard, S., "Ultimate Capacity of Plates in Transverse Compression", Det Norske Veritas Report No. 79-0104, February, 1979.

31. Smith, C.S. "Imperfection Effects and Design Tolerances in Ships and Offshore Structures", Transaction, Institute of Engineers and Shipbuilders, Scotland, Vol. 124, February, 1981.

32. Valsgaard, S., "Ultimate Capacity of Plates in Biaxial In-Plane Compression", Det Norske Veritas Report No. 78-678, March, 1979.

33. Dier, A.F. and Dowling, P.J., "Strength of Ships Plating: Plates Under Combined Lateral Loading and Biaxial Compression", CESLIC Report SP8, Imperial College, London, November, 1980.

34. Okada, H., et al. "Compressive Strength of Long Rectangular Plates Under Hydrostatic Pressure", Journal Society Naval Architecture, Japan, Vol. 146, Nov 1979.

35. Harding, J.E. et al. "Ultimate Load Behavior of Plates under Combined Direct and Shear In-Plane Loading", Proceedings of International Symposium on Steel Plated Structures, Crosby Lockwood Staples, London, 1977.

36. Hughes, O., and Franklin, P., "Definition and Validation of a Practical Rationally-Based Method for the Fatigue Analysis and Design of Ship Hulls", SNAME T&R Report No. R-41, February, 1993.

37. Newman, J. C., Jr., "Fatigue Crack Growth Analysis of Structures (FASTRAN) -- A Closure Model", COSMIC, 1984.

38. Berens, A.P., et al., "Risk Analysis For Aging Aircraft Fleets", The University of Dayton Research Institute, WL-TR-91.

39. "Methods and Models for Predicting Fatigue Crack Growth Under Random Loading", ASTM STP #748, 1981.

40. Parks, D.M., "The Inelastic Line-Spring: Estimates of Elastic-Plastic Fracture Mechanics Parameters for Surface-Cracked Plates and Shells", Transactions of the ASME, Vol. 103, August, 1981.

41. Kumar, V., German, M.D., and Schumacher, B.I., "Analysis of Elastic Surface Cracks in Cylinders Using the Line-Spring Model and Shell Finite Element Method", Journal of Pressure Vessel Technology, Vol. 107, November, 1985.

42. Kumar, V. and German, M.D., "Studies of the Line-Spring Model for Non-linear Crack Problems", Transactions of the ASME, Vol. 107, November, 1985.

43. Du, Z.Z. and Hancock, J.W., "Stress Intensity Factors of Semi-Elliptical Cracks in a Tubular Welded Joint Using Line Springs and 3D Finite Elements", Journal of Pressure Vessel Technology, Vol. 111, August, 1989.

44. Chen, Y.K., et al., "Ultimate Strength of Ship Structures", Transaction SNAME, Vol. 91, 1983.

45. Kutt, L.M., et al., "Evaluation of the Longitudinal Ultimate Strength of Various Ship Hull Configuration", Transactions, SNAME, Vol. 93, 1985.

46. Skaar, K.T., et al., "How low can steel weight go with safety and economy?", PRADS '87, Norway, June, 1987.

47. Valsgaard, S. & Steen, E., "Ultimate Hull Girder Strength Margins in Present Class Requirements", Marine Structural Inspection and Monitoring Symposium, presented by the SSC and SNAME, March 1991.

48. Ueda, Y. and Rashed, S.M.H., "The Idealized Structural Unit Method and its Application to Deep Girder Structures", Computers and Structures, Vol. 18, No. 2, 1984.

49. International Ship Structures Congress (ISSC) : "Non-Linear Structural Response", Report of Committee II.2, Genoa, 1985

50. Det Norske Veritas (DnV): "Buckling Strength Analysis of Mobile Offshore Units", Classification Notes, Note No. 30.1, Rev. 1987.

51. Valsgaard, S., "Numerical Design Predictions of the Capacity of Plates in Biaxial In-Plane Compression", Computers and Structures, Vol. 12, 1980.

52. Valsgaard, S. and Foss, G., "Buckling Research in Det Norske Veritas", Chapter 18, Buckling of Shells in Offshore Structures, Granada, London, 1982.

53. Carlsen, C.A., "A parametric study of collapse of stiffened plates in compression", The Structural Engineer, Vol. 58B(2), 1980.

54. Hellan, K., "Introduction to Fracture Mechanics", McGraw-Hill, 1984.

55. Y. Ueda and S.M.H. Rashed, "An Ultimate Transverse Strength Analysis of Ship Structure", J. of Society of Naval Architects of Japan, Vol. 136, 1974.

56. Y. Ueda and S.M.H. Rashed, "The Idealized Structural Unit Method and Its Application to Deep Girder Structures", Computers and Structures, Vol. 18, 1984.

57. Y. Ueda and S.M.H. Rashed and J.K. Paik, "Plate and Stiffened Plate Units of the Idealized Structural Unit Method (1st Report)", J. of Society of Naval Architects of Japan, Vol. 156, 1984.

58. Y. Ueda, S.M.H. Rashed and J.K. Paik, "Plate and Stiffened Plate Units of the Idealized Structural Unit Method (2nd Report)", J. of Society of Naval Architects of Japan, Vol. 159, 1986.

59. Y. Ueda, S.M.H. Rashed and M. Katayama, "Ultimate Strength Analysis of Double Bottom Structures by Idealized Structural by Idealized Structural Unit Method", J. of Society of Naval Architects of Japan, Vol. 138, 1975.

60. Y. Ueda, et al., "Ultimate Strength Analysis of Double Bottom Structures in Stranding Conditions", Proc. of 3rd International Symposium on Practical Design of Ships and Mobile Units, Trondheim, Norway, 1987.

61. J.K. Paik, et al., "Damage and Strength Analysis of Double Bottom Structures in Stranding", Proc. of the Autumn Meeting of Society of Naval Architects of Korea, 1990.

62. J.K. Paik, "Ultimate Strength Analysis of Ship Structures by Idealized Structural Unit Method", Dr. Dissertation, Osaka University, Japan, 1987.

63. J.K. Paik, "Ultimate Longitudinal Strength Analysis of the Double Skin Tanker by Idealized Structural Unit Method", Proc. of the Autumn Meeting of Society of Naval Architects of Korea, 1990.

64. J.K. Paik and D.H. Lee, "Ultimate Longitudinal Strength-Based Safety and Reliability Assessment of Ship's Hull Girder", J. of Society of Naval Architects of Japan, Vol. 168, 1990.

65. S.M.H. Rashed, "Ultimate Strength and Post-Ultimate Strength Behavior of Damaged Tubular Structural Members", Division of Marine Structures, Norwegian Institute of Technology, Report No. Sk/R52, 1980.

66. Y. Ueda and S.M.H. Rashed, "Behavior of Damaged Tubular Structural Members", J. of Energy Resources Technology, ASME, Vol. 107, 1985.

67. Y. Ueda, S.M.H. Rashed and K. Nakacho, "New Efficient and Accurate Method of Non-linear Analysis of Offshore Frames (The Idealized Structural Unit Method)", J. of Energy Resources Technology, ASME, Vol 107, 1985.

68. S.M.H. Rashed, et al., "Ultimate Strength of Jack-Up Rigs in Survival and Punch-Through Conditions", Proc. of 3rd International Symposium on Practical Design of Ships and Mobile Units, Trondheim, Norway, 1987.

69. T. Yao, J. Taby and T. Moan, "Ultimate Strength and Post-Ultimate Strength Behavior of Damaged Tubular Members in Offshore Structures", J. of Offshore Mechanics and Arctic Engineers, ASME, Vol. 110, 1988.

70. J.K. Paik and B.C. Shin, "Theoretical and Experimental Study for the Progressive Collapse Strength Analysis of Tubular Offshore Structures", Proc. of 1st Pacific/Asia Offshore Mechanics Symposium, Seoul, Korea, 1990.

71. J.K. Paik and H.K. Lim, "A Study on the Ultimate Strength Analysis of Frame Structures by Idealized Structural Unit Method", Proc. of the Autumn Meeting of Computational Structural Engineering Institute of Korea, 1990.

72. Paik, J.K. and Lim, H.K., "Progressive Collapse Strength Analysis of Jacket Type Offshore Structure", Proc. of the Autumn Meeting of Korea Committee for Ocean Resources and Engineering, 1990.

73. Rutherford, S.E. and Caldwell, J.B., "Ultimate Longitudinal Strength of Ships: A Case Study", SNAME Transactions, Vol. 98, 1990.

74. Hughes, O.F., "Ship Structural Design", published by SNAME, N. Jersey, 1988.

75. Melitz, D.T., Robertson, E.J. & Davison, N.J., "Structural Performance Management of VLCCs - An Owner's Approach", Marine Technology, Vol. 29, No. 4, Oct. 1992.

76. Bishop, R.E.D. and Price, W.G., "A Unified Dynamic Analysis of Ship Response to Waves", Transactions, RINA, Vol. 119, 1977.

77. Bishop, R.E.D., Price, W.G. and Tam, P.K.Y., "On the Dynamics of Slamming", Transactions, RINA, Vol. 20, 1978.

78. Shi, W.B. and Thompson, P.A., "Aspects of Vulnerability of Bulk Carrier Structures", RINA, International Conference on Bulk Carriers and Tankers - The Way Ahead, December, 1992.

79. Petersen, E. and Valsgaard, S., "Collision Resistance of Marine Structures, in Structural Crash-Worthiness" (ed. N. Jones and T. Wierzhicki), Butterworths, 1983.

80. The Norwegian Petroleum Directorate (NPD), "Regulation for Structural Design of Loadbearing Structures Intended for Exploitation of Petroleum Resources", 1985.

81. Amdahl, J., Taby, J. and Granli, T., "Progressive Collapse Analysis of Mobile Platforms", Proceedings of 3rd International Symposium on Practical Design of Ships and Mobile Units (PRADS), Norway, June, 1987.

82. Moan, T., "Advances in the Design of Offshore Structures for Damage Tolerance", International Conference on Advances in Marine Structures, ARE, Dumfermline, Scotland, May, 1986.

83. Wood, H.A., "The USAF Approach to Structural Life Management", Proceedings of International Symposium on The Role of Design, Inspection and Redundancy in Marine Structural Reliability, Committee on Marine Structures, Marine Board, National Research Council, National Academy Press, Washington, D.C., 1983.

84. Negaard, Gordon, R., "The History of Aircraft Structural Integrity Program", Aerospace Structures Information and Analysis Center (ASIAC) Report No. 680.1B, 1980.

85. King, T.T., "Some Developments in the Air Force Aircraft Structural Integrity Program (ASIP)", AFFDL-TR-70-144, AF Flight Dynamics Laboratory, Wright-Patterson AFB, Ohio, September 1970.

86. Burns, J.G., et al., "Aging Aircraft Structural Damage Analysis", Fatigue Management: 72nd Meeting of the AGARD Structures and Materials Panels, Bath, UK, April-May, 1991.

87. Warren, D.S., "Design and Inspection Interrelation for Commercial Jet Transport Structure", Proceedings of International Symposium on The Role of Design, Inspection and Redundancy in Marine Structural Reliability, Committee on Marine Structures, Marine Board, National Research Council, National Academy Press, Washington, D.C., 1983.

88. Santos, D., "Fatigue Management for the A-7P", Fatigue Management: 72nd Meeting of the AGARD Structures and Materials Panels, Bath, UK, April-May, 1991.

89. MCIC-HB-01, Damage Tolerance Design Handbook, May, 1984.

90. Report No. 2-53440/7R-5928, Vol. 1, Damage Tolerance and Fatigue Assessment, 31 January, 1977.

91. SDM-1000, "Practical Techniques for the Development of Mode I, Linear Elastic Stress Intensity Solutions For Typical Structural Details", July, 1985.

5.0 ULTIMATE STRENGTH ANALYSIS OF A TYPICAL TANKER

The purpose of this section is to illustrate the methodology proposed to assess the residual strength on a damaged tanker. This section draws on, section 2.0 - to identify damage locations, section 3.0 - for applicable local failure criteria and section 4.0 - for ultimate strength analysis at the global level. Based on findings of section 2.0 and hull survey records of the tanker, two damage locations were identified. Since damage at both locations was in the form of cracking, fracture criteria discussed in section 3.0 were used for failure assessment at the local level. On the basis of the local analysis, damaged components which where assessed as ineffective in carrying further load were neglected in the global analysis. The global analysis to evaluate the ultimate collapse strength, both in the intact and damaged condition, was carried out using ULTSTR, which is a simple ultimate strength program described in section 4.0.

5.1 Description of the Problem

5.1.1 Tanker Configuration

A single skin tanker as shown in figure 5-1, of length 239.57m, breadth 32m, depth 17.37m and displacement 85,000 tons was chosen for the case study. The structural configuration at midship of the tanker, which has a transverse frame spacing of 3.0m, is shown in figure 5-2.

5.1.2 Locations

Locations were selected based on the tanker's hull survey records. Two instances of damage were chosen. The first instance was cracking of the side shell longitudinal No. 8 in a wing ballast tank. The longitudinal was located near the summer loadline, approximately four tenths of the depth below the upper deck. Longitudinals in this region have been identified, based upon service experience (section 2.0) and analytically in reference [1], as being susceptible to fatigue cracking. The other instance was cracking of bottom longitudinal No. 24, at its connection with the transverse frame. Since this location is close to the extreme fiber of the cross-section, it is in a highly stressed region and therefore, any damage could be potentially catastrophic.

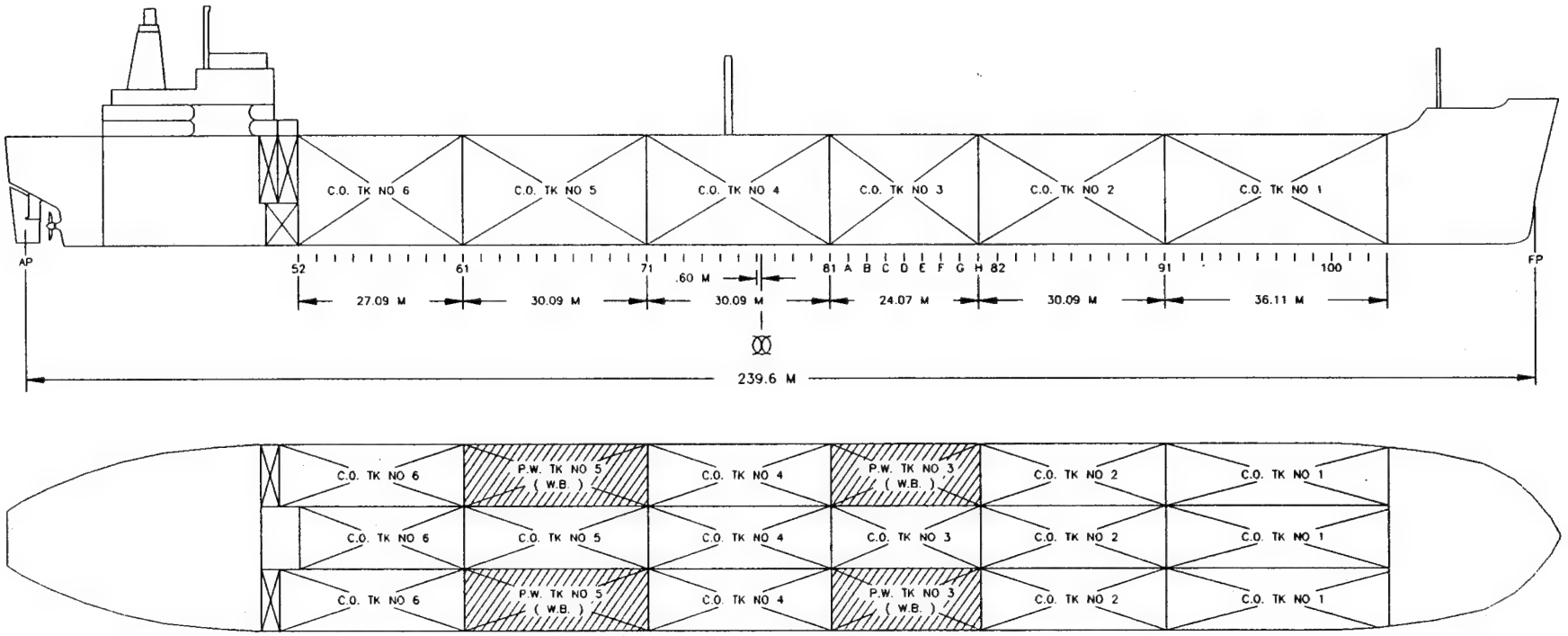

PARTICULARS	
LENGTH (O.A.)	246.9 M
LENGTH (B.P.)	239.6 M
BREADTH (MLD)	32.0 M
DEPTH (MLD)	17.37 M
DRAFT (SUMMER)	13.26 M
C_b	0.83
VELOCITY	16 KNOTS

FIGURE 5.1 PROFILE AND PLAN VIEW OF A 85,000 TANKER

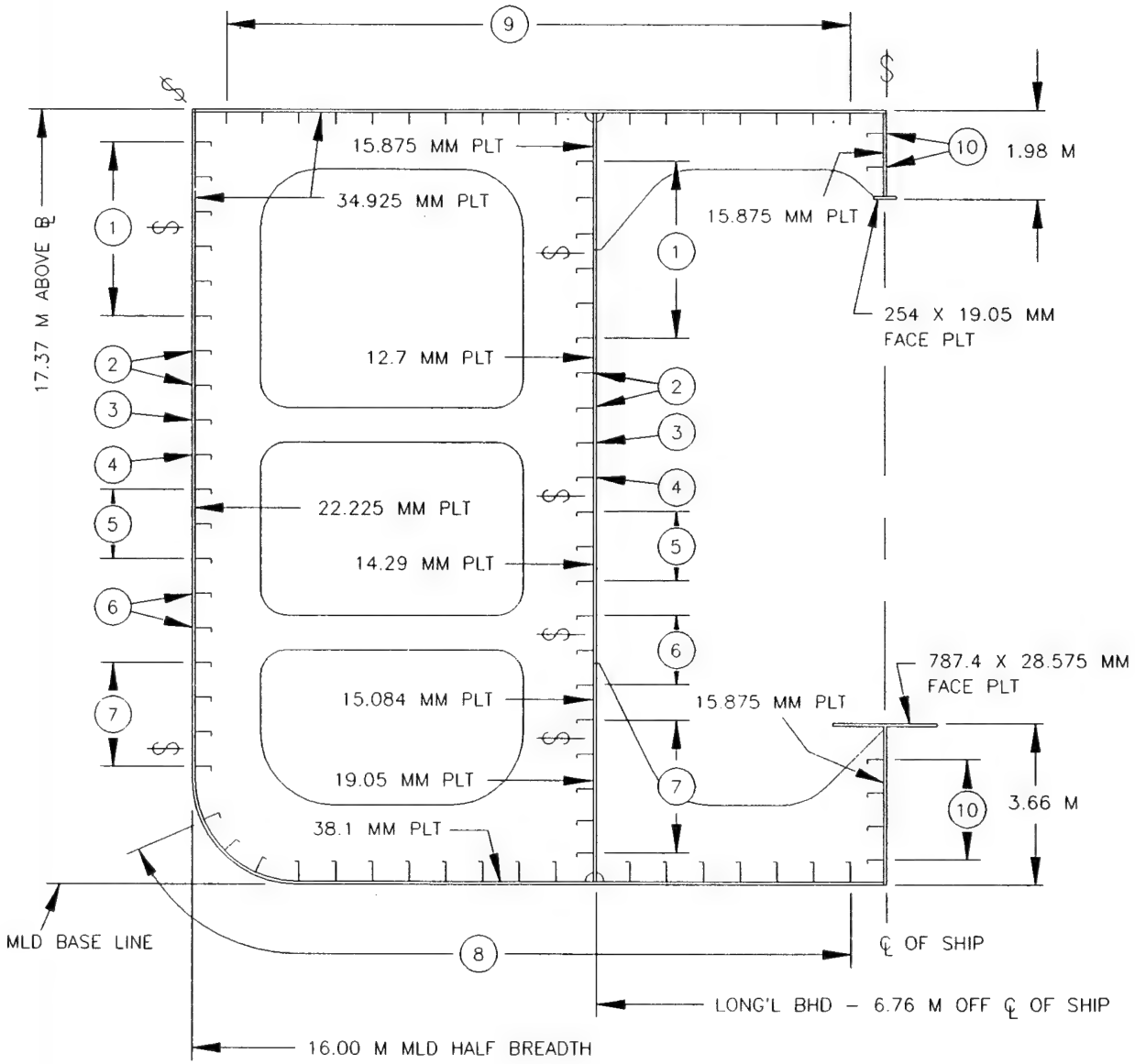

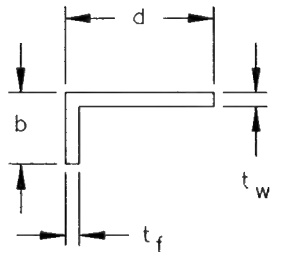

ALL MATERIAL – 'MS' STEEL

STF ID#	d^*	t_w^*	b^*	t_f^*
1	203.2	12.7	101.6	12.7
2	228.6	12.7	101.6	12.7
3	228.6	14.3	101.6	14.3
4	239.4	10.8	101.6	14.6
5	287.0	9.4	88.9	17.8
6	314.7	9.5	101.6	15.5
7	364.5	10.1	85.7	16.5
8	441.3	17.8	101.6	15.9
9	280.0	35.0	00.0	00.0
10	177.8	11.1	101.6	11.1

*ALL VALUES IN MM

FIGURE 5.2 MIDSHIP SECTION OF 85,000 TON TANKER

5.1.3 Type of Damage and Criteria

At the local level, structural components are well designed to guard against ductile forms of failure like buckling and yielding. The results of the limited damage survey presented in section 2.0 indicates that fatigue cracking is a documented form of failure for tankers. There are few useful guidelines in the marine industry to assess a cracked structure. For this reason PD 6493 [2] was chosen to determine critical crack length and crack growth history.

5.1.4 Loading

For the determination of fatigue inducing loads, the ABS guide on Fatigue Strength Assessment of Tankers [3] was followed. The guide identifies the following three primary load components that cause fatigue:

(1) hull girder bending moments (vertical and horizonal)

(2) external hydrodynamic pressure and

(3) internal tank loads (inertial fluid loads and added static head due to vessel motion).

The guide considers loads that arise from ordinary wave induced loads. It does not take into account wave impact loads, whipping, springing, tank fluid sloshing or vibrating forces due to machinery or propellers.

Eight load cases (LC1-LC8), depending on the internal tank loading pattern and the draft, are used for the assessment. The loading patterns for various internal tank arrangements are shown in figure 5-3, reproduced from [3]. Relevant coefficients and correlation factors to be used to calculate the individual load components and combined loads are provided in the guide and have been reproduced in table 5-1.

Depending on the location of the structural component in the ship, different combinations of the load cases are to be used to find the appropriate stress range. Vertically, the ship cross-section has been divided into two zones. Zone A comprises the deck and bottom structure, side shell and all longitudinal bulkhead structure within 15% of the ship's molded depth, D, from deck or bottom. The rest 70% of D, comprising of the side shell and all longitudinal bulkhead structures constitutes zone B. These zones are shown schematically in figure 5-4. The appropriate stress range for each zone is calculated based on the fluctuating load due to two selected load cases acting together. For Zone A, the greater value of (LC1 & LC2) or (LC3 & LC4) is used and for Zone B, the greater of (LC5 & LC6) or (LC7 & LC8).

TABLE 5-1 LOAD COMBINATIONS*

	L.C.1	L.C.2	L.C.3	L.C.4	L.C.5	L.C.6	L.C.7	L.C.8
A. HULL GIRDER LOADS								
Vertical B.M	Sag (-)	Hog (+)	Sag (-)	Hog (+)	Hog (+)	Sag (-)	Sag (-)	Hog (+)
k_c	1.0	1.0	0.7	0.7	0.3	0.3	0.4	0.4
Vertical S.F.	(+)	(-)	(+)	(-)	(-)	(+)	(+)	(-)
k_c	0.5	0.5	1.0	1.0	0.3	0.3	0.4	0.4
Horizontal B.M.					(+)	(-)	(-)	(+)
k_c	0.0	0.0	0.0	0.0	0.3	0.3	1.0	1.0
Horizontal S.F.					(+)	(-)	(-)	(+)
k_c	0.0	0.0	0.0	0.0	0.3	0.3	0.5	0.5
B. EXTERNAL PRESSURE								
k_c	0.5	0.5	0.5	1.0	0.5	1.0	0.5	1.0
k_{l0}	-1.0	1.0	-1.0	1.0	-1.0	1.0	-1.0	1.0
C. INTERNAL TANK PRESSURE								
k_c	0.4	0.4	1.0	0.5	1.0	0.5	1.0	0.5
W_v	0.75	-0.75	0.75	-0.75	0.25	-0.25	0.4	-0.4
W_l	Fwd BHD 0.25	Fwd BHD -0.25	Fwd BHD 0.25	Fwd BHD -0.25	-	-	Fwd BHD 0.2	Fwd BHD -0.2
	Aft BHD -0.25	Aft BHD 0.25	Aft BHD -0.25	Aft BHD 0.25	-	-	Aft BHD -0.2	Aft BHD 0.2
W_t	-	-	-	-	PORT BHD -0.75	PORT BHD 0.75	PORT BHD -0.4	PORT BHD 0.4
	-	-	-	-	STBD BHD 0.75	STBD HBD -0.75	STBD BHD 0.4	STBD BHD -0.4
C_ϕ, Pitch	-1.0	1.0	-1.0	1.0	0.0	0.0	-0.7	0.7
C_θ, Roll	0.0	0.0	0.0	0.0	1.0	-1.0	0.7	-0.7
D. REFERENCE WAVE HEADING AND MOTION OF SHIP								
Heading Angle	0	0	0	0	90	90	60	60
Heave	Down	Up	Down	Up	Up	Down	Down	Up
Pitch	Bow Down	Bow Up	Bow Down	Bow Up	-	-	Bow Down	Bow Up
Roll	-	-	-	-	STBD Down	STBD Up	STBD Down	STBD Up

* K_u = 1.0 for all load components.

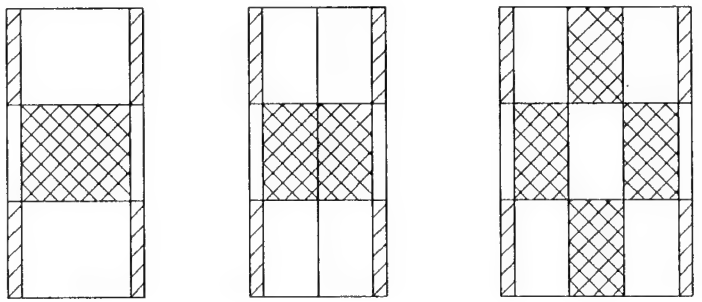

a) LOAD CASES #1, 3 & 7, 2/3 DESIGN DRAFT

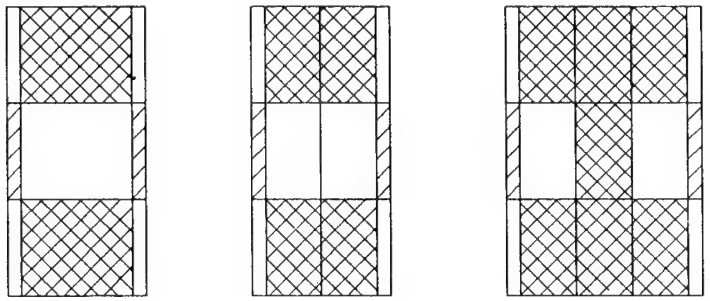

b) LOAD CASES #2, 4 & 8 DESIGN DRAFT

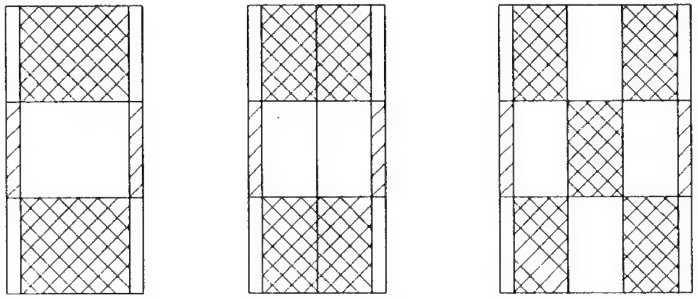

c) LOAD CASES #5, 2/3 DESIGN DRAFT

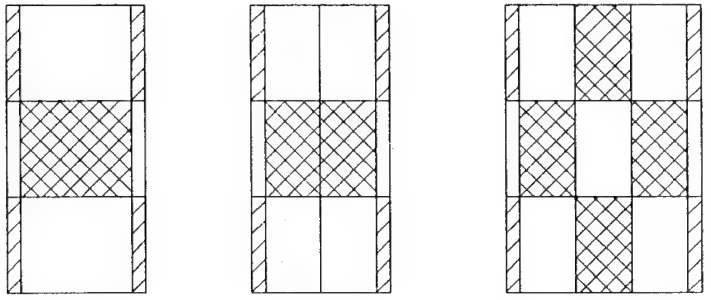

d) LOAD CASES #6, 2/3 DESIGN DRAFT

FIGURE 5.3 TANK LOADING PATTERNS

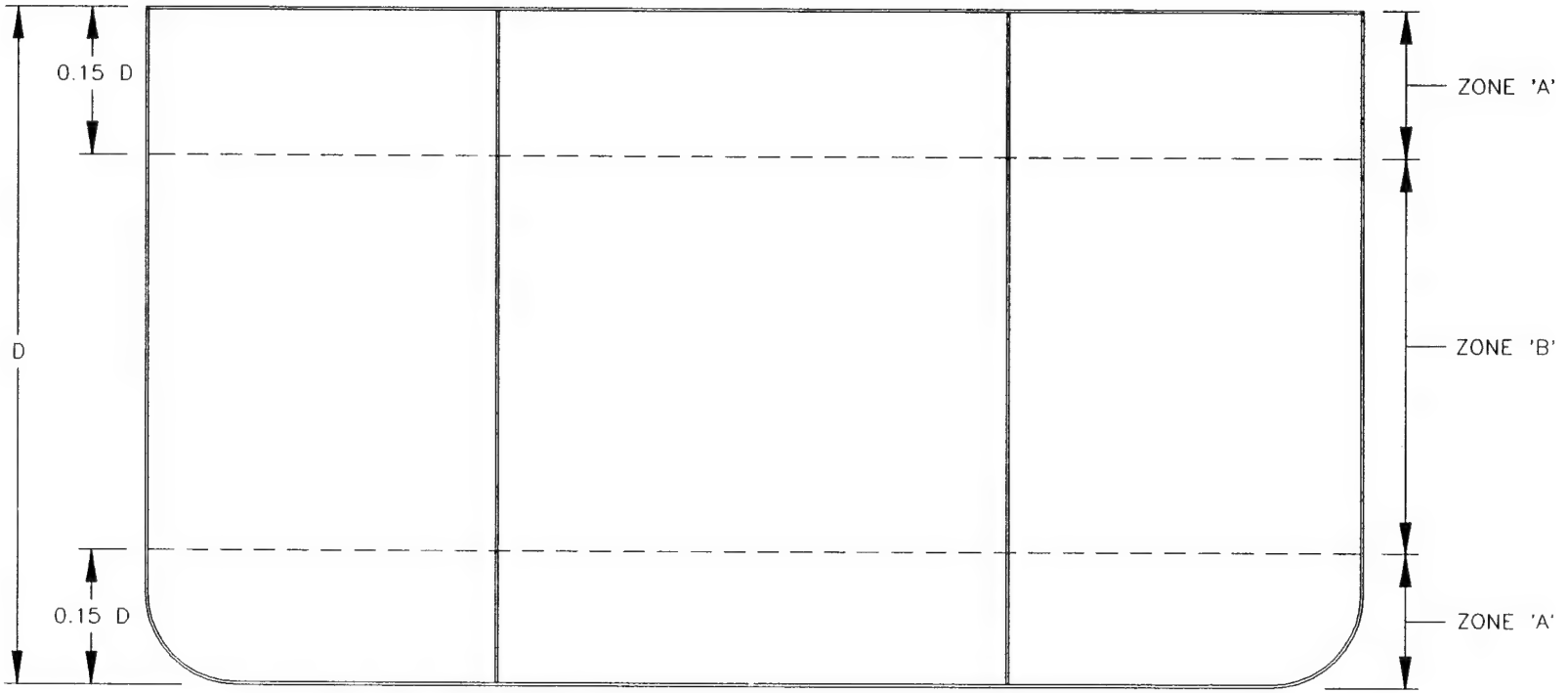

FIGURE 5.4 SCHEMATIC SHOWING THE ZONE A & ZONE B OF A TANKER CROSS SECTION

5.2 Local Level Analysis

Analysis at the local level involves determination of the critical crack length and development of a crack growth history. Damage at the two locations mentioned above, have been analyzed in the following two examples. While in example 1, the ratio of the nominal tensile stress, σ_1, acting on the cracked structure to the yield strength, σ_y, is less than 0.5, in example 2 it is greater than 0.5. Therefore, crack assessment was carried out at level one of PD 6493 for example 1 and at level two for example 2.

5.2.1 Example 1

In this example, cracking of the web of the side shell longitudinal No. 8 in No. 5 starboard ballast tank is analyzed. The longitudinal, is an angle bar with a web depth of 228.6 mm, flange width of 101.6 mm and thickness of 12.7 mm. The crack occurred between frames 66 and 67. It extends for 178 mm in the web of the stiffener and 76 mm in the flange. A description of the longitudinal with the crack and the adjoining region is shown schematically in figure 5-5. The longitudinal is located 11.01m above the baseline, which is about 60% of D and therefore in zone B. The analysis was divided into two parts. In the first part, the allowable crack length was determined based on the stresses calculated using equations found in [3] and crack assessment procedures of [2]. In part 2, crack growth analysis was performed by numerical integration of Paris' equation. The details of these procedures are provided below.

Part 1 - <u>Determination of Allowable Crack Length</u>

<u>Methodology</u>: According to PD 6493, the normal tensile stress, σ_1, acting on the cracked structure can be resolved into the primary stress, P, due to the externally applied load, secondary stress, Q, due to residual stresses and peak stress, F, due to concentrations caused by local discontinuities. The stress due to hull girder bending make up the membrane component of the primary stress, P_m, while the local bending of the stiffener due to external and internal pressure loads make up the bending component, P_b. Values of hull bending moments, which were calculated according to [3], are presented in table 5-2 along with the corresponding stress values for the following sectional properties of the tanker:

Moment of inertia about the horizontal N.A.	I_{yy}	$= 2.82 \times 10^6$ m^2-cm^2
Moment of inertia about the vertical N.A.	I_{zz}	$= 5.51 \times 10^6$ m^2-cm^2
Height of N.A. above baseline		= 8.57m
Vertical distance of SSL No. 8 from the N.A.	y	= 2.44m
Transverse distance of SSL No. 8 from the C.L.	z	= 16.00m

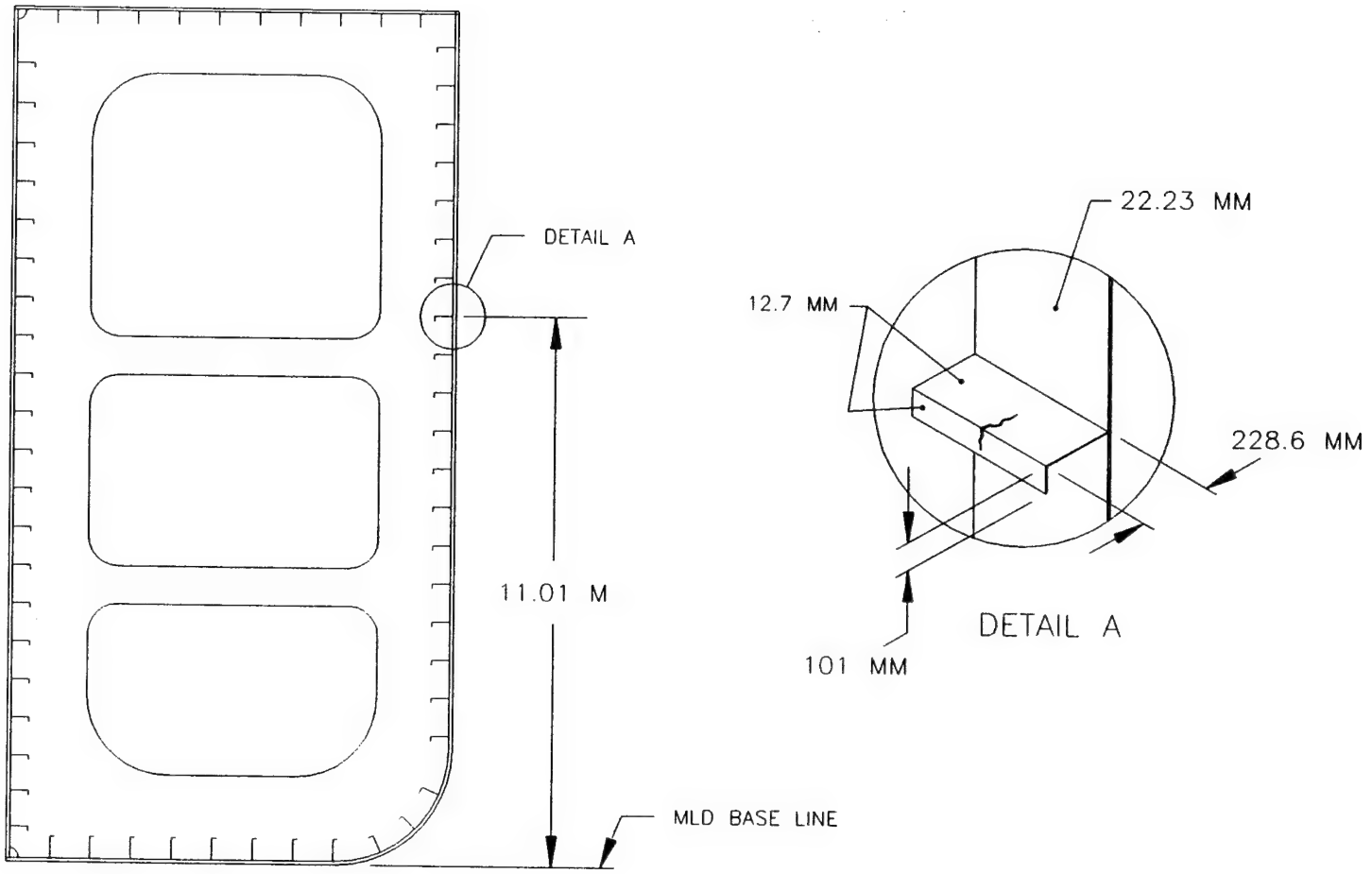

FIGURE 5.5 DESCRIPTION OF DAMAGE AT FR 66 1/2, SIDE SHELL LONGITUDINAL NO.8, EXAMPLE 1.

TABLE 5-2 BENDING MOMENT AND STRESSES AT SSL No. 8

	Bending Moment (N-m)	Stresses (N/mm^2)
Still Water B.M.	2.52×10^9	22.0
Vertical Wave B.M. (Sagging)	-1.14×10^9	-10.0
Vertical Wave B.M. (Hogging)	1.07×10^9	9.0
Horizontal Wave B.M.	$\pm 1.38 \times 10^9$	± 40.0

For crack analysis only tensile stresses are considered, therefore an average of the absolute values of the vertical wave bending stresses due to sagging and hogging was considered along with the still water bending stress and horizontal wave bending stress to determine P_m. Therefore,

$$P_m = 22 + 1/2\ (10+9) + 40 = 71.5\ N/mm^2$$

The stress range, f^*_{r2}, caused by the local bending of the stiffener due to pressure loading was computed according to the following formula given in [3]

$$f^*_{r2} = C_t\ M/SM \qquad (5.1)$$

where,

C_t = 1.5; correction factor for combined bending and torsional stress,

SM = 4.916 $m\text{-}cm^2$; sectional modulus of the longitudinal and the associated effective plating at the flange,

M = $k \cdot p \cdot s \cdot l^2$; bending moment at the supported ends of the longitudinal.

In the above expression for M,

k = 1.15/12; factor accounting for the fixity of the stiffener,

s = 800 mm; stiffener spacing,

l = 2.25m; unsupported span of the stiffener,

and p = 0.045 N/mm^2; total range of the net fluctuating pressure, based on equations found in [3].

Based on the above values, f^*_{r2} = 54 N/mm^2 for this crack location.

P_b, the bending component of the primary stress was taken as half of the stress range f^*_{r2}, which fluctuates between compression and tension. Therefore,

$$P_b = 0.5 \times 54 = 27 \text{ N/mm}^2$$

Because the crack is located on a longitudinal stiffener in an area between two transverse frames, with no connecting members in the vicinity, the secondary stress, Q, due to welding and peak stress, F, due to local discontinuities were assumed to be absent.

The material properties of the longitudinal stiffener were assumed to be those of Grade A mild steel. The data listed below are from [4] for plate thickness less than 25 mm.

Steel Type (Grade)	Young's Modulus E(N/mm^2)	Yield Strength σ_y(N/mm^2)	Ultimate Strength σ_u(N/mm^2)	Fractures Toughness K_{IC}(N/mm$^{1.5}$)	Minimum Service Temperature (°C)
MS (A)	207000	235	440	2136	0

As mentioned in [5], the likely range of fracture toughness, δ_{CR}, for mild steel grades lies between 0.15 mm and 0.60 mm at 0°C - 20°C and normal strain rates. In this example, at an operating temperature of 20°C, δ_{CR} was assumed to be 0.25 mm.

Fracture assessment in this example was carried out at level 1 of PD 6493. This is an initial screening level which provides very conservative results. At this level the maximum tensile stress, σ_1, is taken to be uniform and equal to the maximum sum of the values of the stress components ($P_m + P_b + Q + F$). Since Q and F were assumed to be zero,

$$\sigma_1 = P_m + P_b = 71.5 + 27 = 98.5 \text{ N/mm}^2$$

Depending on the fracture toughness values, which could be based on the K-method or the δ-method, two allowable crack lengths were obtained.

K-Method:

$$\bar{a}_m = \frac{1}{2\pi}\left(\frac{K_{mat}}{\sigma_1}\right)^2 \tag{5.2}$$

where $K_{mat} = K_{IC}$. Therefore,

$$\bar{a}_m = \frac{1}{2\pi}\left(\frac{2136}{98.5}\right)^2 = 72 \text{ mm}$$

CTOD-Method:

$$\bar{a}_m = \frac{\delta_{mat} E}{2\pi\left(\frac{\sigma_1}{\sigma_y}\right)^2 \sigma_y} \qquad \text{for } \frac{\sigma_1}{\sigma_y} \leq 0.5 \tag{5.3}$$

$$\bar{a}_m = \frac{\delta_{mat} E}{2\pi\left[\frac{\sigma_1}{\sigma_y} - 0.25\right]\sigma_y} \qquad \text{for } \frac{\sigma_1}{\sigma_y} > 0.5$$

where $\delta_{mat} = \delta_{CR}$. Since,

$$\frac{\sigma_1}{\sigma_y} = \frac{98.5}{235} = 0.42 < 0.5$$

Therefore,

$$\bar{a}_m = \frac{0.25 \text{x} 207000}{2\pi\ (0.42)^2\ 235} = 199 \text{ mm}$$

Finite Width Correction: If the calculated $\bar{a}_m$ exceeds one twentieth of the width, W, of the component, which in this case is the depth of the web of the longitudinal stiffener (228.6 mm), PD 6493 suggests a finite width correction to be applied to $\bar{a}_m$:

$$\bar{a}_{m(cor)} = \bar{a}_m \left[\frac{1}{1 + \left(\frac{\bar{a}_m}{W} \right)} \right] \tag{5.4}$$

On applying this correction, the allowable crack lengths were:

K-Method - 56 mm
CTOD - 106 mm

In level 1 assessment, a check against plastic collapse of the component was made separately by calculating the collapse ratio, S_r. Plastic collapse occurs due to the overall yielding of the uncracked ligaments of the cross-section. S_r is the ratio of effective net section stress, σ_n, to the flow strength, σ_f, of the component which should not exceed 0.8.

For flat plates, PD 6493 suggest the following formula to calculate σ_n:

$$\sigma_n = \frac{P_b + (P_b^2 + 9P_m^2)^{0.5}}{3\left\{1 - \frac{a}{W}\right\}} \tag{5.5}$$

where "a" is the crack length and the flow strength, σ_f, is defined as the lesser of the average of yield strength, σ_y, and ultimate tensile strength, σ_u, or $1.2\sigma_y$. Therefore,

$$\sigma_f = \min\left\{\frac{\sigma_u + \sigma_y}{2},\ 1.2\sigma_y\right\} = 282\ N/mm^2 \tag{5.6}$$

The S_r values calculated based on the allowable crack length of 56 mm and 106 mm were 0.38 and 0.53 respectively which are less than 0.8 implying they would not result in plastic collapse.

The allowable crack length predicted by the K-method is conservative because it is based on fracture toughness value, K_{IC}, determined from coupon tests under plain strain conditions. Plain strain conditions imply high degree of constraint around the cracked region. The fracture toughness, δ_{CR}, used in the CTOD method are based on experiments which allow for plasticity of the specimen and hence are close to conditions experienced by real structures under minimum constraint. In this example, the crack is assumed to be in a region of relatively low constraint. Therefore the crack length, 106 mm, predicted by the CTOD method was considered to be the maximum allowable crack length.

Part 2 - Crack Growth Analysis by the General Procedure

Methodology: To determine the relationship between crack length and time, PD 6493 suggests integration of the Paris' equation which is:

$$\frac{da}{dN} = C(\Delta K_I)^m \qquad (5.7)$$

where,

da/dN is the rate of crack propagation

'C' and 'm' are constants depending on the material, environment and frequency of the applied load.

ΔK_I is the range of stress intensity factor corresponding to the applied stress cycles and instantaneous crack length.

For structural ferritic steels operating in marine environments at temperatures up to 20°C, PD 6493 suggests the use of following values for 'C' and 'm':

$C = 2.3 \times 10^{-12}$
$m = 3.0$

The threshold stress intensity factor, ΔK_{th}, below which there is no crack growth was assumed to be 63 $N \cdot mm^{-3/2}$ per PD 6493.

ΔK_I for a through thickness crack was calculated using the following expression from PD 6493:

$$\Delta K_I = (\Delta P_m + \Delta P_b) \left\{\pi a \, \mathrm{Sec} \, \frac{\pi a}{W}\right\}^{0.5} \qquad (5.8)$$

where,

ΔP_m is the primary membrane stress range
ΔP_b is the primary bending stress range
a is the instantaneous crack length and
W is the width of the component.

ΔP_m results from horizonal and vertical hull girder bending due to waves. Still water bending is not considered since it is a steady, unfluctuating stress which does not contribute to fatigue crack growth. Therefore,

$$\Delta P_m = |\sigma_{VS}| + |\sigma_{VH}| + 2|\sigma_H| \qquad (5.9)$$

where σ_{VS} and σ_{VH} are the vertical bending stresses due to sagging and hogging respectively and σ_H is the horizontal wave bending stress. Using the values of the stresses from table 5-2,

$$\Delta P_m = 10 + 9 + 2(40) = 99 \text{ N/mm}^2.$$

ΔP_b is the stress range due to local bending of the stiffener caused by the fluctuating pressure load and was calculated previously as f^*_{r2} in equation (5.1). Thus,

$$\Delta P_b = 54 \text{ N/mm}^2.$$

In the absence of a measured stress spectrum acting on the ship, a stress spectrum was generated from data available from [4]. This data reflects short-term simulated North-Sea conditions used for fatigue studies in the offshore industry. This condition consists of eleven wave heights or sea states. The maximum significant wave height is 16m. For each sea-state, its significant wave height, H_{si}, fraction of time spent in that sea-state, p_i, and its frequency, f_i are presented in table 5-3. The stress spectrum was obtained by assuming the maximum stress range, $\sigma_{r\,max}$, which is the sum of ΔP_m and ΔP_b, corresponds to the maximum significant wave height. The other stress ranges, σ_{ri}, were obtained as follows:

$$\sigma_{ri} = (H_{si}/H_{s\,max})\,\sigma_{r\,max}$$

In this example it was assumed that:

(a) the length of each voyage is 30 days or 0.08 year and
(b) for short term damage estimation, the stress spectrum is repeated every month.

The number of cycles, n_i corresponding to a particular stress range was calculated as:

$$n_i = p_i \, f_i \, T$$

where, T = 2627895 sec (30 days).

TABLE 5-3 SHORT TERM NORTH SEA STRESS SPECTRUM

Wave Level	H_{si} (m)	p_i	f_i (Hz)	σ_{ri} (N/mm^2)	n_i (Cycles)
1	16.0	0.0000368	0.0976	153.20	9
2	14.5	0.0000932	0.1040	138.83	25
3	13.0	0.0003700	0.1090	124.47	106
4	11.5	0.0022000	0.1200	110.11	694
5	10.0	0.0073000	0.1330	95.75	2551
6	8.5	0.0135000	0.1440	81.39	5109
7	7.0	0.0265000	0.1600	67.02	11142
8	5.5	0.0600000	0.1780	52.66	28066
9	4.0	0.2100000	0.1990	38.30	109820
10	2.5	0.4900000	0.2230	23.94	287150
11	1.0	0.1900000	0.2710	9.57	135310

The stress ranges, σ_{ri} and number of cycles, n_i, are shown in table 5-3. Crack growth under variable amplitude loading is affected by the sequence of application of the stress ranges in the spectra. As demonstrated in references [6, 7], the root mean square (rms) value of the stress spectra can be used in the calculation of ΔK. The rms value of the stress ranges was calculated using the following formula:

$$\Delta\sigma_{rms} = \sqrt{\frac{\sum_{i=1}^{K} n_i \sigma_{ri}^2}{\sum_{i=1}^{K} n_i}} \qquad (5.10)$$

where,

K = number of stress ranges; 11 in this case
n_i = number of cycles for the i^{th} stress range
σ_{ri} = value of the i^{th} stress range,
$\Delta\sigma_{rms}$ = root mean square value of the stress ranges.

For the assumed stress spectrum, which has a maximum stress range, $\sigma_{r\,max}$ = 153 N/mm^2, the $\Delta\sigma_{rms}$ was calculated to be 30.3 N/mm^2. This value was used in calculating the stress intensity factor range, ΔK used in the crack growth equation (5.7).

Therefore,

$$\Delta K_{rms} = \Delta\sigma_{rms}\left\{\pi\ a\ Sec\left(\frac{\pi a}{W}\right)\right\}^{0.5} \tag{5.11}$$

The crack propagation equation (5.7), was integrated numerically using a step by step procedure. These steps are explained below:

1. Determination of a_j: Starting with an initial crack length, a_0, at each step 'j' the crack length was increased by a predetermined increment, Δa. Increments are either uniform or logrithmic. Logrithmic increments are used when the desired number of increments is small. The present work utilized logrithmic increments, calculated as,

$$\Delta a = \frac{\log(a_f) - \log(a_0)}{N_{inc}} \tag{5.12}$$

where:

a_f = 106 mm ; the final crack length
a_0 = 0.005 mm; assumed initial crack length
N_{inc} = 100; number of increments

so that the crack length at the end of the jth increment is

$$a_j = 10^{\log(a_0) + j\Delta a} \tag{5.13}$$

2. Determination of ΔK_j: ΔK_j used for the calculation was assumed to be constant over each increment and was based on the crack length at the end of the increment. Therefore:

$$\Delta K_j = \Delta\sigma_{rms}\left\{\pi\ a_j\ Sec\left(\frac{\pi a_j}{W}\right)\right\}^{0.5} \tag{5.14}$$

3. Determination of N_j: The number of cycles used in extending the crack over each increment, N_j, was calculated using equation (5.7). Thus,

$$N_j = \frac{a_j - a_{(j-1)}}{C(\Delta K_j)^m} \qquad (5.15)$$

where,

a_{j-1} is the crack length at the beginning of the j^{th} step, and a_j is the crack length at the end of the j^{th} step.

The cumulative sum of the number of cycles at each step, N_1, N_2, ...N_j gave the total number of cycles expended to reach the crack length, a_j, at the end of the j^{th} step.

The results of the crack growth analysis are shown in figure 5-6.

Conclusions:

Based on assumptions on loading, stress estimation, generation of the sea-spectra and the conservatism of the procedures of PD 6493 in determining critical crack length, an allowable crack length of 106 mm was determined. A crack longer than the allowable may lead to unstable fracture. Therefore the observed crack of 178 mm on the web of the longitudinal is not-permissible. From the results of crack growth analysis done in Part 2, it is evident that it takes little over 6 voyages for an initial crack of length 0.005 mm to reach an allowable length of 106 mm. Therefore considering a factor of safety of 2, this crack should be repaired within approximately three months of its discovery.

5.2.2 Example 2

At frame 81B of No. 3 port ballast tank, cracks were found at the attachment welds of the vertical flat bar stiffener to the bottom longitudinal No. 24 on the aft side of the transverse web frame. A schematic of the region is shown in figure 5-7. In this example, crack assessment was performed at level 2 of PD 6493 since the ratio of nominal tensile stress to the yield strength was greater than 0.5. At this level plastic collapse is implicitly taken into account through interaction curves. A similar analysis, as done in example 1, was carried out for this example, the results of which are presented below.

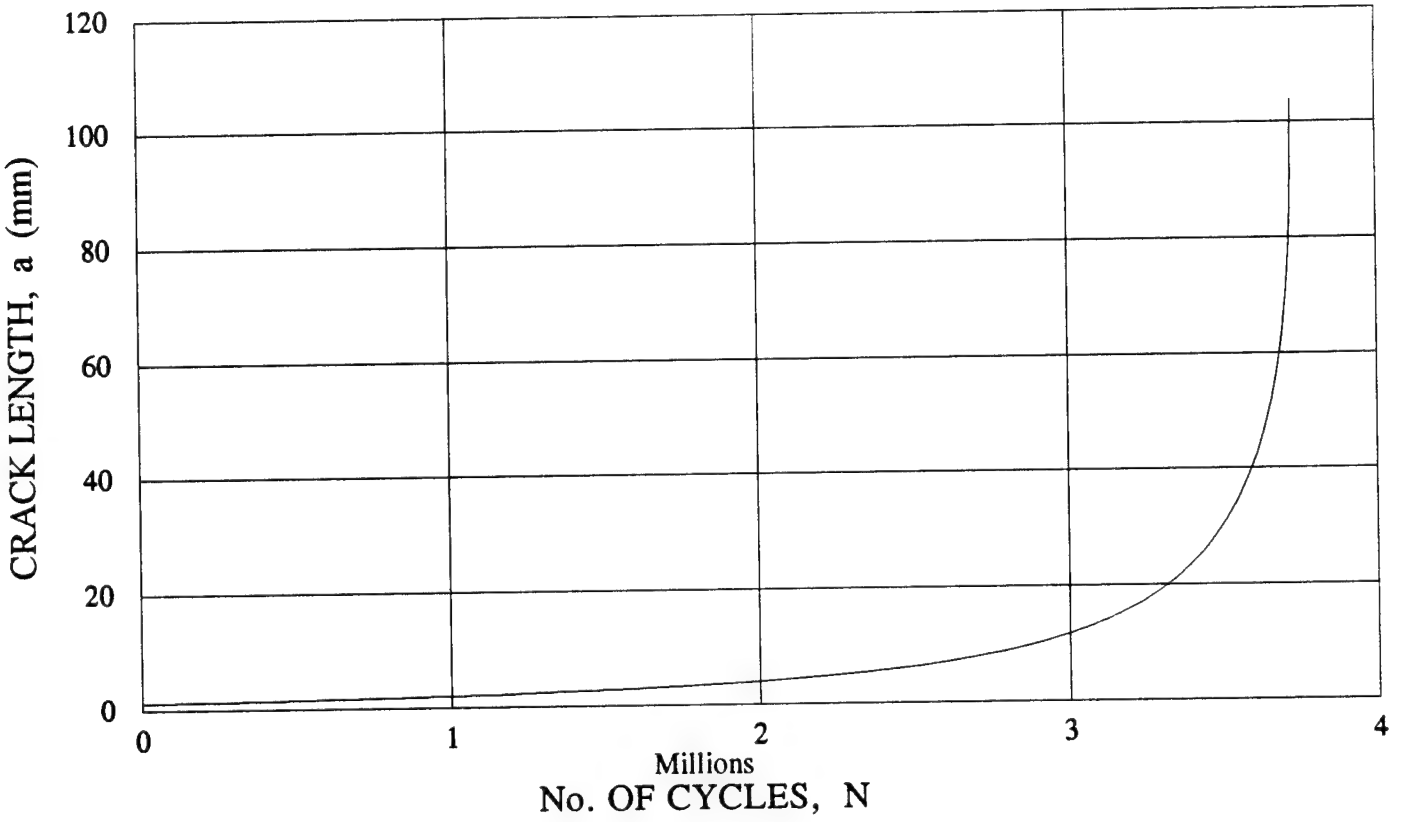

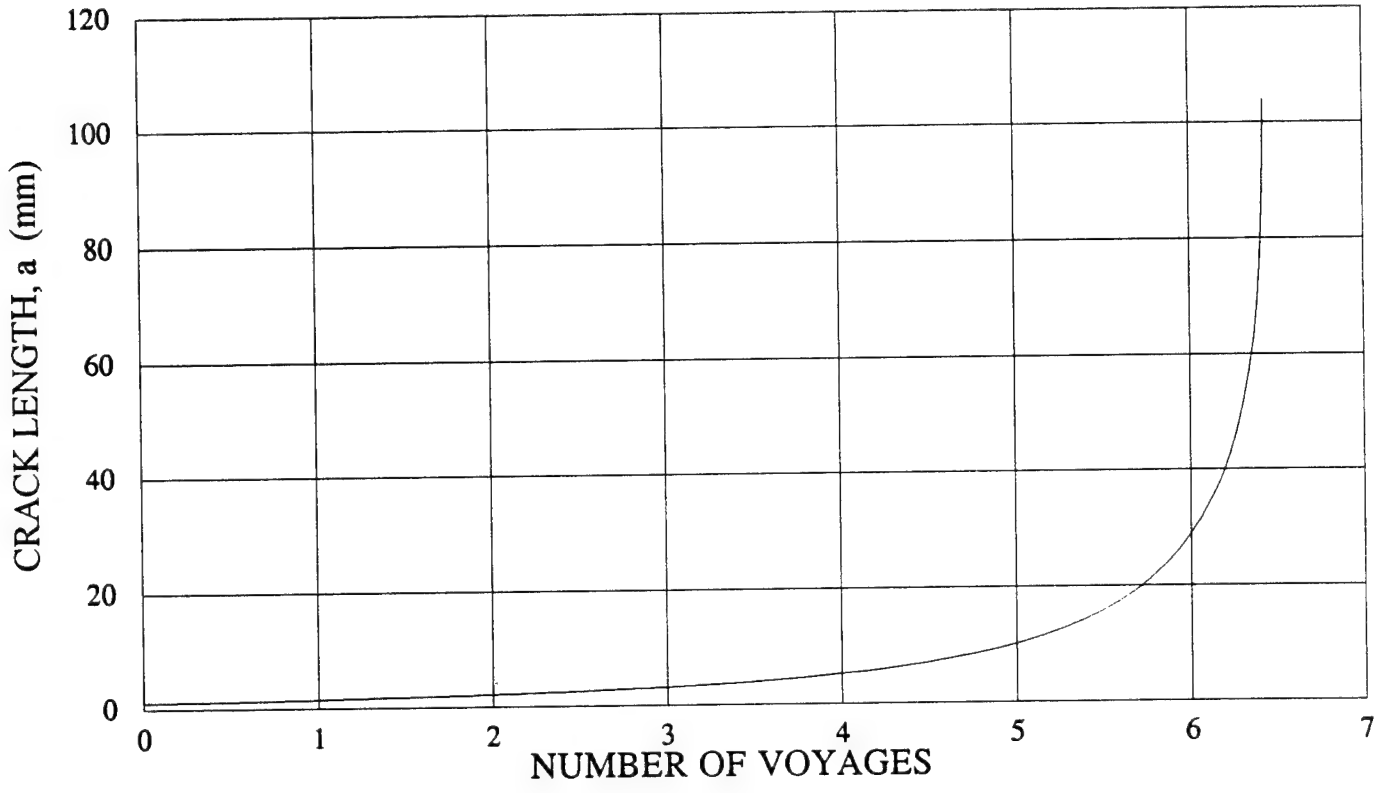

FIGURE 5.6 CRACK GROWTH PROFILE, EXAMPLE 1

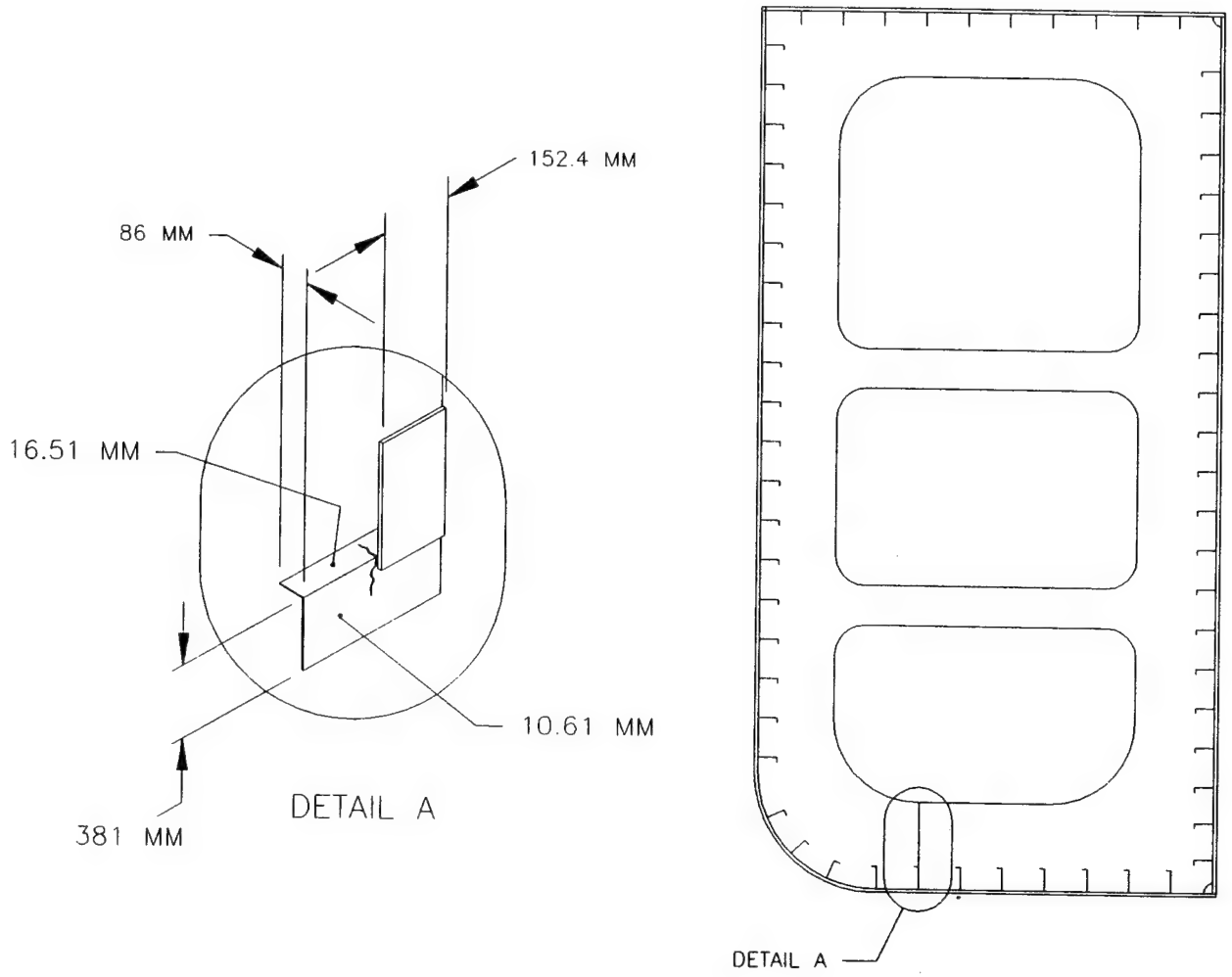

FIGURE 5.7 DESCRIPTION OF DAMAGE AT FR 81B, BOTTOM LONGITUDINAL NO.24, EXAMPLE 2.

Part 1 - Determination of Allowable Crack Length:

Hull bending moments and pressures were calculated in accordance with the ABS guide [3] for Zone A. The calculation of hull girder stresses in zone A neglects the contribution of horizontal wave bending moment, per [3]. Values of hull bending moments and stresses are presented in table 5-4 for the following section properties:

Moment of inertia about the horizontal N.A.	$I_{yy} = 2.82 \times 10^6$ m^2-cm^2
Moment of inertia about the vertical N.A.	$I_{zz} = 5.51 \times 10^6$ m^2-cm^2
Height of N.A. above baseline	= 8.57m
Vertical distance of BL No. 24 from the N.A.	y = 8.57m
Transverse distance of BL No. 24 from the C.L.	z = 11.82m

TABLE 5-4 BENDING MOMENT AND STRESSES AT BL #24

	Bending Moment (N-m)	Stresses (N/mm^2)
Still Water B.M.	2.52×10^9	76.0
Vertical Wave B.M. (Sagging)	-3.18×10^9	-97.0
Vertical Wave B.M. (Hogging)	2.98×10^9	91.0
Horizontal Wave B.M.	0.0	0.0

The stress range, f^*_{r2}, caused by the local bending of the stiffener due to pressure loading was computed to be 15 N/mm^2 according to equation (5.1) based on the following values:
C_t = 1.5, K = 1.15/12, SM = 19 m-cm^2, s = 845 mm, l = 2.86m and p = 0.03 N/mm^2 (see example 1 for explanation of the symbols). The resulting primary membrane stress, P_m, and bending stress, P_b, were 170 N/mm^2 and 7.5 N/mm^2 respectively. Since the tanker has been in service for over 20 years, the effect of residual weld stress was assumed to be negligible. Fracture assessment in this example was carried out at level 2 of PD 6493. At this level, the allowable crack length was determined by the following equation:

$$\bar{a}_m = \frac{E\sigma_y\delta_{mat}\left\{\left[S_r\left\{\frac{8}{\pi^2}\ln\sec\left(\frac{\pi}{2}S_r\right)\right\}^{-0.5}\right]-\rho\right\}^2}{\pi(Y\sigma)^2} \qquad (5.16)$$

where,

ρ is the plasticity correction factor, which is 0.0 in this example. (Since secondary (residual) stresses are assumed to be 0.)

For an edge crack under axial loading and bending, $Y\sigma$ is the sum of the membrane component, $(Y\sigma)_m$ and the bending component, $(Y\sigma)_b$. These were calculated using the following expressions:

$$(Y\sigma)_m = \frac{M_{km}P_m}{\mathrm{Cos}\left(\pi\frac{\alpha}{2}\right)}\sqrt{\frac{2}{\pi\alpha}\tan\frac{\pi\alpha}{2}}\left[0.752 + 2.20\alpha + 0.37\left(1 - \sin\frac{\pi\alpha}{2}\right)^3\right]$$

$$(Y\sigma)_b = \frac{M_{kb}P_b}{\mathrm{Cos}\left(\pi\frac{\alpha}{2}\right)}\sqrt{\frac{2}{\pi\alpha}\tan\frac{\pi\alpha}{2}}\left[0.923 + 0.199\left(1 - \mathrm{Sin}\frac{\pi\alpha}{2}\right)^4\right] \qquad (5.17)$$

where,

α = a/W; is the ratio of the crack length to the width of the specimen as shown in figure 5-8.

M_{km}, M_{kb} are the membrane and bending stress concentration factors due to local discontinuity, these were assumed to be 1.0 since they could not be precisely determined.

In equation 5.15, $Y\sigma$ & S_r are function of crack length, a. Therefore an iterative procedure was adopted to determine $\bar{a}_m$. For the same material properties as used in example 1, the allowable crack length was found to be 59 mm and the plastic collapse ratio, S_r was 0.71.

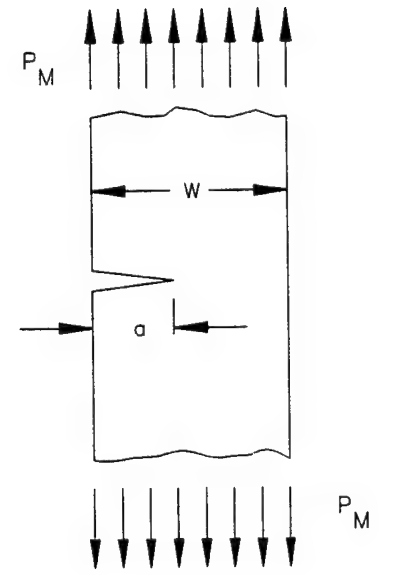

$$\alpha = a / \Omega$$

$$Y(\alpha) = \sqrt{\frac{2}{\pi\alpha} \tan\frac{\pi\alpha}{2}} \; * \; \frac{0.752 + 2.20\alpha + 0.37\left(1 - \sin\frac{\pi\alpha}{2}\right)^3}{\cos\frac{\pi\alpha}{2}}$$

EDGE CRACK UNDER AXIAL LOAD

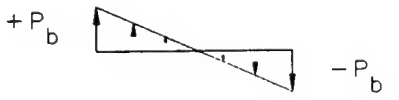

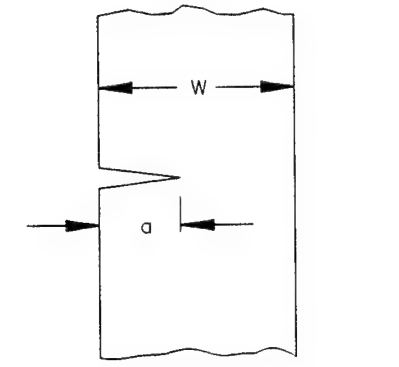

$$\alpha = a / \Omega$$

$$Y(\alpha) = \sqrt{\frac{2}{\pi\alpha} \tan\frac{\pi\alpha}{2}} \; * \; \frac{0.923 + 0.199\left(1 - \sin\frac{\pi\alpha}{2}\right)^4}{\cos\frac{\pi\alpha}{2}}$$

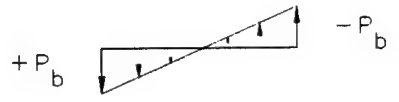

EDGE CRACK UNDER BENDING

FIGURE 5.8 'Y' FOR COMPONENT WITH EDGE CRACK UNDER AXIAL TENSION AND BENDING

Crack Growth Analysis:

In this example, crack growth analysis was performed using the same procedure as of example 1. Assuming the same short term North Sea Spectrum as example 1, a stress spectrum was generated. Using the rms value of the stress ranges in this spectrum, a crack growth profile over time was developed in a fashion similar to example 1. As can be seen from figure 5-9, it takes about 4 voyages for an initial crack of length 0.005 mm to become critical. Pertinent data is given below:

ΔP_m = 187.4 N/mm^2
ΔP_b = 15.0 N/mm^2
$\sigma_{r\,max}$ = 202.4 N/mm^2
$\Delta\sigma_{rms}$ = 40.1 N/mm^2

Conclusions:

In example 2 the effect of the fluctuating pressure load due to the seaway, is less pronounced. This is evident from the values of f^*_{r2} which are, 54 N/mm^2 in example 1 and 15 N/mm^2 in example 2. But the total tensile stress acting at the bottom shell plating, in example 2, is much higher than that acting at the side shell longitudinal No. 8, in example 1. Therefore in example 2, the critical crack length is smaller, and also the rate of crack propagation is faster.

5.3 Global Level Analysis

To assess the consequences of the local damage analyzed in the previous sub-sections on the overall strength of the tanker, ULTSTR [8] was used to study the ultimate ductile strength in the intact and damaged condition. Although ULTSTR was developed at DTRC by the US Navy for evaluation of the ultimate strength of naval ships it can be used for any ship structure including tankers. It is based on the "component approach" as mentioned earlier. Some of the limitations of ULTSTR are:

(1) no consideration for interaction of failure modes

(2) no consideration for failure by tripping in the elasto-plastic range

(3) no treatment of 3-dimensional effects;

Nevertheless for the purpose of comparative studies, it is relatively easy to use and less time consuming than a full 3-dimensional finite element analysis.

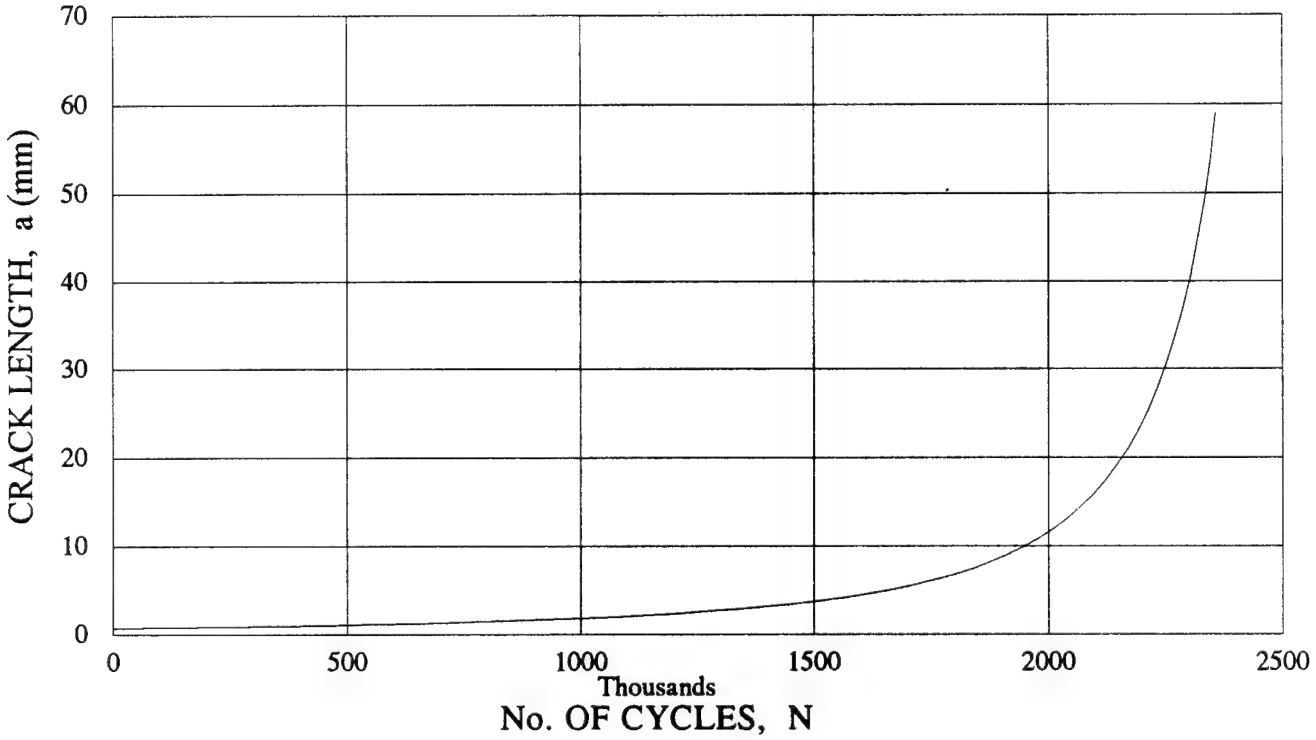

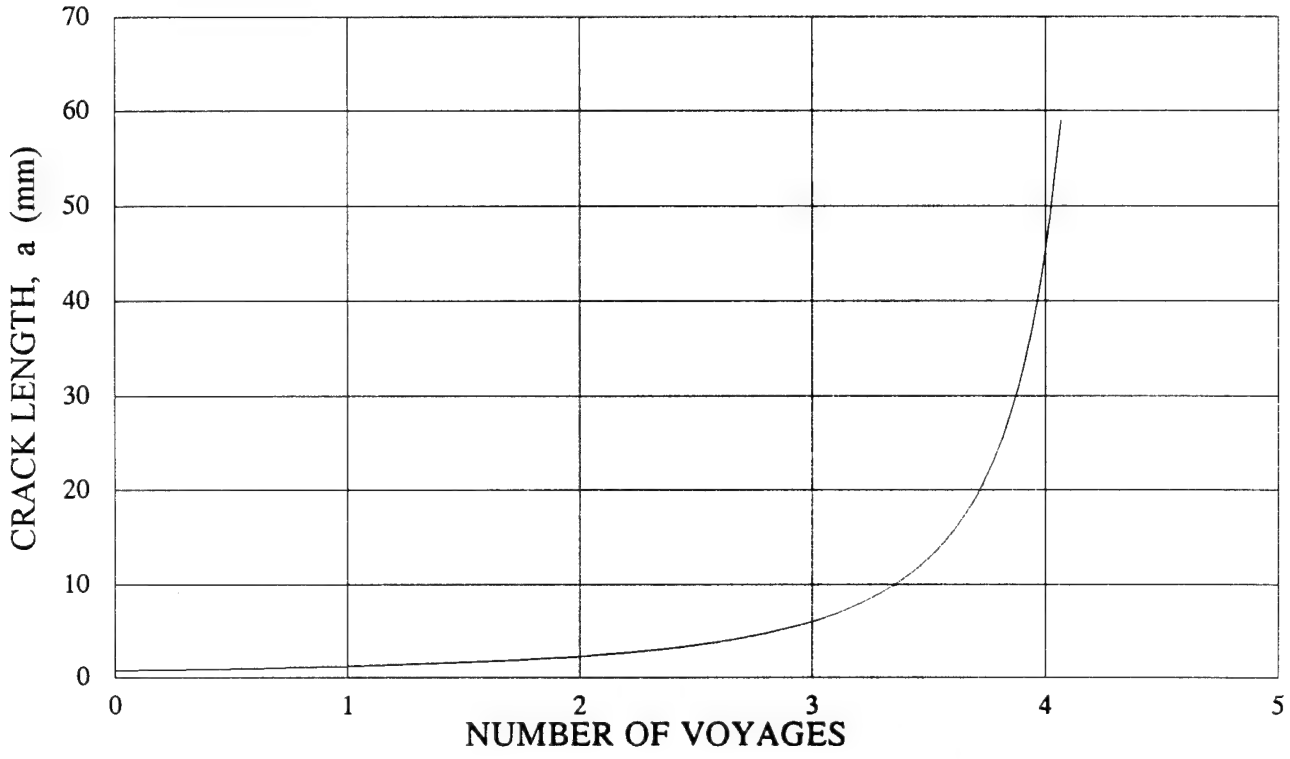

FIGURE 5.9 CRACK GROWTH PROFILE, EXAMPLE 2

To assess the residual strength of the damaged tanker, first its reserve strength which is the ratio of the ultimate moment capacity (intact) to the allowable design bending moment was determined. The design bending moment, M_{Des}, was calculated from ABS [9] rules. ULTSTR runs of the intact tanker were performed in hogging and sagging conditions, to determine its ultimate capacity. Since the tanker is symmetric about the centerplane, only half the midship section was explicitly modeled while the other half was modeled implicitly using the "MIRROR" option of ULTSTR. The whole midship was discretized into 105 gross-panels and 25 hard-corner elements as shown schematically in figure 5-10. While vertical structures, like the side shell plating and the longitudinal bulkhead, were finely discretized because of the linear variation of the normal stress across the depth, transverse structures like the main deck and bottom plating, were divided into just two gross panels, due to the uniform distribution of the normal stress across them. By specifying the transverse frame spacing as the column-buckling and tripping length of the stiffeners making up the gross-panels, effects of the transverse structures like bulkheads and frames were incorporated. Results of these analyses are presented below:

Design Bending Moment	5.600×10^9 N•m
Intact Ultimate Bending Moment (Hogging)	6.868×10^9 N•m
Reserve Capacity, REF (Hogging)	1.23
Intact Ultimate Bending Moment (Sagging)	6.744×10^9 N•m
Reserve Capacity, REF (Sagging)	1.20

A plot of the bending moment versus the applied curvature, figure 5-11 shows a drastic fall in the moment capacity once the ultimate moment is reached. Thus implying very little capability for load redistribution. The primary mode of failure which leads to the onset of ultimate collapse was found to be stiffener tripping at the upper deck and bottom shell plating.

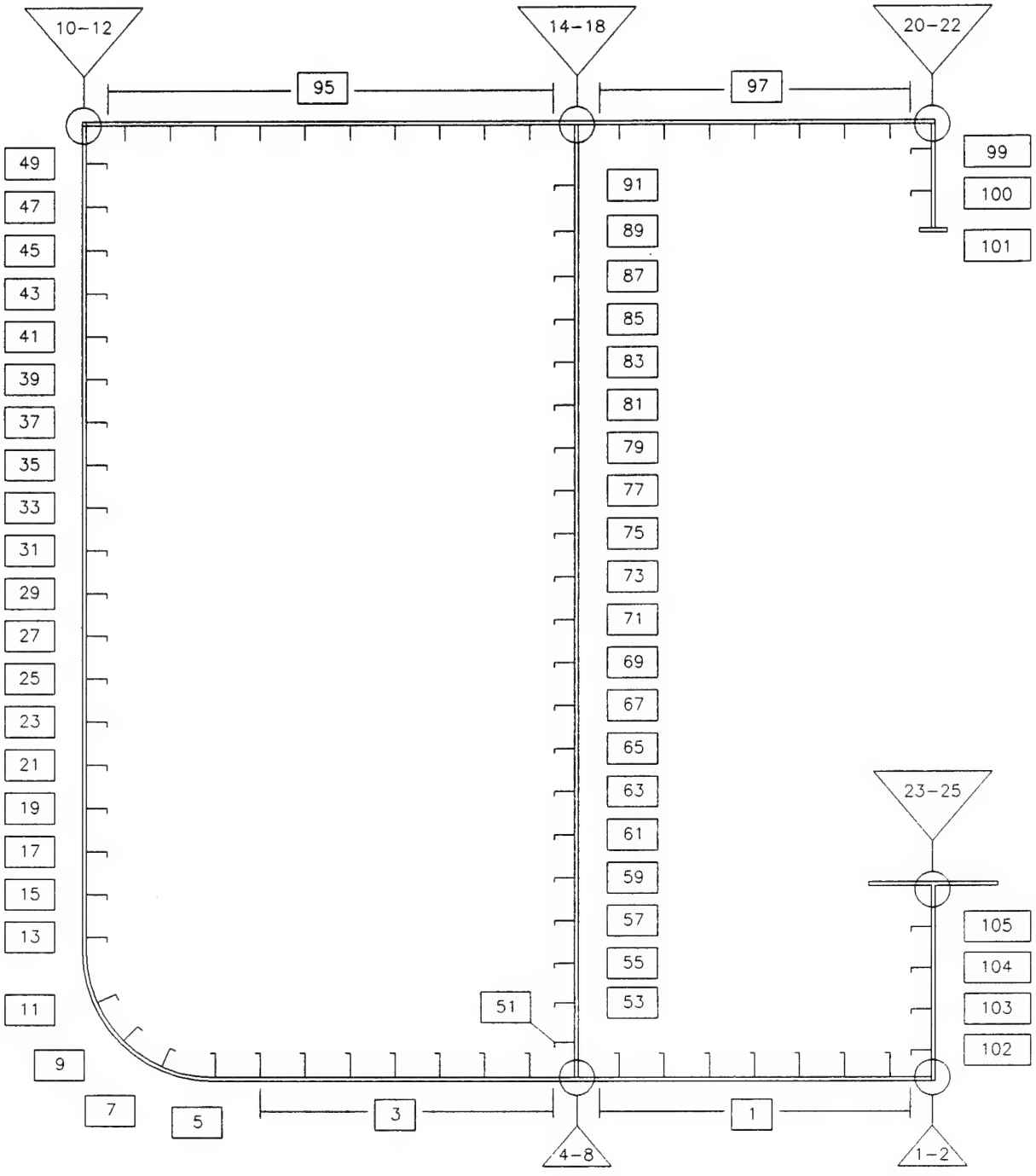

FIGURE 5.10 DISCRETIZATION OF TANKER CROSS–SECTION INTO GROSS PANELS ' □ ' AND HARD CORNERS △

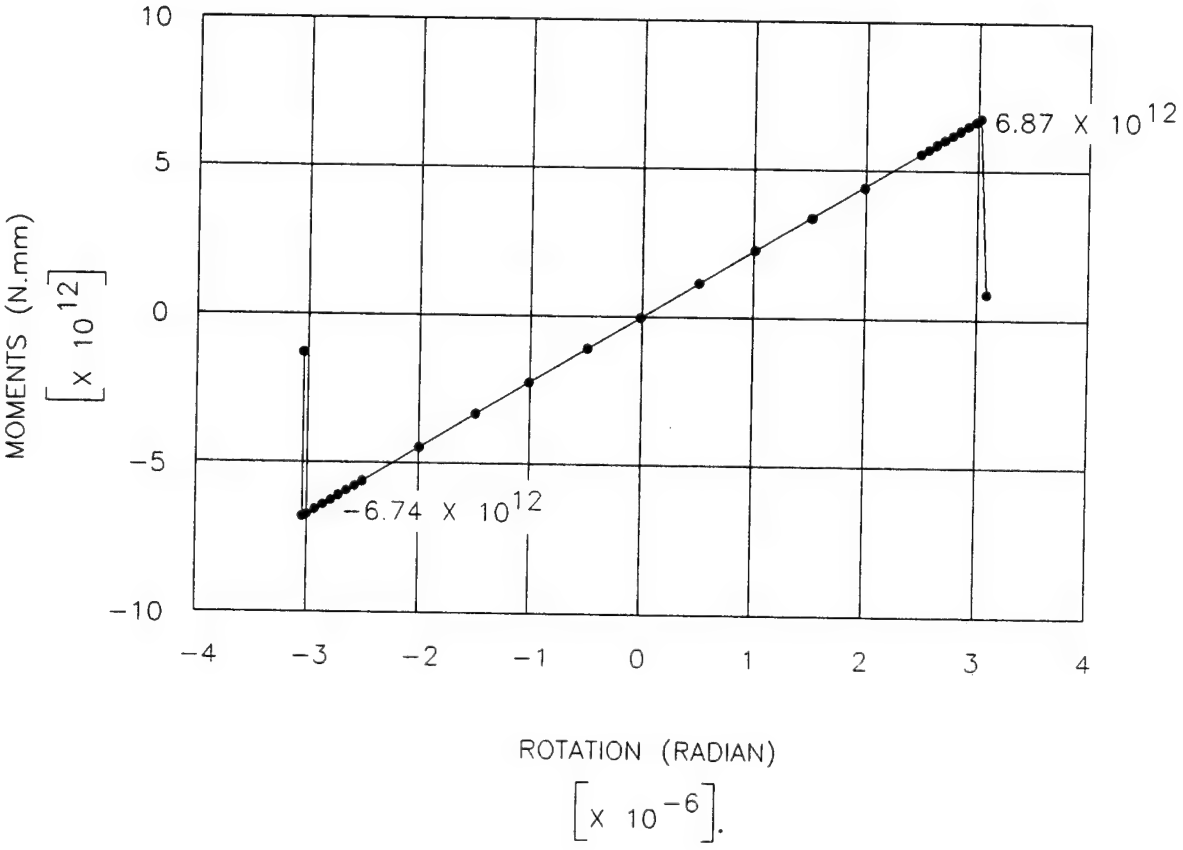

FIGURE 5.11 ULTIMATE MOMENT CAPACITY OF THE 85,000 TON TANKER

The local damages to the structural components analyzed in section 5.2 were fatigue cracks. Most of the time these cracks propagate into regions of low stress intensities and hence their growth gets retarded. To precisely determine the extent of the cracks, stress fields acting in the area adjoining the cracks need to be determined. This requires a full 3-dimensional analysis. To integrate the affect of these local damages into the global response, without resorting to a full scale 3-dimensional finite element analysis, a conservative approach was adopted. In this approach, portions of the tanker's cross-section in the vicinity of the damage were considered ineffective and hence neglected in the ULTSTR model. In addition to the two damage locations, analyzed in section 5.2, eight other critical locations were identified based on service life experience and accordingly the tanker was divided into 10 zones, A-J as shown in figure 5-12. Ten ULTSTR runs were performed and the results are presented in table 5-5. In these ten cases, the first 8 represented damage in the form of cracks and were modeled by complete removal of the affected gross panels from the port side of the cross-section. In cases 9 and 10, permanent deformation in zone C was simulated by assigning the gross panels in this zone initial distortion of 254 and 508 mm respectively which are about 8 and 16 percent of the transverse frame spacing. From the table, it can be seen (case 1-4) that damages in portions of the main deck or bottom shell plating result in relatively significant loss of ultimate strength in comparison to damages in other zones (cases 5-7) of the tankers. For comparison, in case 8, all gross panels in zones G, H, I & J were eliminated resulting in about 6% reduction in cross-sectional area - almost the same as that due to elimination of zone C (case 3), but the residual strength (RIF) in hogging decreased only by 6% whereas in case 3 it decreased by 14%.

The product of the residual strength index (RIF) and the reserve capacity (REF), is a good indicator for the purpose of residual strength assessment. The value of this product, which can be considered as a safety factor, should never be less than one.

Therefore,

$$FS = RIF \times REF = \frac{M_{Ult}(Damaged)}{M_{Ult}(Intact)} * \frac{M_{Ult}(Intact)}{M_{Des}} > 1.0 \qquad (5.18)$$

For each of the ten cases in table 5-5, these factors of safety were computed and it was found that in cases 1 and 4, they were less than one. Thus implying that operation of the vessel with damage in these zones could adversely affect the overall strength of the vessel.

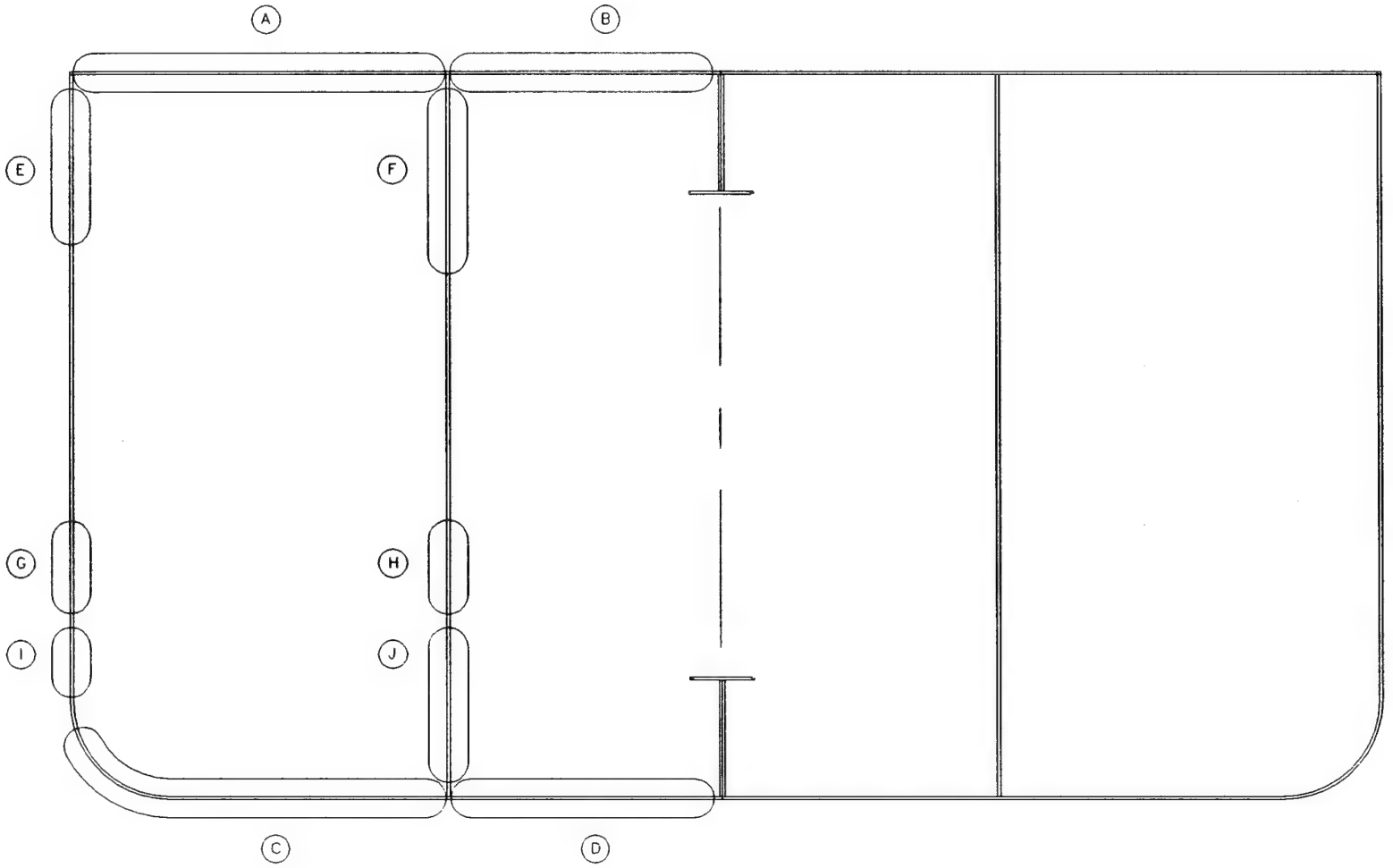

FIGURE 5.12 CRITICAL LOCATIONS OF THE TANKER

TABLE 5-5 RESIDUAL STRENGTH FACTORS OF DAMAGED TANKER

Case No.	Damaged Zone	Area (% change)	RIF* (Sag)	FS** (Sag)	RIF* (Hog)	FS** (Hog)
1	A	-8	0.79	0.95	0.93	1.14
2	B	-6	0.85	1.02	0.96	1.18
3	C	-10	0.95	1.14	0.78	0.96
4	D	-6	0.98	1.18	0.86	1.06
5	E & F	-5	0.93	1.12	1.00	1.23
6	G & I	-3	1.00	1.20	0.97	1.19
7	H & J	-3	1.00	1.20	0.99	1.22
8	G, H, I & J	-6	1.00	1.20	0.94	1.16
9	Permanent Set in C = 254 mm		1.00	1.20	0.90	1.11
10	Permanent Set in C = 508 mm		1.00	1.20	0.88	1.08

* $RIF = \frac{M_{ULT}(\text{Damaged})}{M_{ULT}(\text{Intact})}$

** FS = RIF x REF, where

$REF = \frac{M_{ULT}(\text{Intact})}{M_{ULT}(\text{Des})}$

REF (Sag) = 1.20

REF (Hog) = 1.23

5.4 References

1. Hughes, O. and Franklin, P., "Definition and Validation of a Practical Rationally-Based Method for the Fatigue Analysis and Design of Ship Hulls", SNAME, T&R Report No. R-41, February, 1993.

2. "Guidance on the Methods for Assessing the Acceptability of Flaws in Fusion Welded Structures, PD 6493: 1991", Published by the British Standards Institution (BSI).

3. ABS "Guide for the Fatigue Strength Assessment of Tankers", June 1992.

4. "Ship Design Manual - Marine Structures", Chapter 6, Part 8, Published by British Ship Research Association (BSRA).

5. Shi, W.B. and Thompson, P.A., "Aspects of Vulnerability of Bulk Carrier Structures", RINA, International Conference on Bulk Carriers and Tankers - The Way Ahead, December, 1992.

6. Rolfe, S.T. and Barsom, J.M., "Fracture and Fatigue Control in Structures - Applications of Fracture Mechanics", Published by Prentice - Hall, Inc. 1977, New Jersey.

7. Chang, J.B. and Hudson, C.M., editors, "Methods and Models for Predicting Fatigue Crack Growth Under Random Loading", ASTM STP 748, 1981.

8. Adamchak, J.C., "ULTSTR: A Program for Estimating the Collapse Moment of a Ship's Hull Under Longitudinal Bending", Report No. DTNSRDC - 82/076, October, 1982.

9. ABS Rules For Classing and Building Steel Vessels, 1992.

6.0 CONCLUSIONS AND RECOMMENDATIONS FOR FUTURE WORK

The primary objectives of this project were,

- Introduce the subject of residual strength assessment of damaged marine structures to the practicing ship structural engineering community.

- Summarize the state of the art technology and methods available in the marine and non-marine industry for quantifying residual strength.

- Recommend future work that will further integrate existing engineering procedures in the areas of crack growth, permanent deformation and ultimate strength emphasizing cost effective methods.

Background

Residual strength can be defined as the remaining strength in a structure once a component has failed or has been so severely damaged as to be ineffective. Thus residual strength can be viewed as the ultimate capacity for a damaged structure and therefore is an important indicator of the structures damage tolerance.

The current design process assumes that, the application of small deflection linear elastic theory provides the appropriate measure of structural performance at the global response level, for most marine structures. From such a global assessment of the structure's response, the forces applied to individual members are then compared with the local member capability assessed in terms of ultimate strength. Approaches to the determination of local member ultimate strength may include non-linear, large deflection or plastic type analysis.

It is important to note that the response and capability of a marine structure following some form of damage is evaluated by identifying the effect of local member failure on the overall structural integrity. The effects of local damage must be integrated upward to the global structural level to insure that correct load transfer paths are determined to realistically simulate the extent of damage on the overall system behavior. This local-global response approach required for assessing the residual strength of damaged marine structures represents a reverse approach from the global-local response approach used in the current structural design process. This was the underlying principle of this investigation.

Conclusions

The following conclusions, based on the results of this pilot project are presented below:

1. The theories, methods and computational tools for assessing the residual strength of damaged marine structures due to normal operating loads exist but they are scattered in literature and no standardized procedure for their application has been established.

2. Assessment of residual strength of continuous structures like ships is very complex and expensive. Two methods of analysis are possible: an approximate 2-dimensional procedure (the indirect method) or a 3-dimensional non-linear finite element analysis (the direct method). While the indirect method is economical and good for quick assessment of damage consequences, it predicts very conservative results because of the numerous assumptions on the stress fields, boundary conditions and extent of the damage modeled. The direct method is more fundamental in nature with very few assumptions and overcomes most of the limitations of the indirect method. But it is not a very practical method. It is an expensive method which requires a high level of expertise and considerable amount of computational resources.

3. The accuracy of the ultimate strength analysis programs used in either methods is hard to predict since limited amount of full scale test data are available for comparison. Few comparisons of the predictions of these programs with experimental data indicate that these programs can at the best be used for comparative studies.

4. Data collection and subsequent analysis of damage records for both ship and offshore structures in the context of total fleet years of service, damage tolerant features and the time relationship between occurrence of damage and subsequent detection and repair is difficult. Meaningful conclusions will require a lot of data, thoroughly processed, and will be expensive to collect.

5. Critical locations of damage are a function of ship type and structural configuration.

6. The dominant form of damage in marine structures due to normal operating loads is fracture and excessive permanent deformation. Most of the time these fractures are in the form of fatigue cracking on secondary members and are repaired before they reach their critical length or propagate into regions of low stress. The level of inherent ductility of ship structures, make them very tolerant to excessive permanent deformation.

7. The effect of local damage, such as permanent deformation, on the global response of the structure can be modeled by available ultimate strength programs. Modeling the extent of fracture damage is subjective and requires an understanding of the structural configuration and stress fields. The estimate of the impact of crack like damages, on the global response, can be accomplished by using aerospace industry developed technology and modifying it for marine structural applications.

8. Structural members that are not very highly stressed in intact conditions play an important role in redistributing forces when damage takes place. Consequently these members are more critical to the damaged structure behavior than the intact structure behavior.

9. Ultimate strength and the manner of hull girder collapse are strongly affected by hard corners in the cross-section. In terms of ultimate strength, hard corners should be incorporated into the design by judicious use of structural bulkheads and secondary structural components.

10. Although this report addresses residual strength assessment of structures damaged due to normal operating loads, it is important to note that the ultimate strength prediction methods reviewed in this report are applicable to assess damage caused by random accidents such as collisions and groundings. The only difference is that since the assessment is done after the actual accident, the exact location and the extent of the damage is better defined.

Recommendations for Future Work

Based on the above conclusions, the following recommendations are presented for future work:

1. Research into development and validation of an integrated computer program for residual strength assessment of damaged marine structures. Specifically the program should be capable of:

- full 3-dimensional geometric modeling of the ship structure
- stress-analysis, with provisions for modeling material and geometric non-linearities and crack like defects
- computing spectral wave loading given the sea state, heading and duration
- crack growth predictions
- ultimate strength predictions

2. In order to account for the role of residual strength in the development of limit state design criteria, critical locations susceptible to damage for specific ship types (i.e. bulk carriers, tankers and containerships) should be identified by:

(a) stress analysis using finite element procedures and

(b) extensive research of available casualty records.

The results obtained from 2(a) and 2(b) should be correlated in terms of the following three categories:

(i) slow crack growth structure - designs where stress levels are limited to assure that cracks will not grow to critical sizes during specified periods which depend on the degree of inspectability.

(ii) crack arrest fail safe structures - designs that stop unstable, rapid propagation of cracks within a continuous area of structure and subsequent growth is slow enough to permit detection prior to complete failure.

(iii) multiple load path fail safe structure - structure designed in segments such that localized damage is contained within one or two segments and the remaining structure exhibits slow crack growth and provides sufficient strength until subsequent inspection.

3. For specific ship types, with documented design information, calculate the reserve and residual strength using both the 2-dimensional component method and the 3-dimensional non-linear finite element method. Compare the results of both methods and examine the sensitivity of the ultimate strength prediction to the following:

- damage modeling assumptions
- amplitude and shape of permanent deformations
- locations of fracture damage
- loss of transverse structure
- loss of hull girder shear area
- location of hard corners vs. fracture initiation.

4. Compare the results of these studies to full scale tests simulating damaged ship structure.

5. For quick assessment of crack like defects, develop charts of fracture toughness data through actual testing. These testings should be conducted for various typical structural configurations susceptible to cracking.

6. Besides development of analytical procedures, research has to be focussed on the development and installation of a fully integrated hull surveillance system. The research should specifically address such issues as:

(i) real-time monitoring of hull stresses, accelerations and fatigue.

(ii) selection of measuring instruments to withstand the harsh marine environment.

(iii) strategic positioning of these instruments on the ship to measure the desired response.

(iv) provision for direct link between the stress monitoring system and the ship's loading computers.

The goals of the surveillance system should be:

- to compare instantaneous measured stresses to the maximum permissible stress for the vessel and provide a feedback.

- monitor stress reversals for evaluation of cumulative fatigue damage.

- to store the data acquired during voyages to be used later on-shore to help plan and forecast long-term repair and maintenance strategies.

Project Technical Committee Members

The following persons were members of the committee that represented the Ship Structure Committee to the Contractor as resident subject matter experts. As such they performed technical review of the initial proposals to select the contractor, advised the contractor in cognizant matters pertaining to the contract of which the agencies were aware, and performed technical review of the work in progress and edited the final report.

Mr. Jack Spencer	American Bureau of Shipping
LCDR Doug O'Reilly	Directorate Ship Engineering, Canada
Mr. Neil Pegg	Defence Research Establishment Atlantic, Canada
Mr. Francis J. Scotto	American Bureau of Shipping
Mr. James White	U.S. Coast Guard Research and Development
Mr. Jerry Snyder	Naval Sea Systems Command
Mr. Phil Alman	U.S. Coast Guard
Ms. Maria Ximenes	Chevron Shipping
Mr. William Siekierka	Naval Sea Systems Command, Contracting Officer's Technical Representative
Dr. Robert Sielski Mr. Alex Stavovy	National Academy of Science, Marine Board Liaison
CDR Steve Sharpe	U.S. Coast Guard, Executive Director Ship Structure Committee

COMMITTEE ON MARINE STRUCTURES

Commission on Engineering and Technical Systems

National Academy of Sciences – National Research Council

The COMMITTEE ON MARINE STRUCTURES has technical cognizance over the interagency Ship Structure Committee's research program.

Peter M. Palermo Chairman, Alexandria, VA
Subrata K. Chakrabarti, Chicago Bridge and Iron, Plainfield, IL
John Landes, University of Tennessee, Knoxville, TN
Bruce G. Collipp, Marine Engineering Consultant, Houston, TX
Robert G. Kline, Marine Engineering Consultant, Winona, MN
Robert G. Loewy, NAE, Rensselaer Polytechnic Institute, Troy, NY
Robert Sielski, National Research Council, Washington, DC
Stephen E. Sharpe, Ship Structure Committee, Washington, DC

LOADS WORK GROUP

Subrata K. Chakrabarti Chairman, Chicago Bridge and Iron Company, Plainfield, IL
Howard M. Bunch, University of Michigan, Ann Arbor, MI
Peter A. Gale, John J. McMullen Associates, Arlington, VA
Hsien Yun Jan, Martech Incorporated, Neshanic Station, NJ
John Niedzwecki, Texas A&M University, College Station, TX
Solomon C. S. Yim, Oregon State University, Corvallis, OR
Maria Celia Ximenes, Chevron Shipping Co., San Francisco, CA

MATERIALS WORK GROUP

John Landes, Chairman, University of Tennessee, Knoxville, TN
William H Hartt, Florida Atlantic University, Boca Raton, FL
Horold S. Reemsnyder, Bethlehem Steel Corp., Bethlehem, PA
Barbara A. Shaw, Pennsylvania State University, University Park, PA
James M. Sawhill, Jr., Newport News Shipbuilding, Newport News, VA
Bruce R. Somers, Lehigh University, Bethlehem, PA
Jerry G. Williams, Conoco, Inc., Ponca City, OK

RECENT SHIP STRUCTURE COMMITTEE PUBLICATIONS

SSC-363 Uncertainties in Stress Analysis on Marine Structures by E. Nikolaidis and P. Kaplan 1991

SSC-364 Inelastic Deformation of Plate Panels by Eric Jennings, Kim Grubbs, Charles Zanis, and Louis Raymond 1991

SSC-365 Marine Structural Integrity Programs (MSIP) by Robert G. Bea 1992

SSC-366 Threshold Corrosion Fatigue of Welded Shipbuilding Steels by G. H. Reynolds and J. A. Todd 1992

SSC-367 Fatigue Technology Assessment and Strategies for Fatigue Avoidance in Marine Structures by C. C. Capanoglu 1993

SSC-368 Probability Based Ship Design Procedures: A Demonstration by A. Mansour, M. Lin, L. Hovem, A. Thayamballi 1993

SSC-369 Reduction of S-N Curves for Ship Structural Details by K. Stambaugh, D. Lesson, F. Lawrence, C-Y. Hou, and G. Banas 1993

SSC-370 Underwater Repair Procedures for Ship Hulls (Fatigue and Ductility of Underwater Wet Welds) by K. Grubbs and C. Zanis 1993

SSC-371 Establishment of a Uniform Format for Data Reporting of Structural Material Properties for Reliability Analysis by N. Pussegoda, L. Malik, and A. Dinovitzer 1993

SSC-372 Maintenance of Marine Structures: A State of the Art Summary by S. Hutchinson and R. Bea 1993

SSC-373 Loads and Load Combinations by A. Mansour and A. Thayamballi 1994

SSC-374 Effect of High Strength Steels on Strength Consdierations of Design and Construction Details of Ships by R. Heyburn and D. Riker 1994

SSC-375 Uncertainty in Strength Models for Marine Structures by O. Hughes, E. Nikolaidis, B. Ayyub, G. White, P. Hess 1994

SSC-377 Hull Structural Concepts For Improved Producibility by J. Daidola, J. Parente, and W. Robinson 1994

SSC-378 The Role of Human Error in Design, Construction and Reliability of Marine Structures by R. Bea 1994

SSC-379 Improved Ship Hull Structural Details Relative to Fatigue by K. Stambaugh, F. Lawrence and S. Dimitriakis 1994

SSC-380 Ship Structural Integrity Information System by R. Schulte-Strathaus, B. Bea 1995

Ship Structure Committee Publications - A Special Bibliography